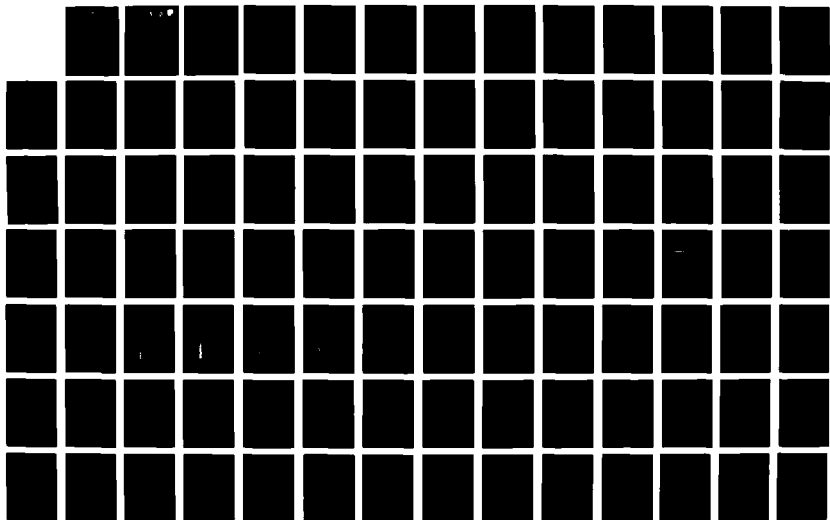AD-A261 796

CONSIDERATIONS OF THE ERROR VARIANCES OF TIME-AVERAGED
ESTIMATORS FOR CORRELATED PROCESSES(U) ROME LAB
GRIFFISS AFB NY   J N MICHELS DEC 92 RL-TR-92-339

1/2

UNCLASSIFIED   XC-RL/GRIFFISS   NL

AD-A261 796

RL-TR-92-339
In-House Report
December 1992

DTIC
S ELECTE
MAR 2 3 1993
C
D

CONSIDERATIONS OF THE ERROR VARIANCES OF TIME-AVERAGED ESTIMATORS FOR CORRELATED PROCESSES

James H. Michels

93   3 22 012

93-05920

Rome Laboratory
Air Force Materiel Command
Griffiss Air Force Base, New York

This report has been reviewed by the Rome Laboratory Public Affairs Office (PA) and is releasable to the National Technical Information Service (NTIS). At NTIS it will be releasable to the general public, including foreign nations.
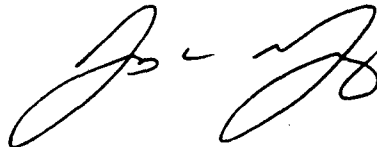
RL-TR-92-339 has been reviewed and is approved for publication.

APPROVED:

JOSEPH POLNIASZEK, Acting Chief
Surveillance Technology Division
Surveillance & Photonics Directorate

FOR THE COMMANDER:

JAMES W. YOUNGBERG, LtCol, USAF
Deputy Director
Surveillance & Photonics Directorate

If your address has changed or if you wish to be removed from the Rome Laboratory mailing list, or if the addressee is no longer employed by your organization, please notify RL (OCTM) Griffiss AFB NY 13441-5700. This will assist us in maintaining a current mailing list.

Do not return copies of this report unless contractual obligations or notices on a specific document require that it be returned.

REPORT DOCUMENTATION PAGE

Form Approved
OMB No. 0704-0188

1. AGENCY USE ONLY (Leave Blank)	2. REPORT DATE December 1992	3. REPORT TYPE AND DATES COVERED In-House Jun 91 - Oct 92

4. TITLE AND SUBTITLE
CONSIDERATIONS OF THE ERROR VARIANCES OF TIME-AVERAGED
ESTIMATORS FOR CORRELATED PROCESSES

5. FUNDING NUMBERS
PE - 62702F
PR - 4506
TA - 17
WU - 67

6. AUTHOR(S)
James H. Michels

7. PERFORMING ORGANIZATION NAME(S) AND ADDRESS(ES)
Rome Laboratory (OCTM)
26 Electronic Parkway
Griffiss AFB NY 13441-4514

8. PERFORMING ORGANIZATION REPORT NUMBER
RL-TR-92-339

9. SPONSORING/MONITORING AGENCY NAME(S) AND ADDRESS(ES)
Rome Laboratory (OCTM)
26 Electronic Parkway
Griffiss AFB NY 13441-4514

10. SPONSORING/MONITORING AGENCY REPORT NUMBER

11. SUPPLEMENTARY NOTES
Rome Laboratory Project Engineer: James H. Michels/OCTM (315) 330-4431

12a. DISTRIBUTION/AVAILABILITY STATEMENT
Approved for public release; distribution unlimited

12b. DISTRIBUTION CODE

13. ABSTRACT (Maximum 200 words)

This report considers the sample and error variances of both time-averaged correlation function and parameter estimators for stationary discrete complex processes. Analytic expressions for the variance of the biased, time-averaged auto and cross-channel correlation function estimators of stationary discrete complex processes are developed. These expressions relate the variance of these estimators not only to the size of the observation windows used to obtain the estimates, but also to the correlation of the processes as well. They provide a performance measure which can be used to specify the window size of the observation interval required to achieve a specific value of this variance. A unique aspect of this development is the determination of the functional dependence of these expressions in terms of the process temporal and cross-channel correlation. Validation of the analytic expressions is obtained using Monte-Carlo simulation. Furthermore, computed results are presented for the error variances of several parameter estimators for which analytical expressions are lacking. Their performance is compared to that of the exact Cramer-Rao bound as a function of process correlation and data window size. Both Gaussian and non-Gaussian processes are considered as well as both single and multichannel processes.

14. SUBJECT TERMS
Autoregressive Processes, Parameter Estimation, Random Processes, Cramer-RAO Bound, Error Variance, Ergodicity

15. NUMBER OF PAGES
116

16. PRICE CODE

17. SECURITY CLASSIFICATION OF REPORT UNCLASSIFIED	18. SECURITY CLASSIFICATION OF THIS PAGE UNCLASSIFIED	19. SECURITY CLASSIFICATION OF ABSTRACT UNCLASSIFIED	20. LIMITATION OF ABSTRACT U/L

ACKNOWLEDGEMENTS

DTIC QUALITY INSPECTED 1

Accesion For	
NTIS CRA&I	☑
DTIC TAB	☐
Unannounced	☐
Justification	
By	
Distribution /	
Availability Codes	
Dist	Avail and / or Special
A-1	

CONTENTS

LIST OF TABLES

1.0 INTRODUCTION

Ergodicity is the condition which enables time-averaged statistics of random processes to approximate those obtained by ensemble averages. Although this condition is often assumed in estimation and other signal processing applications, the dependence of the ergodic behavior of random processes upon fundamental process characteristics (such as the temporal and cross-channel correlation, and the process variance) and its implications on estimation performance evaluation is not often considered. The ergodicity condition for auto- and cross-channel correlation functions expressed in terms of these fundamental process characteristics is derived in this paper. Specifically, analytic expressions are developed for the variance of the biased, time-averaged correlation functions for stationary discrete complex processes. If these variances approach zero in the limit of infinitely large sample sizes, the ergodic condition holds. The expressions derived here pertain to the general case of Gaussian processes with unconstrained quadrature components where the bandpass processes are, in general, non-stationary [5]. In addition, the analytic expressions are simplified for the special case of complex processes with constrained correlation between the Gaussian quadrature components yielding stationary narrowband bandpass processes.

The expressions developed here for the time-averaged correlation function estimators provide a performance measure which can be used to specify the window size of the observation interval required to achieve a specific value of this variance. As an example, the increase in sample window size required to achieve a specific value of the variance of the time-averaged correlation functions is quantitatively related to the increase in temporal correlation as well as the variance of the underlying process. Validity of the analytic expressions is presented using a multichannel process synthesis method described in [1,2].

Next, Monte-Carlo simulations are used to measure the error variance of several parameter estimators using zero-mean time series whose covariances are functions of a parameter vector. Both Gaussian and non-Gaussian processes are considered. In this analysis, the parameter vectors are varied to simulate processes with various temporal and cross-channel correlation; ie., processes ranging from narrowband to broadband. The dependence of the parameter estimators upon process correlation is contrasted with that of the time averaged correlation function estimators. It is noted that the performance of these two

1

classes of estimators have markedly different dependence on process temporal correlation. Finally, the performance of the parameter estimators is compared to the exact Cramer-Rao bound.

2.0 PROCESS DEFINITION

In this chapter, we define the multichannel autoregressive (AR) process, the relation between the AR coefficients and the correlation matrix of the processes known as the Yule-Walker equation, a wide class of non-Gaussian processes known as Spherically Invariant Random Processes (SIRP's); and finally, a brief description of the procedure used to synthesize these processes enabling the control of the temporal and cross-channel correlation.

2.1 MULTICHANNEL AUTOREGRESSIVE (AR) PROCESSES

The multichannel forward autoregressive (AR) process $\underline{x}(n)$ is expressed as

$$\underline{x}(n) = -\sum_{k=1}^{M} A^H(k)\underline{x}(n-k) + \underline{u}(n) \qquad (2.1)$$

where $A^H(k)$ is the kth JxJ matrix coefficient for the Jx1 vector AR process $\underline{x}(n)$ of model order M and $\underline{u}(n)$ is the Jx1 forward white noise driving vector with covariance matrix $[\Sigma_f]_u$. We note that $A^H(k)$ is expressed in terms of the Hermitian operation for notational convenience, but is not restricted to be a Hermitian matrix. It will be shown later that this notation enables us to express the Yule-Walker equation in terms of row vectors containing the Hermitian transpose operation. For the single channel case, the terms in eq(2.1) are scalers. Thus,

$$x(n) = -\sum_{k=1}^{M} a^*(k)x(n-k) + u(n) \qquad (2.2)$$

The vector $\underline{u}(n)$ from eq(2.1) can be expressed as

$$\underline{u}(n) = C_v\underline{v}(n) \qquad (2.3)$$

where $\underline{v}(n)$ is a Jx1 white noise vector with JxJ diagonal covariance matrix D_v. Eq(2.3) enables us to obtain

$$[\Sigma_f]_u \equiv E[\underline{u}(n)\underline{u}^H(n)] = E[C_v\underline{v}(n)\underline{v}^H(n)C_v^H] \tag{2.4a}$$

$$= C_v E[\underline{v}(n)\underline{v}^H(n)]C_v^H \tag{2.4b}$$

$$= C_v D_v C_v^H \tag{2.4c}$$

For the special case

$$D_v = E[\underline{v}(n)\underline{v}^H(n)] = I \tag{2.5}$$

where I is the JxJ identity matrix, eq(2.4c) reduces to

$$[\Sigma_f]_u = C_v C_v^H. \tag{2.6}$$

Eq.(2.6) indicates that the JxJ matrix C_v can be obtained by the Cholesky decomposition of $[\Sigma_f]_u$. The above relationships are utilized in the process synthesis procedure described in section 2.4 and reference [2]. Alternatively, eq(2.3) could have been expressed as

$$\underline{u}(n) = L_z\underline{z}(n) \tag{2.7}$$

where L_z is a unit diagonal lower triangular matrix and the vector process $\underline{z}(n)$ is a white noise vector uncorrelated in time, whose components are also uncorrelated across channels. The covariance matrix of $\underline{u}(n)$ is expressed as

$$[\Sigma_f]_u \equiv E[\underline{u}(n)\underline{u}^H(n)] = E[L_z\underline{z}(n)\underline{z}^H(n)L_z^H] \tag{2.8a}$$

$$= L_z E[\underline{z}(n)\underline{z}^H(n)]L_z^H \tag{2.8b}$$

$$= L_z D_z L_z^H \tag{2.8c}$$

where

$$D_z = E[\underline{z}(n)\underline{z}^H(n)]. \tag{2.9}$$

Eq(2.8c) denotes the LDL^H decomposition of $[\Sigma_f]_u$ provided D_z is a real, diagonal matrix. Furthermore, the channel variances are contained along the diagonal elements of D_z.

4

2.2. THE YULE-WALKER EQUATIONS

In this subsection, we present the relationship between the matrix coefficients $A^H(k)$ of eq(2.1), the covariance matrix $[\Sigma_f]_u$ of the forward AR white noise driving vector defined in eqs(2.4), and the known correlation matrix $[R_{xx}]$ of the vector $\underline{x}(n)$. The latter is defined as

$$[R_{xx}] = E[\underline{\underline{x}}_{n-M,n} (\underline{\underline{x}}_{n-M,n})^H]. \qquad (2.10)$$

where

$$\underline{\underline{x}}^T_{n-M,n} = [\underline{x}^T(n-M)\ \underline{x}^T(n-M+1)...\underline{x}^T(n)] \qquad (2.11)$$

We first introduce the reversed order correlation matrix $[\tilde{R}_{xx}]_{M+1}$ defined as

$$[\tilde{R}_{xx}] = E[\underline{\underline{x}}_{n,n-M}(\underline{\underline{\tilde{x}}}_{n,n-M})^H] \qquad (2.12)$$

where

$$\underline{\underline{x}}^T_{n,n-M} = [\underline{x}^T(n)\ \underline{x}^T(n-1)...\underline{x}^T(n-M)] \qquad (2.13)$$

and ~ denotes time order reversal. We note that the matrix $[\tilde{R}_{xx}]$ is the correlation matrix of $\underline{\underline{\tilde{x}}}_{n-M,n} = \underline{\underline{x}}_{n,n-M}$ in contrast to $[R_{\underline{xx}}]$ which is the correlation matrix of the vector $\underline{\underline{x}}_{n-M,n}$ defined in eq(2.11).

The relationship between $A^H(k)$, $[\Sigma_f]_u$ and $[\tilde{R}_{\underline{xx}}]$ is expressed by the augmented Yule-Walker equations [9,10]; ie.,

$$\underline{A}^H\ [\tilde{R}_{\underline{xx}}] = \{[\Sigma_f]_u^H\ [0]...[0]\} \qquad (2.14)$$

where

$$\underline{A}^H = [I\ A^H(1)\ A^H(2)...A^H(M)] \qquad (2.15a)$$

$$[\Sigma_f]_u^H = E[\underline{u}(n)\underline{u}^H(n)]\ = [\Sigma_f]_u \qquad (2.15b)$$

$$\underline{u}^T(n) = [u_1(n)\ u_2(n)\ ...u_J(n)] \qquad (2.15c)$$

5

The corresponding equation for the wide-sense stationary, backward AR process is expressed as

$$\underline{x}(n) = -\sum_{k=1}^{M} B^H(k)\underline{x}(n+k) + \underline{u}_b(n) \qquad (2.16)$$

where we specifically denote the backward white noise driving vector $\underline{u}_b(n)$ with the subscript b. The covariance matrix of $\underline{u}_b(n)$ is expressed as

$$[\Sigma_b]_u = E[\underline{u}_b(n)\ \underline{u}_b^H(n - l) \qquad (2.17)$$

The corresponding equation for the backward Yule-Walker equations are expressed as

$$\underline{B}^H [\tilde{R}_{xx}] = \{[0]...[0]\ [\Sigma_b]_u^H\} \qquad (2.18)$$

where

$$\underline{B}^H = [B^H(M)...B^H(1)\ I]. \qquad (2.19)$$

2.3 NON-GAUSSIAN AUTOREGRESSIVE PROCESSES

In this section, we discuss the generalization of the single channel autoregressive processes defined in eq(2.2) to a class of non-Gaussian random processes known as spherically invariant random processes (SIRP) [7,16,17,18]. The non-Gaussian form of the random process x(n) is introduced through the white noise driving term u(n). Following Rangaswami [16], we first define a spherically invariant random vector (SIRV) as a random vector (real or complex) whose PDF is uniquely determined by the specification of a mean vector, a covariance matrix and a characteristic first order PDF. A spherically invariant random process (SIRP) is a random process (real or complex) such that every random vector obtained by sampling this process is an SIRV. An important theorem in the theory of such processes is the representation theorem [Yao] stated as follows.

6

Theorem 1 If a random vector is an SIRV, then there exists a non-negative random variable S such that the PDF of the random vector conditioned on S is a multivariate Gaussian PDF.

For the simulation of an SIRV, we consider the product

$$\underline{u}_{1,N} = \underline{z}_{1,N} S \qquad (2.20)$$

where $\underline{u}_{1,N} = [u_1 \ u_2 \ ... \ u_N]^T$ denotes the SIRV, $\underline{z}_{1,N} = [z_1 \ z_2 \ ... \ z_N]^T$ is a Gaussian random vector with zero mean and covariance matrix M and S is a real, non-negative random variable with characteristic PDF $f_S(s)$. Statistical independence between $\underline{z}_{1,N}$ and S is assumed for convenience. In [7], several characterisic PDF's for $f_S(s)$ are considered which provide various PDF's for $f_U(u)$. Among others, they include the Chi, Weibull, Generalized Rayleigh, Rician, the K-distribution, Laplace, Cauchy, Student-t and, as a special case, the Gaussian. In section 5.3.2, we consider K-distributed processes using a form of the Gamma distribution for $f_S(s)$.

2.4 PROCESS SYNTHESIS PROCEDURE

In this section, we briefly describe the method used to synthesize the random processes used in this study. The procedure utilizes the multichannel Yule-Walker equation expessed by eq.(2.14). Essentially, the desired temporal and cross-channel correlation are specified in the covariance matrix $[\tilde{R}_{xx}]$, eq(2.14) is solved for the vector of matrix coefficients $\underline{A}^H$ and the matrix $[\Sigma_f]_u^H$. The $A^H(k)$ coefficients contained in $\underline{A}^H$ are used in eq(2.1) directly for the desired order M of the process. The matrix $[\Sigma_f]_u^H$ is used in eq(2.6) to determine the matrix C_v. This matrix in turn is used in eq(2.3) to provide the white noise driving term $\underline{u}(n)$ in eq(2.1). We note that $\underline{u}(n)$ provides the cross-channel correlation through the Hermitian covariance matrix $[\Sigma_f]_u$.

In [2], we describe a method to incorporate the desired correlation properties into $[\tilde{R}_{xx}]$. This is accomplished through the use of 'shaping functions' which enable us to modify the shape of the correlation functions contained in the correlation matrix. For the cross-correlation function, we consider

7

$$R_{ij}(l) = \frac{(\rho_{ij})\sigma_{ii}\sigma_{jj}f(\lambda_{ij}, l - l_{ij})}{f(\lambda_{ij}, l - l_{ij})\big|_{l=0}} \exp\{j[\theta_{ij}(l) - \theta_{ij}(0)]\} \qquad (2.21a)$$

$$= \frac{|\rho_{ij}|\sigma_{ii}\sigma_{jj}f(\lambda_{ij}, l - l_{ij})}{f(\lambda_{ij}, l - l_{ij})\big|_{l=0}} \exp\{j[\theta_{ij}(l)]\} \qquad (2.21b)$$

where ρ_{ij} is the complex cross-channel correlation parameter such that $\rho_{ij} = R_{ij}(0)/\sigma_{ii}\sigma_{jj}$, λ_{ij} is the one-lag temporal cross-correlation parameter, l_{ij} is the lag value at which the cross-correlation function peaks and $\theta_{ij}(l)$ is the phase of the cross-correlation function. By definition,

$$\rho_{ij} = |\rho_{ij}| \exp[j\theta_{ij}(0)] \qquad (2.22)$$

Expressions for $R_{ji}(l)$ are obtained from eq(2.21b) using the property

$$R_{ji}(l) = R_{ij}^{*}(-l). \qquad (2.23)$$

These equations provide us with a useful description of the cross-correlation function in terms of the complex cross-correlation coefficient ρ_{ij}, the standard deviations σ_{ii} and σ_{jj} of the channel i and j processes, respectively, and the one-lag temporal cross-correlation parameter, λ_{ij}. For the autocorrelation function (i=j), we have $|\rho_{ii}| = 1$ since any given channel process is totally correlated with itself at zero lag. Also, $\theta_{ii}(0) = 0$ since $\theta_{ii}(l)$ is an odd function of l. Since the function $f(\bullet)$ for the autocorrelation function has a peak value of unity at l=0 and noting that $l_{ii} = 0$, eq(2.21b) for i=j reduces to

$$R_{ii}(l) = \sigma_{ii}^{2} f(\lambda_{ii}, l) \exp\{j\theta_{ii}(l)\} \qquad (2.24)$$

where λ_{ii} is the one-lag temporal autocorrelation parameter and is a measure of the correlation magnitude between consecutive samples such that $0 \leq \lambda_{ii} \leq 1$. At lag value l=0, eq.(2.24) becomes $R_{ii}(0) = \sigma_{ii}^{2}$ which is, as expected, the variance of the zero mean, channel i process.

EXAMPLE Gaussian Shaped Correlation Functions

In [2], the special cases of Gaussian, exponential and sinc shaped correlation functions are considered using the forms given in eqs(2.21b) and (2.24). For cross-correlation functions with Gaussian shaped magnitudes, for example, we use

$$f(\lambda_{ij}, l - l_{ij}) = (\lambda_{ij})^{(l-l_{ij})^2} \tag{2.25}$$

so that eq(2.21b) becomes

$$R_{ij}(l) = \frac{|\rho_{ij}|\sigma_{ii}\sigma_{jj}(\lambda_{ij})^{(l-l_{ij})^2}}{(\lambda_{ij})^{l^2_{ij}}}\exp\{j\theta_{ij}(l)\} \tag{2.26}$$

For the autocorrelation function (i=j) with Gaussian shaped magnitudes, we have (dropping the subscript i for notational convenience)

$$R(l) = \sigma^2 f(\lambda,l)\exp[j\theta(l)] = \sigma^2 (\lambda)^{l^2} \exp[j\theta(l)] \tag{2.27}$$

where

$$f(\lambda,l) = (\lambda)^{l^2} = \exp[- 2\pi^2\mu^2T^2l^2] \tag{2.28a}$$

and

$$\lambda = \exp[-2\pi^2\mu^2T^2] \tag{2.28b}$$

is a real constant such that $0 \le \lambda \le 1$ and T is the sample period. In ref [2], we show that μ^2 is the variance (which determines the width) of the corresponding Gaussian shaped spectra.

EXAMPLE Exponentially Shaped Correlation Functions

For the exponentially shaped cross-channel correlation function, we use the expression

9

$$R_{ij}(l) = \frac{|\rho_{ij}|\sigma_{ii}\sigma_{jj}(\lambda_{ij})^{|l-l_{ij}|}}{(\lambda_{ij})^{|l_{ij}|}}\exp\{j\theta_{g_{ij}}(l)\} \qquad (2.29)$$

while the autocorrelation function becomes

$$R_{ii}(k) = \sigma_{ii}^2 (\lambda_{ii})^{|k|} \exp[j\theta_{ii}(l)]. \qquad (2.30)$$

In the above discussion, we have proposed the use of functional forms to characterize the magnitude and phase of the correlation functions. The motivation for this approach is that it will allow for flexibility in modeling random processes with various correlation and spectral shape. We note, however that at this point we have not constrained these functions to meet all the criteria that are necessary and sufficient to characterize correlation functions. In fact, determining all of these conditions in a general formulation is a difficult task. In [2], we note several constraints for the correlation functions including the important condition of positive semi-definiteness of the correlation matrix.

3.0 VARIANCE OF THE TIME-AVERAGED CORRELATION FUNCTIONS

3.1 VARIANCE OF THE AUTOCORRELATION FUNCTION ESTIMATOR

The ensemble correlation function is defined as the expectation of lagged products of a given stationary process when averaged over an ensemble of realizations. If this function is equal to the time-averaged correlation function obtained from a single realization, the process is called auto- or cross-correlation ergodic. Consider the time-averaged estimate of the <u>biased</u>[†] correlation function using N_T observation time samples

$$\hat{R}_{ijT_b}(l,N_T) = \begin{cases} \dfrac{1}{N_T} \displaystyle\sum_{n=0}^{N_T-l-1} x_i(n)x_j^*(n-l) & 0 \le l \le N_T-1 \\[3em] \dfrac{1}{N_T} \displaystyle\sum_{n=0}^{N_T-|l|-1} x_i^*(n)x_j(n-|l|) & -(N_T-1) \le l \le 0. \end{cases} \tag{3.1}$$

The variance of the autocorrelation (j=i) estimator $\hat{R}_{iiT_b}(l,N_T)$ is expressed as

$$V_{B_{ii}}(l,N_T) =$$

$$= E\left\{ [\hat{R}_{iiT_b}(l,N_T) - E[\hat{R}_{iiT_b}(l,N_T)]][\hat{R}_{iiT_b}^*(l,N_T) - E[\hat{R}_{iiT_b}^*(l,N_T)] \right\} \tag{3.2a}$$

$$= E[\hat{R}_{iiT_b}(l,N_T)\hat{R}_{iiT_b}^*(l,N_T)] - E[\hat{R}_{iiT_b}(l,N_T)]E[\hat{R}_{iiT_b}^*(l,N_T)]. \tag{3.2b}$$

We now consider each term within the expectation operations expressed in eq(3.2b). Using eq(3.1) in the first term on the RHS of eq(3.2b), we have for positive and negative l

$$\hat{R}_{iiT_b}(l,N_T)\hat{R}_{iiT_b}^*(l,N_T) = \frac{1}{N_T^2} \sum_{n=0}^{N_T-l-1} \sum_{p=0}^{N_T-l-1} x_i(n)x_i^*(n-l)x_i^*(p)x_i(p-l)$$

[†] In this paper, we consider the biased estimator for the correlation functions since it ensures positive semi-definiteness. In [2], the unbiased estimator is presented as well as an estimator with unlimited data.

$$0 \leq l \leq N_T - 1 \qquad (3.3a)$$

$$= \frac{1}{N_T^2} \sum_{n=0}^{N_T-|l|-1} \sum_{p=0}^{N_T-|l|-1} x_i^*(n)x_i(n-|l|)x_i(p)x_i^*(p-|l|)$$

$$-(N_T-1) \leq l \leq 0 \qquad (3.3b)$$

so that

$$E[\hat{R}_{iiT_b}(l,N_T)\hat{R}_{iiT_b}^*(l,N_T)] = \frac{1}{N_T^2} \sum_{n=0}^{N_T-l-1} \sum_{p=0}^{N_T-l-1} E[x_i(n)x_i^*(n-l)x_i^*(p)x_i(p-l)]$$

$$0 \leq l \leq N_T - 1 \qquad (3.4a)$$

$$= \frac{1}{N_T^2} \sum_{n=0}^{N_T-|l|-1} \sum_{p=0}^{N_T-|l|-1} E[x_i^*(n)x_i(n-|l|)x_i(p)x_i^*(p-|l|)]$$

$$-(N_T-1) \leq l \leq 0 \qquad (3.4b)$$

For the second term in eq(3.2b), eqs.(3.1) enable us to obtain

$$E[\hat{R}_{iiT_b}(l,N_T)] = \frac{1}{N_T} \sum_{n=0}^{N_T-l-1} R_{ii}(l) \qquad 0 \leq l \leq N_T - 1 \qquad (3.5a)$$

$$= \frac{1}{N_T} \sum_{n=0}^{N_T-|l|-1} R_{ii}^*(l) \qquad -(N_T-1) \leq l \leq 0. \qquad (3.5b)$$

so that

$$E[\hat{R}_{iiT_b}(l,N_T)]E[\hat{R}_{iiT_b}^*(l,N_T)] =$$

$$= \frac{1}{N_T^2} \sum_{n=0}^{N_T-l-1} \sum_{p=0}^{N_T-l-1} |R_{ii}(l)|^2 \qquad 0 \leq l \leq N_T \qquad (3.6a)$$

$$= \frac{1}{N_T^2} \sum_{n=0}^{N_T-|l|-1} \sum_{p=0}^{N_T-|l|-1} |R_{ii}(l)|^2 \qquad -(N_T-1) \leq l \leq 0. \qquad (3.6b)$$

Using eqs(3.4) and (3.6) in the expression

$$V_{B_{ii}}(l,N_T) = E[\hat{R}_{iiT_b}(l,N_T)\hat{R}_{iiT_b}^*(l,N_T)] - E[\hat{R}_{iiT_b}(l,N_T)]E[\hat{R}_{iiT_b}^*(l,N_T)] \qquad (3.7)$$

12

we obtain

$$V_{B_{ii}}(l,N_T) = \frac{1}{N_T^2} \sum_{n=0}^{N_T-l-1} \sum_{p=0}^{N_T-l-1} \left\{ E[x_i(n)x_i^*(n-l)x_i^*(p)x_i(p-l)] - |R_{ii}(l)|^2 \right\}$$

$$\text{for} \quad 0 \le l \le N_T - 1 \tag{3.8a}$$

$$= \frac{1}{N_T^2} \sum_{n=0}^{N_T-|l|-1} \sum_{p=0}^{N_T-|l|-1} \left\{ E[x_i^*(n)x_i(n-|l|)x_i(p)x_i^*(p-|l|)] - |R_{ii}(l)|^2 \right\}$$

$$\text{for} \quad -(N_T-1) \le l \le 0. \tag{3.8b}$$

We now define

$$\phi(n,l) = x_i(n)x_i^*(n - l) \tag{3.9a}$$

and

$$R_{\phi\phi}(k,l) = E[\phi(n,l)\phi^*(n - k,l)] \tag{3.9b}$$

so that, assuming stationarity, the covariance of $\phi(n,l)$ *can be expressed as*

$$C_{\phi\phi}(k,l) = E\left[\left\{ \phi(n,l) - E[\phi(n,l)] \right\} \left\{ \phi^*(n-k,l) - E[\phi^*(n-k,l)] \right\} \right] \tag{3.10a}$$

$$= R_{\phi\phi}(k,l) - E[\phi(n,l)]E[\phi^*(n-k,l)]. \tag{3.10b}$$

Also, from eq(3.9a)

$$E[\phi(n,l)] = R_{ii}(l) \tag{3.11a}$$

and

$$E[\phi^*(n-k,l)] = R_{ii}^*(l) \tag{3.11b}$$

so that (3.10b) becomes

$$C_{\phi\phi}(k,l) = R_{\phi\phi}(k,l) - |R_{ii}(l)|^2 \tag{3.12a}$$

$$= E[x_i(n)x_i^*(n - l)x_i^*(n - k)x_i(n - l - k)] - |R_{ii}(l)|^2. \tag{3.12b}$$

Using eq(3.12b) in (3.8)

$$V_{B_{ii}}(l, N_T) = \frac{1}{N_T^2} \sum_{n=0}^{N_T-l-1} \sum_{p=0}^{N_T-l-1} C_{\phi\phi}(n-p, l) \qquad 0 \le l \le N_T - 1 \qquad (3.13a)$$

$$= \frac{1}{N_T^2} \sum_{n=0}^{N_T-|l|-1} \sum_{p=0}^{N_T-|l|-1} C_{\phi\phi}^*(n-p, |l|) \qquad -(N_T-1) \le l \le 0. \qquad (3.13b)$$

Using $k = n - p$ where

$$-(N_T - l - 1) \le k \le N_T - l - 1 \qquad \text{for} \qquad 0 \le l \le N_T - 1 \qquad (3.14a)$$

$$-(N_T - |l| - 1) \le k \le N_T - |l| - 1 \qquad \text{for} \qquad -(N_T-1) \le l \le 0. \qquad (3.14b)$$

We also note that eq(3.14b) holds for all l so that

$$V_{B_{ii}}(l, N_T) = \frac{1}{N_T^2} \sum_{k=-(N_T-l-1)}^{N_T-l-1} [N_T - |l| - |k|] \, C_{\phi\phi}(k, l) \qquad 0 \le l \le N_T - 1 \qquad (3.15a)$$

$$= \frac{1}{N_T^2} \sum_{k=-(N_T-|l|-1)}^{N_T-|l|-1} [N_T - |l| - |k|] \, C_{\phi\phi}^*(k, |l|) \qquad -(N_T-1) \le l \le 0. \qquad (3.15b)$$

However, for negative lag l, we have

$$C_{\phi\phi}^*(k, |l|) = C_{\phi\phi}(k, l) \qquad (3.16)$$

and eqs(3.15) can be written as

$$V_{B_{ii}}(l, N_T) = \frac{1}{N_T} \sum_{k=-(N_T-|l|-1)}^{N_T-|l|-1} \left[1 - \frac{|l| + |k|}{N_T} \right] C_{\phi\phi}(k, l) \qquad (3.17)$$

for both positive and negative values of l. For processes with zero-mean, jointly stationary Gaussian quadrature components, the imaginary terms in $C_{\phi\phi}(k, l)$

cancel when summed over positive and negative values of k (Appendix A) so that

$$V_{B_{ii}}(l,N_T) = \frac{1}{N_T} \sum_{k=-(N_T-|l|-1)}^{N_T-|l|-1} \left[1 - \frac{|l|+|k|}{N_T} \right] Re\{C_{\phi\phi}(k,l)\}. \qquad (3.18a)$$

$$= \frac{1}{N_T} \sum_{k=-(N_T-|l|-1)}^{N_T-|l|-1} \left[1 - \frac{|l|+|k|}{N_T} \right] \left[|R_{ii}(k)|^2 + Re\{F_{ii}(l,k)\} \right] \qquad (3.18b)$$

where

$$R_{ii}(k) = E[x_i(n)x_i^*(n - k)] \qquad (3.19)$$

and

$$F_{ii}(l,k) = E[x_i(n)x_i(n - l - k)]E[x_i^*(n - l)x_i^*(n - k)]. \qquad (3.20)$$

Using eq(A.6b) in Appendix A, it can be shown that in the special case where the quadrature components maintain the relations

$$R_{ii}^{II}(l) = R_{ii}^{QQ}(l) \qquad (3.21a)$$

and

$$R_{ii}^{IQ}(l) = - R_{ii}^{QI}(l) \qquad (3.21b)$$

then

$$Re\{F_{ii}(l,k)\} = 0 \qquad \text{for all } l,k. \qquad (3.22)$$

We note that eqs.(21) hold for the special case of wide-sense stationarity of the narrowband bandpass processes [2]. In this case, eq(3.18b) becomes

$$V_{B_{ii}}(l,N_T) = \frac{1}{N_T} \sum_{k=-(N_T-|l|-1)}^{N_T-|l|-1} \left[1 - \frac{|l|+|k|}{N_T} \right] |R_{ii}(k)|^2. \qquad (3.23)$$

3.2 VARIANCE OF THE CROSS-CORRELATION FUNCTION ESTIMATOR

Analogous to the derivation leading to eq(3.18b), the variance of the biased, time-averaged cross-correlation function estimator for processes described by the general Gaussian case noted in section 3.1 has been shown [2] to be

15

$$V_{B_{ij}}(l,N_T) = \frac{1}{N_T} \sum_{k=-(N_T-|l|-1)}^{N_T-|l|-1} \left[1 - \frac{|l|+|k|}{N_T} \right] Re\left[R_{ii}(k)R_{jj}^*(k) + F_{ij}(l,k) \right] \qquad (3.24)$$

where

$$F_{ij}(l,k) = E[x_i(n)x_j(n-l-k)]E[x_i^*(n-l)x_j^*(n-k)]. \qquad (3.25)$$

We note that the term $Re[F_{ij}(l,k)]$ will contribute a dependence of $V_{B_{ij}}(l,N)$ upon cross-correlation terms such as the cross-correlation parameter $|\rho_{ij}|$ defined in section 2.4 and [1,2]. In [2], we show that for joint wide-sense stationarity of narrowband multichannel bandpass processes,

$$R_{ij}^{II}(l) = R_{ij}^{QQ}(l) \qquad (3.26a)$$

and

$$R_{ij}^{IQ}(l) = - R_{ij}^{QI}(l) \qquad (3.26b)$$

which leads to $F_{ij}(l,k)=0$. Under these conditions, eq(3.24) reduces to

$$V_{B_{ij}}(l,N_T) = \frac{1}{N_T} \sum_{k=-(N_T-|l|-1)}^{N_T-|l|-1} \left[1 - \frac{|l|+|k|}{N_T} \right] Re\left[R_{ii}(k)R_{jj}^*(k) \right]. \qquad (3.27)$$

Thus, for joint wide-sense stationarity of the narrowband multichannel bandpass processes, the variance of the cross-channel correlation function estimator is independent of the cross-channel correlation. This result is verified via simulated results in sections 5.2 and 5.4.

3.3 SAMPLE VARIANCE OF THE CORRELATION FUNCTION

Consider N_R realizations of the random process $x_i(n)$. Let each realization be indexed by the integer α; $\alpha=1,2,...,N_R$. Corresponding to the realization with index α, let $\hat{R}_{ijT_b}(l,N_T|\alpha)$ be the biased, time-averaged cross-correlation function estimate using N_T observation samples. The sample variance of the time-averaged

cross-correlation function estimate is computed from N_R statistically independent realizations using the expression

$$\text{Var}[\hat{R}_{ijT_b}(l,N_T):N_R] = \frac{1}{N_R-1} \sum_{\alpha=1}^{N_R} |\hat{R}_{ijT_b}(l,N_T|\alpha) - \bar{\hat{R}}_{ijT_b}(l,N_R|\alpha)|^2 \tag{3.28}$$

where

$$\bar{\hat{R}}_{ijT_b}(l,N_R|\alpha) = \frac{1}{N_R} \sum_{\alpha=1}^{N_R} \hat{R}_{ijT_b}(l,N_T|\alpha). \tag{3.29}$$

The autocorrelation function is obtained for i=j. Eq.(3.28) is used to compute the variance of the time-averaged auto- and cross-correlation function estimators in chapter 5 for comparison with eqs(3.23) and (3.27), respectively.

3.4 ERGODICITY CONSIDERATIONS

In section 2.4 and [1,2], we presented functional forms for the auto- and cross-correlation functions to obtain desired temporal and cross-channel correlation of the processes to be synthesized. Using eq(2.30) in eqs(3.23) and (3.27), we obtain [2], respectively

$$V_{B_{ii}}(l,N_T) = \frac{1}{N_T} \sum_{k=-(N_T-|l|-1)}^{N_T-|l|-1} \left[1 - \frac{|l|+|k|}{N_T} \right] \sigma_{ii}^4 \, (\lambda_{ii})^{2|k|} \tag{3.30}$$

and

$$V_{B_{ij}}(l,N_T) = \frac{1}{N_T} \sum_{k=-(N_T-|l|-1)}^{N_T-|l|-1} \left[1 - \frac{|l|+|k|}{N_T} \right] \sigma_{11}^2 \, (\lambda_{11})^{|k|} \sigma_{22}^2 \, (\lambda_{22})^{|k|} \cdot$$

$$\cos[\theta_{ii}(l) - \theta_{jj}(l)]. \tag{3.31}$$

When invoking the ergodic assumption, one would like the variances of the estimators expressed by eqs.(3.30) and (3.31) to be suitably small so that the time-averaged correlation function is a satisfactory approximation to the ensemble correlation function. For a given λ_{ii} and σ_{ii}^2, these analytic expressions provide a means for determining the required N_T to minimize the variance to a specified level. A unique aspect of this development is the determination of these expressions in terms of both the observation window size N_T, the process parameters σ_{ii}^2 and λ_{ii} and, for $V_{B_{ij}}(l,N_T)$, the phase angles $\theta_{ii}(l)$ and $\theta_{jj}(l)$. These expressions indicate that for $\lambda_{ii}<1$, their limit approaches zero as N_T approaches infinity. Thus, for stationary processes, ergodicity holds in all cases except for total temporal correlation (ie., $\lambda_{ii}=1$). In this case, $V_{B_{ii}}(l,N_T)=\sigma_{ii}^4$; ie., the square of the process variance. Furthermore, as σ_{ii}^2 and λ_{ii} change, eqs(3.30) and (3.31) provide a quantitative measure expressing the requirements on the observation window size to obtain time-averaged correlation function estimates which yield a close approximation to the ensemble averaged correlation functions.

Figure 1 is a plot of the error variance $V_{B_{ii}}(l,N_T)$ for the biased, time-averaged autocorrelation function estimator versus the number of time samples N_T used in the estimate. Each curve is plotted for a specific value of the temporal

18

correlation parameter λ_{ii} while σ_{ii}^2 was fixed at a value of 4. As these curves reveal, the error variance decreases with increasing N_T, however, the rate of the decrease is highly dependent upon the temporal correlation of the processes; ie., for processes with low temporal correlation (λ_{ii} approaching zero), $V_{B_{ii}}(l,N_T)$ diminishes rapidly for increasing N_T. However, for processes with high temporal correlation (λ_{ii} approaching unity), $V_{B_{ii}}(l,N_T)$ decreases slowly. At $\lambda_{ii} = 1$, the process is no longer ergodic, so that the error variance no longer decreases as a function of N_T.
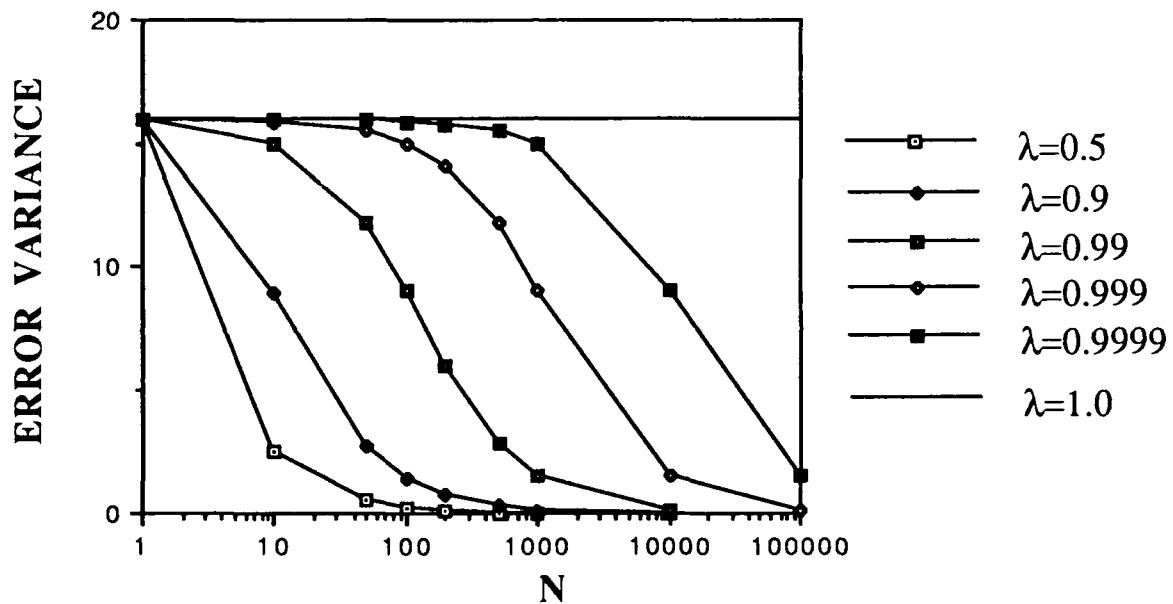
Figure 1 Variance $V_{B_{ii}}(l,N_T)$ at $l=0$ for the time-averaged autocorrelation function estimator as a function of N_T time samples with the one-lag temporal correlation λ_{ii} as a parameter and $\sigma_{ii}^2=4$.

19

3.5 THE NORMALIZED CORRELATION FUNCTION

The normalized time-averaged auto- and cross-correlation function estimators are briefly discribed in this section. They are defined, respectively, as

$$\hat{r}_{ii}(l,N_T) = \hat{R}_{ii}(l,N_T)/\hat{R}_{ii}(0,N_T) \tag{3.32}$$

and

$$\hat{r}_{ij}(l,N_T) = \hat{R}_{ij}(l,N_T)/\hat{R}_{ij}(0,N_T). \tag{3.33}$$

Specific forms of the estimators such as the biased correlation function estimator presented in eq(3.1) are used to evaluate the numerator and denominators of eqs.(3.32) and (3.33). The normalized forms differ significantly from the corresponding unnormalized form presented above in as much as the variance of the estimates have a significantly different dependence upon process correlation. We note that each estimator is expressed as a ratio of two random variables. Each of these random variables, however, is highly correlated; ie., they are each computed using the same observation data. As a result, the deviation of $\hat{R}_{ij}(l,N_T)$ about its mean level will be 'tracked' similarly by $\hat{R}_{ij}(0,N_T)$; ie., if $\hat{R}_{ij}(l,N_T)$ lies above (or below) its mean level, likewise, $\hat{R}_{ij}(0,N_T)$ will lie above (or below) its mean level. As a result, the normalized correlation function estimator will be closer to its respective mean and its associated variance is reduced. As noted above, its dependence upon process correlation will be quite unlike that of the ordinary correlation function estimators. In fact, it will be similar to that of the parameter estimators described later (see section 4.5).

The variances associated with the estimators described by eqs(3.32) and (3.33) are difficult to develop since they involve ratios of two correlated random variables. In [17], a taylor series expansion is used to derive approximate expressions for the variance of these estimators.

4.0 AUTOREGRESSIVE PROCESS PARAMETER ESTIMATORS

In this chapter, we describe the three parameter estimators used in this study; namely, the multichannel Strand-Nuttall estimator [11,12] and two versions of the Yule-Walker estimator [9,10]. In addition, we present a recursive method used to calculate the multichannel matrix coefficients known as the Levinson-Wiggins-Robinson method. The Burg estimator [13] and the multichannel Strand-Nuttall estimator are equivalent for the single channel case.

Expressions for the error variance of time-averaged parameter estimators are difficult to determine. However, the Cramer-Rao bound (CRB) provides a reference for the performance of the estimators. An analytic expression for the exact Cramer-Rao bound (CRB) of unbiased AR parameter estimates has been presented [6]. The expression was shown to converge to the asymptotic form of the CRB for large measurement time sample sizes. In chapter 5.0, we show simulated results for the error variances of the estimators and compare these results to the exact CRB as a function of the correlation of the processes.

4.1 THE YULE-WALKER ESTIMATOR

The Yule-Walker estimator used in this study initially uses estimates in the covariance matrix of eq.(2.14). The Yule-Walker equation is then solved to obtain the estimates of the parameters and the white driving noise covariance matrix. The two versions of the Yule-Walker estimators used in this study differ in that the estimates of the covariance matrix are obtained using either the biased or the unbiased covariance estimator. They are refered to here as the Yule-Walker with biased covariance (YWBC) estimator and the Yule-Walker with unbiased covariance (YWUBC) estimator, respectively. The biased covariance estimator is expressed in eq.(3.1). The corresponding unbiased estimator is obtained by replacing the denominator of eq.(3.1) by N_T-l. We point out, however, that although the covariance estimator may be unbiased, the corresponding Yule-Walker (YWUBC) estimator is not unbiased.

4.2 THE LEVINSON-WIGGINS-ROBINSON RECURSION

We now develop a recursive procedure to determine the multichannel forward and backward matrix coefficients. The procedure was initially presented

by Wiggins and Robinson [16] based on the scalar version of Levinson [14]. The approach presented in this subsection, however, is similar to that used by Strand [11]. Consider the pth order update of the multichannel forward PEF coefficient expressed in the form

$$
\underline{A}_p = \begin{bmatrix} A_p(0) \\ A_p(1) \\ A_p(2) \\ \vdots \\ A_p(p-1) \\ A_p(p) \end{bmatrix} = \begin{bmatrix} A_{p-1}(0) \\ A_{p-1}(1) \\ A_{p-1}(2) \\ \vdots \\ A_{p-1}(p-1) \\ [0] \end{bmatrix} + \begin{bmatrix} [0] \\ B_{p-1}(p-1) \\ \vdots \\ B_{p-1}(2) \\ B_{p-1}(1) \\ B_{p-1}(0) \end{bmatrix} [\Gamma_f]_p \qquad (4.1)
$$

where $[\Gamma_f]_p$ is a constant matrix called the forward reflection coefficient matrix and $A_p(0) = A_{p-1}(0) = B_{p-1}(0) = I$, the JxJ identity matrix. The update equation is therefore expressed as

$$
\begin{aligned}
A_p(k) &= A_{p-1}(k) + B_{p-1}(p-k)[\Gamma_f]_p & k&=1,2,\dots,p-1 & (4.2a) \\
&= [\Gamma_f]_p & k&=p & (4.2b) \\
&= [0] & k&>p & (4.2c) \\
&= A_p(0) = I & k&=0. & (4.2d)
\end{aligned}
$$

Consider the order update of the backward PEF coefficient as

$$
\underline{B}_p = \begin{bmatrix} B_p(p) \\ B_p(p-1) \\ \vdots \\ B_p(1) \\ B_p(0) \end{bmatrix} = \begin{bmatrix} [0] \\ B_{p-1}(p-1) \\ \vdots \\ B_{p-1}(1) \\ B_{p-1}(0) \end{bmatrix} + \begin{bmatrix} A_{p-1}(0) \\ A_{p-1}(1) \\ \vdots \\ A_{p-1}(p-1) \\ [0] \end{bmatrix} [\Gamma_b]_p \qquad (4.3)
$$

where $[\Gamma_b]_p$ is the backward reflection coefficient matrix. The update equation is expressed as

$$
B_p(k) = B_{p-1}(k) + A_{p-1}(p-k)[\Gamma_b]_p \qquad k=1,2,\dots,p-1 \qquad (4.4a)
$$

$$= [\Gamma_b]_p \qquad\qquad k=p \qquad\qquad (4.4b)$$

$$= [0] \qquad\qquad k>p \qquad\qquad (4.4c)$$

$$= B_p(0) = I \qquad\qquad k=0. \qquad\qquad (4.4d)$$

We now determine the conditions under which the above equations hold. First, we take the Hermitian transpose of eq(4.1) and postmultiply both sides of the equation by $[\tilde{R}_{\underline{xx}}]_{p+1}$. For the LHS, the normal equations provide

$$\underline{A}_p^H [\tilde{R}_{\underline{xx}}]_{p+1} = \{ [\Sigma_f]_p^H [0] \ ... \ [0] \} \qquad\qquad (4.5a)$$

where $[\Sigma_f]_p^H$ is the JxJ forward error covariance matrix for a pth order filter. Each side of eq(4.5a) is a vector of matrices containing p+1 matrix elements. Taking the Hermitian transpose of $\underline{A}_p$ in eq(4.1) and using it in (4.5a), we also have

$$\underline{A}_p^H [\tilde{R}_{\underline{xx}}]_{p+1} = \{ \underline{A}_{p-1}^H [0] \} [\tilde{R}_{\underline{xx}}]_{p+1} + [\Gamma_f]_p^H \{ [0] \ \underline{B}_{p-1}^H \} [\tilde{R}_{\underline{xx}}]_{p+1} \qquad (4.5b)$$

so that

$$\{ [\Sigma_f]_p^H [0] \ ... \ [0] \} = \{ \underline{A}_{p-1}^H [0] \} [\tilde{R}_{\underline{xx}}]_{p+1} + [\Gamma_f]_p^H \{ [0] \ \underline{B}_{p-1}^H \} [\tilde{R}_{\underline{xx}}]_{p+1}. \qquad (4.5c)$$

Let us now introduce a partitioned form of $[\tilde{R}_{\underline{xx}}]_{p+1}$ such that

$$[\tilde{R}_{\underline{xx}}]_{p+1} = \begin{bmatrix} R_{xx}(0) & R_{xx}(1) & R_{xx}(2) & ... & R_{xx}(p) \\ R_{xx}(-1) & R_{xx}(0) & R_{xx}(1) & ...R_{xx}(p-1) \\ \vdots & \vdots & \vdots & \vdots & \vdots \\ R_{xx}(1-p) & R_{xx}(2-p) & R_{xx}(3-p) & ... & R_{xx}(1) \\ R_{xx}(-p) & R_{xx}(1-p) & R_{xx}(2-p) & ... & R_{xx}(0) \end{bmatrix} = \begin{bmatrix} [\tilde{R}_{\underline{xx}}]_p & (\underline{S}_{xx})_p \\ (\underline{S}_{xx})_p^H & [R_{xx}(0)] \end{bmatrix} \qquad (4.6)$$

where $(\underline{S}_{xx})_p$ is a vector containing p matrix elements and is defined as

$$(\underline{S}_{xx})_p^H = [R_{xx}(-p),R_{xx}(1-p),...,R_{xx}(-1)]. \qquad\qquad (4.7)$$

We now consider

$$\{\underline{A}_{p-1}^{H} \ [0]\} \ [\tilde{R}_{\underline{xx}}]_{p+1} = \{\underline{A}_{p-1}^{H} \ [0]\} \begin{bmatrix} [\tilde{R}_{\underline{xx}}]_p & (\underline{S}_{xx})_p \\ (\underline{S}_{xx})_p^{H} & [R_{xx}(0)] \end{bmatrix} \qquad (4.8a)$$

$$= \{\underline{A}_{p-1}^{H}[\tilde{R}_{\underline{xx}}]_p \quad \underline{A}_{p-1}^{H}(\underline{S}_{xx})_p\}. \qquad (4.8b)$$

However, we can reduce the order of eq(4.5a) by one and obtain the Hermitian transposed vector which will now contain p matrix elements, so that

$$\underline{A}_{p-1}^{H}[\tilde{R}_{\underline{xx}}]_p = \{[\Sigma_f]_{p-1}^{H} \ [0] \ ... \ [0]\}. \qquad (4.9)$$

Let us now define

$$[\Delta]_p^{H} \equiv \underline{A}_{p-1}^{H}(\underline{S}_{xx})_p = \{I \ A_{p-1}^{H}(1) \ A_{p-1}^{H}(2) \ ... \ A_{p-1}^{H}(p-1)\} \begin{bmatrix} R_{xx}(p) \\ R_{xx}(p-1) \\ \vdots \\ R_{xx}(1) \end{bmatrix} \qquad (4.10a)$$

$$= R_{xx}(p) + \sum_{k=1}^{p-1} A_{p-1}^{H}(k)R_{xx}(p-k). \qquad (4.10b)$$

Substituting eqs(4.9) and (4.10a) in (4.8b), we have

$$\{\underline{A}_{p-1}^{H} \ [0]\} \ [\tilde{R}_{\underline{xx}}]_{p+1} = \{[\Sigma_f]_{p-1}^{H} \ [0] \ ... \ [0] \ [\Delta]_p^{H}\}. \qquad (4.11)$$

We will utilize this expression later. We now repartitioned $[\tilde{R}_{xx}]_{p+1}$ into the form given by

$$[\tilde{R}_{\underline{xx}}]_{p+1} = \begin{bmatrix} R_{xx}(0) & R_{xx}(1) & R_{xx}(2) & ... & R_{xx}(p) \\ R_{xx}(-1) & R_{xx}(0) & R_{xx}(1) & ...R_{xx}(p-1) \\ \vdots & \vdots & \vdots & \vdots & \vdots \\ R_{xx}(1-p) & R_{xx}(2-p) & R_{xx}(3-p)... & R_{xx}(1) \\ R_{xx}(-p) & R_{xx}(1-p) & R_{xx}(2-p)... & R_{xx}(0) \end{bmatrix} = \begin{bmatrix} R_{xx}(0) & (\underline{R}_{xx})_p^{H} \\ (\underline{R}_{xx})_p & [\tilde{R}_{\underline{xx}}]_p \end{bmatrix} \qquad (4.12)$$

where

$$(\underline{R}_{xx})_p^{H} = [R_{xx}(1) \ R_{xx}(2) \ ... \ R_{xx}(p)]. \qquad (4.13)$$

We now consider

24

$$\{[0] \quad \underline{B}_{p-1}^H\}[\tilde{R}_{\underline{xx}}]_{p+1} = \{[0] \quad \underline{B}_{p-1}^H\} \begin{bmatrix} R_{xx}(0) \, (\underline{R}_{xx})_p^H \\ (\underline{R}_{xx})_p \, [\tilde{R}_{\underline{xx}}]_p \end{bmatrix} \qquad (4.14a)$$

$$= \{\underline{B}_{p-1}^H(\underline{R}_{xx})_p \quad \underline{B}_{p-1}^H[\tilde{R}_{\underline{xx}}]_p\}. \qquad (4.14b)$$

However, from the backward multichannel normal equations, we have

$$\underline{B}_{p-1}^H[\tilde{R}_{\underline{xx}}]_p = \{[0] \, ... \, [0] \, [\Sigma_b]_{p-1}^H\}. \qquad (4.15)$$

Let us now define

$$[\Delta']_p^H \equiv \underline{B}_{p-1}^H \, (\underline{R}_{xx})_p \qquad (4.16a)$$

$$= \{B_{p-1}^H(p-1) \, B_{p-1}^H(p-2) \, ... \, B_{p-1}^H(1) \, I\} \begin{bmatrix} R_{xx}(-1) \\ R_{xx}(-2) \\ \vdots \\ R_{xx}(-p) \end{bmatrix} \qquad (4.16b)$$

$$= R_{xx}(-p) + \sum_{k=1}^{p-1} B_{p-1}^H(k)R_{xx}(k-p). \qquad (4.16c)$$

Substituting eqs(4.15) and (4.16a) into (4.14b), yields

$$\{[0] \quad \underline{B}_{p-1}^H\}[\tilde{R}_{\underline{xx}}]_{p+1} = \{[\Delta']_p^H \, [0] \, ... \, [0] \, [\Sigma_b]_{p-1}^H\}. \qquad (4.17)$$

Using eqs(4.11) and (4.17) in (4.5c), we obtain

$$\{[\Sigma_f]_p^H \, [0] \, ... \, [0]\} = \{[\Sigma_f]_{p-1}^H \, [0] \, ... \, [0] \, [\Delta]_p^H\}$$
$$+ [\Gamma_f]_p^H \, \{[\Delta']_p^H \, [0] \, ... \, [0] \, [\Sigma_b]_{p-1}^H\}. \qquad (4.18)$$

And so, in order for eq(4.1) to hold, we must satisfy eq(4.18). From eq(4.18), we have

$$[\Sigma_f]_p^H = [\Sigma_f]_{p-1}^H + [\Gamma_f]_p^H \, [\Delta']_p^H \qquad (4.19)$$

and

$$[0] = [\Delta]_p^H + [\Gamma_f]_p^H \, [\Sigma_b]_{p-1}^H. \qquad (4.20)$$

From eqs(4.20) and (4.2b), we have

$$[\Gamma_f]_p^H = A_p^H(p) = - [\Delta]_p^H \left\{ [\Sigma_b]_{p-1}^H \right\}^{-1}.$$ (4.21)

We must now return to eq(4.3) and carry out a similar procedure that was carried out for eq(4.1); ie., we post-multiply $\underline{B}_p^H$ by $[\tilde{R}_{xx}]_{p+1}$ so that

$$\underline{B}_p^H [\tilde{R}_{xx}]_{p+1} = \left\{ [0] \ldots [0] [\Sigma_b]_p^H \right\}.$$ (4.22)

For the first term on the RHS of eq(4.3), we postmultiply by the partitioned form of eq(4.12). In this case, we obtain the same results as expressed in eqs(4.14a) through (4.17). For the second term on the RHS, we postmultiply by the partitioned form of eq(4.6) so that we obtain the same results as expressed in eqs(4.8) through (4.11). Substituting these results into eq(4.22), we have

$$\left\{ [0] \ldots [0] \ [\Sigma_b]_p^H \right\} = \left\{ [\Delta']_p^H \ [0] \ldots [0] \ [\Sigma_b]_{p-1}^H \right\}$$

$$+ \ [\Gamma_b]_p^H \left\{ [\Sigma_f]_{p-1}^H \ [0] \ldots [0] \ [\Delta]_p^H \right\}. \tag{4.23}$$

Eq(4.23) must therefore be maintained in order for the recursion in eq(4.3) to hold. From the above equation, we have

$$[\Sigma_b]_p^H = [\Sigma_b]_{p-1}^H + \ [\Gamma_b]_p^H \ [\Delta]_p^H \tag{4.24}$$

$$[0] = [\Delta']_p^H + \ [\Gamma_b]_p^H \ [\Sigma_f]_{p-1}^H. \tag{4.25}$$

From eqs(4.25) and (4.4b), we have

$$[\Gamma_b]_p^H = B_p^H(p) = - \ [\Delta']_p^H \left\{ [\Sigma_f]_{p-1}^H \right\}^{-1}. \tag{4.26}$$

Before summarizing the pertinent recursion equations used to estimate the forward and backward coefficient matrices, we can at this point develop several important relationships. Using equations (4.21) and (4.25) in (4.19), we obtain

$$[\Sigma_f]_p^H = [\Sigma_f]_{p-1}^H + \ [\Gamma_f]_p^H \ [\Delta']_p^H \tag{4.27a}$$

$$= [\Sigma_f]_{p-1}^H - A_p^H(p) \ [\Gamma_b]_p^H \ [\Sigma_f]_{p-1}^H. \tag{4.27b}$$

Using eq(4.26) in (4.27b), we have

$$[\Sigma_f]_p^H = [\Sigma_f]_{p-1}^H - A_p^H(p) \ B_p^H(p) \ [\Sigma_f]_{p-1}^H \tag{4.28a}$$

so that

$$[\Sigma_f]_p^H = \left\{ I - A_p^H(p) \ B_p^H(p) \right\} \ [\Sigma_f]_{p-1}^H. \tag{4.28b}$$

Similarly,

$$[\Sigma_b]_p^H = \left\{ I - B_p^H(p) A_p^H(p) \right\} \ [\Sigma_b]_{p-1}^H. \tag{4.29}$$

Let us also consider the matrix identity

$$\{ \underline{A}_{p-1}^H \ [0] \} \ [\tilde{R}_{xx}]_{p+1} \begin{bmatrix} [0] \\ \underline{B}_{p-1} \end{bmatrix} = \left[\{ [0] \ \ \underline{B}_{p-1}^H \} \ [\tilde{R}_{xx}]_{p+1} \begin{bmatrix} \underline{A}_{p-1} \\ [0] \end{bmatrix} \right]^H \tag{4.30}$$

which follows since $[\tilde{R}_{\underline{xx}}]_{p+1}= [\tilde{R}_{\underline{xx}}]_{p+1}^{H}$. Using eqs(4.11) and (4.17) in (4.30), we can write

$$\{[\Sigma_f]_{p-1}^{H} \ [0] \ ... \ [0] \ [\Delta]_p^{H}\} \begin{bmatrix} [0] \\ B_{p-1}(p-1) \\ \vdots \\ B_{p-1}(1) \\ I \end{bmatrix} =$$

$$= \begin{bmatrix} \{[\Delta']_p^{H} \ [0] \ ... \ [0] \ [\Sigma_b]_{p-1}^{H}\} \begin{bmatrix} I \\ A_{p-1}(1) \\ A_{p-1}(2) \\ \vdots \\ A_{p-1}(p-1) \\ [0] \end{bmatrix} \end{bmatrix}^{H} \qquad (4.31)$$

so that after carrying out the matrix multiplications in eq(4.31), we have

$$[\Delta]_p^{H} = [\Delta']_p. \qquad (4.32)$$

Eq(4.32) is useful since it reduces the computations involved in the determination of the reflection coefficient matrices; ie., eqs(4.21) and (4.26) can both be expressed in terms of $[\Delta]_p$, so that

$$[\Gamma_f]_p^{H} = A_p^{H}(p) = - [\Delta]_p^{H}\{[\Sigma_b]_{p-1}^{H}\}^{-1} \qquad (4.33a)$$

$$[\Gamma_b]_p^{H} = B_p^{H}(p) = - [\Delta]_p\{[\Sigma_f]_{p-1}^{H}\}^{-1}. \qquad (4.33b)$$

In the single channel case, the scalar forward and backward prediction error variances are equal. Since $[\Delta]_p$ is a scalar, it follows from eqs(4.33) that $a_p(p)=b_p^{*}(p)$.

We again note that the expressions developed here are in terms of the Hermitian operator as opposed to those often shown in the literature. This stems from the notation used to express the autoregressive equation in eq(2.1) and provides a more consistent notation as stated previously. We now summarize the

pertinent equations for the recursion to update the forward and backward PEF coefficients. First, we have the definitions

$$[\Delta]_p^H \equiv R_{xx}(p) + \sum_{k=1}^{p-1} A_{p-1}^H(k)R_{xx}(p-k) \qquad (4.34a)$$

$$[\Delta']_p^H \equiv R_{xx}(-p) + \sum_{k=1}^{p-1} B_{p-1}^H(k)R_{xx}(k-p). \qquad (4.34b)$$

However, as shown previously

$$[\Delta]_p^H = [\Delta']_p. \qquad (4.35)$$

Hence, we need use only one of the equations in eqs(4.34). Next, from eqs(4.33)

$$[\Gamma_f]_p^H = A_p^H(p) = - [\Delta]_p^H \left\{ [\Sigma_b]_{p-1}^H \right\}^{-1} \qquad (4.36a)$$

$$[\Gamma_b]_p^H = B_p^H(p) = - [\Delta]_p \left\{ [\Sigma_f]_{p-1}^H \right\}^{-1} \qquad (4.36b)$$

where

$$[\Sigma_f]_p^H = \left\{ I - A_p^H(p) \, B_p^H(p) \right\} [\Sigma_f]_{p-1}^H. \qquad (4.37a)$$

$$[\Sigma_b]_p^H = \left\{ I - B_p^H(p) A_p^H(p) \right\} [\Sigma_b]_{p-1}^H. \qquad (4.37b)$$

Then,

$$A_p^H(k) = \begin{cases} A_{p-1}^H(k) + [\Gamma_f]_p^H B_{p-1}^H(p-k) & k=1, 2, ..., p-1 \\ \\ [\Gamma_f]_p^H & k=p \end{cases} \qquad (4.38a)$$

$$B_p^H(k) = \begin{cases} B_{p-1}^H(k) + [\Gamma_b]_p^H A_{p-1}^H(p-k) & k=1, 2, ..., p-1 \\ \\ [\Gamma_b]_p^H & k=p. \end{cases} \qquad (4.38b)$$

We initiate the procedure using the initial conditions for eqs(4.37) as $[\Sigma_f]_0^H = [\Sigma_b]_0^H = R_{xx}(0)$ so that eqs(4.38) provide

$$A_1^H(1) = [\Gamma_f]_1^H = - [\Delta]_1^H \left\{ [\Sigma_b]_0^H \right\}^{-1} \qquad (4.39a)$$

$$= - R_{xx}(1) R_{xx}^{-1}(0) \qquad (4.39b)$$

and

$$B_1^H(1) = [\Gamma_b]_1^H = - [\Delta]_1 \left\{ [\Sigma_f]_0^H \right\}^{-1} \qquad (4.39c)$$

$$= - R_{xx}(-1)R_{xx}^{-1}(0). \tag{4.39d}$$

The procedure continues recursively until the desired order is reached.

4.3 THE STRAND-NUTTALL METHOD

The multichannel harmonic mean algorithm which is a generalization of the Burg method was proposed independently by Strand [11] and Nuttall [12]. In the single channel case, Burg [13] estimated the reflection coefficients directly from the data subject to the constraint of minimizing a performance index consisting of the mean-square values of the estimates of the forward and backward prediction errors. In this case, the scalar forward coefficients of linear prediction are the complex conjugates of the backward coefficients. In the multichannel case, however, the forward and backward reflection coefficient matrices are related by eqs(4.33a) and (4.33b), respectively. These equations indicate that the multichannel forward and backward reflection coefficient matrices have a more complicated relationship than in the scalar case. Specifically, they are related through the forward and backward error covariance matrices. Solving eqs(4.33) for $-[\Delta]_p^H$ and noting that the error covariance matrices are Hermitian, we have

$$-[\Delta]_p^H = A_p^H(p) \, [\Sigma_b]_{p-1}^H = [\Sigma_f]_{p-1}^H \, B_p(p). \tag{4.40}$$

From eq(4.38) at k=p, we have

$$- [\Delta]_p^H = [\Gamma_f]_p^H [\Sigma_b]_{p-1}^H = [\Sigma_f]_{p-1}^H [\Gamma_b]_p. \tag{4.41}$$

These equations show the relationship between the forward and backward reflection coefficients and error covariance matrices as well as the matrix $[\Delta]_p^H$. In the Strand-Nuttall algorithm, it is this latter matrix that we solve for. In eq(4.41), note that the error covariances can be obtained from stage p-1. Two additional well known relationships between the forward and backward error residuals can be expressed as [10,11]

$$\varepsilon_p(n) = \varepsilon_{p-1}(n) + A_p^H(p)\,\beta_{p-1}(n-1) \tag{4.42}$$

and

$$\beta_p(n) = \beta_{p-1}(n-1) + B_p^H(p)\,\varepsilon_{p-1}(n). \tag{4.43}$$

In this section, we will establish a performance function which depends upon estimates of the forward and backward error covariance matrices. This performance function will be minimized with respect to the matrix $[\Delta]_p^H$. In the multichannel case, the reflection coefficients are chosen such that eqs(4.41) through (4.43) are satisfied. These are the constraint equations under which $-[\Delta]_p$ will be selected to minimize the performance function. Using the notation of Nuttall [12], we consider the unbiased error residual matrices over the _available_ data for a filter of order p as

$$E_p \equiv \frac{1}{N-p} \sum_{k=p+1}^{N} \varepsilon_p(k)\varepsilon_p^H(k) = E_p^H \tag{4.44a}$$

$$F_p \equiv \frac{1}{N-p} \sum_{k=p+1}^{N} \beta_p(k)\beta_p^H(k) = F_p^H. \tag{4.44b}$$

Using eqs(4.42) and (4.43) in the above equations and expanding yields

$$E_p \equiv \frac{1}{N-p} \sum_{k=p+1}^{N} [\varepsilon_{p-1}(k)\varepsilon_{p-1}^H(k) + A_p^H(p)\beta_{p-1}(k-1)\varepsilon_{p-1}^H(k) +$$
$$\varepsilon_{p-1}(k)\beta_{p-1}^H(k-1)A_p(p) + A_p^H(p)\beta_{p-1}(k-1)\beta_{p-1}^H(k-1)A_p(p)] \tag{4.45a}$$

and

$$F_p \equiv \frac{1}{N-p} \sum_{k=p+1}^{N} [\beta_{p-1}(k-1)\beta_{p-1}^H(k-1) + B_p^H(p)\varepsilon_{p-1}(k)\beta_{p-1}^H(k-1) +$$
$$\beta_{p-1}(k-1)\varepsilon_{p-1}^H(k)B_p(p) + B_p^H(p)\varepsilon_{p-1}(k)\varepsilon_{p-1}^H(k)B_p(p)] \tag{4.45b}$$

so that

$$E_p = [\hat{R}_{ff}]_{p-1} + A_p^H(p)\,[\hat{R}_{fb}]_{p-1}^H + [\hat{R}_{fb}]_{p-1}A_p(p) + A_p^H(p)[\hat{R}_{bb}]_{p-1}A_p(p) \tag{4.46a}$$

$$F_p = [\hat{R}_{bb}]_{p-1} + B_p^H(p)\,[\hat{R}_{fb}]_{p-1} + [\hat{R}_{fb}]_{p-1}^H B_p(p) + B_p^H(p)[\hat{R}_{ff}]_{p-1}B_p(p) \tag{4.46b}$$

where the estimated time-averaged error covariance matrices are expressed as

$$[\hat{R}_{ff}]_{p-1} = \frac{1}{N-p} \sum_{k=p+1}^{N} \epsilon_{p-1}(k)\epsilon_{p-1}^{H}(k) \tag{4.47a}$$

$$[\hat{R}_{fb}]_{p-1} = \frac{1}{N-p} \sum_{k=p+1}^{N} \epsilon_{p-1}(k)\beta_{p-1}^{H}(k-1) \tag{4.47b}$$

$$[\hat{R}_{fb}]_{p-1}^{H} = \frac{1}{N-p} \sum_{k=p+1}^{N} \beta_{p-1}(k-1)\epsilon_{p-1}^{H}(k) \tag{4.47c}$$

$$[\hat{R}_{bb}]_{p-1} = \frac{1}{N-p} \sum_{k=p+1}^{N} \beta_{p-1}(k-1)\beta_{p-1}^{H}(k-1). \tag{4.47d}$$

In the Strand-Nuttall algorithm, we minimize the sum of the traces of the weighted error matrices

$$I_{sn}([\Delta]_p) = tr(\Lambda_{p-1}E_p) + tr(\Omega_{p-1}F_p) \tag{4.48a}$$

where Λ_{p-1} and Ω_{p-1} are Hermitian, positive definite matrices which weight the matrices E_p and F_p, respectively. These matrices provide arbitrary weights and their selection will be determined later. Eq(4.48a) is the performance function mentioned previously. In the single channel case, we can consider minimizing an index of performance $I_p(\Gamma_p)$ expressed here as the weighted sum of the mean-squared values of the forward and backward prediction errors $\epsilon_p(n)$ and $\beta_p(n)$, respectively; ie.,

$$I_p(\Gamma_p) = aE[|\epsilon_p(n)|^2] + (1-a)E[|\beta_p(n)|^2]. \tag{4.48b}$$

Burg considered the minimization of eq(4.48b) for the case where $a=1/2$. We will show that the minimization of eq(4.48a) as developed here, leads to a generalization of the results obtained by the minimization of eq(4.48b) with $a=1/2$. Using eq(4.40), let us define G_p^H such that

$$G_p^H \equiv - [\Delta]_p^H = A_p^H(p) [\Sigma_b]_{p-1}^H = [\Sigma_f]_{p-1}^H B_p(p). \tag{4.49}$$

Changing notation for the Hermitian error covariance matrices to a form similar to Nuttall's [10], let

$$U_{p-1} \equiv [\Sigma_f]_{p-1} \tag{4.50a}$$

$$V_{p-1} \equiv [\Sigma_b]_{p-1} \tag{4.50b}$$

so that

$$A_p^H(p) = G_p^H[V_{p-1}^{-1}]^H \tag{4.51a}$$

$$B_p^H(p) = G_p[U_{p-1}^{-1}]^H. \tag{4.51b}$$

Using the last two equations together with eqs(4.46), we can write

$$\Lambda_{p-1}E_p + \Omega_{p-1}F_p = \Lambda_{p-1}\left\{ [\hat{R}_{ff}]_{p-1} + G_p^H[V_{p-1}^{-1}]^H[\hat{R}_{fb}]_{p-1}^H + [\hat{R}_{fb}]_{p-1}[V_{p-1}^{-1}]G_p \right.$$
$$\left. + G_p^H[V_{p-1}^{-1}]^H[\hat{R}_{bb}]_{p-1}[V_{p-1}^{-1}]G_p \right\}$$
$$\Omega_{p-1}\left\{ [\hat{R}_{bb}]_{p-1} + G_p[U_{p-1}^{-1}]^H[\hat{R}_{fb}]_{p-1} + [\hat{R}_{fb}]_{p-1}^H[U_{p-1}^{-1}]G_p^H \right.$$
$$\left. + G_p[U_{p-1}^{-1}]^H[\hat{R}_{ff}]_{p-1}[U_{p-1}^{-1}]G_p^H \right\}. \tag{4.52}$$

Taking the trace of eq(4.52) and rearranging terms, we obtain

$$\text{tr}[\Lambda_{p-1}E_p + \Omega_{p-1}F_p] =$$

$$= \text{tr}\left\{ \Lambda_{p-1}[\hat{R}_{ff}]_{p-1} + \Omega_{p-1}[\hat{R}_{bb}]_{p-1} + \Lambda_{p-1}G_p^H[V_{p-1}^{-1}]^H[\hat{R}_{fb}]_{p-1}^H \right.$$
$$\left. + \Omega_{p-1}[\hat{R}_{fb}]_{p-1}^H[U_{p-1}^{-1}]G_p^H \right\}$$
$$+ \text{tr}\left\{ \left[\Lambda_{p-1}[\hat{R}_{fb}]_{p-1}[V_{p-1}^{-1}] + \Lambda_{p-1}G_p^H[V_{p-1}^{-1}]^H[\hat{R}_{bb}]_{p-1}[V_{p-1}^{-1}] \right]G_p \right.$$
$$\left. + \Omega_{p-1}G_p[U_{p-1}^{-1}]^H[\hat{R}_{fb}]_{p-1} + \Omega_{p-1}G_p[U_{p-1}^{-1}]^H[\hat{R}_{ff}]_{p-1}[U_{p-1}^{-1}]G_p^H \right\}. \tag{4.53}$$

We now consider the matrix relation

$$\text{tr}[KL] = \text{tr}[LK] \tag{4.54}$$

where K and L are conformable matrices. Noting that all the above matrices are JxJ, the last two terms in the second trace of eq(4.53) can be reexpressed (ie., with $K = \Omega_{p-1}G_p$ and L defined accordingly for each of these last two terms). G_p can then be factored out in the second trace term so that

$$\mathrm{tr}[\Lambda_{p-1}E_p + \Omega_{p-1}F_p] =$$

$$= \mathrm{tr}\Big\{ \Lambda_{p-1}[\hat{R}_{ff}]_{p-1} + \Omega_{p-1}[\hat{R}_{bb}]_{p-1} + \Lambda_{p-1}G_p^H[V_{p-1}^{-1}]^H[\hat{R}_{fb}]_{p-1}^H$$

$$+ \Omega_{p-1}[\hat{R}_{fb}]_{p-1}^H[U_{p-1}^{-1}]G_p^H\Big\}$$

$$+ \mathrm{tr}\Big\{ \Big[\Lambda_{p-1}[\hat{R}_{fb}]_{p-1}[V_{p-1}^{-1}] + \Lambda_{p-1}G_p^H[V_{p-1}^{-1}]^H[\hat{R}_{bb}]_{p-1}[V_{p-1}^{-1}]$$

$$+ [U_{p-1}^{-1}]^H[\hat{R}_{fb}]_{p-1}\Omega_{p-1} + [U_{p-1}^{-1}]^H[\hat{R}_{ff}]_{p-1}[U_{p-1}^{-1}]G_p^H)\Omega_{p-1}\Big]G_p\Big\}.$$

$$(4.55)$$

Nuttall now minimizes eq(4.55) by choice of G_p^H (in the Hermitian notation used here), subject to eqs(4.41) through (4.43). Eq(4.49) can then be used to solve for the coefficients $A_p^H(p)$ and $B_p^H(p)$ which achieve this minimization. Nuttall [10] points out that the above equation is minimized by setting the coefficient of G_p [contained in the large square brackets of the second trace term of eq(4.55)] equal to a null matrix [15]. Premultiplying this coefficient by $[\Lambda_{p-1}^{-1}]$ and post multiplying by $[\Omega_{p-1}^{-1}]$, we obtain

$$[\hat{R}_{fb}]_{p-1}[V_{p-1}^{-1}][\Omega_{p-1}^{-1}] + G_p^H[V_{p-1}^{-1}]^H[\hat{R}_{bb}]_{p-1}[V_{p-1}^{-1}]\Omega_{p-1}^{-1}$$

$$+ [\Lambda_{p-1}^{-1}][U_{p-1}^{-1}]^H[\hat{R}_{fb}]_{p-1} + \Lambda_{p-1}^{-1}[U_{p-1}^{-1}]^H[\hat{R}_{ff}]_{p-1}[U_{p-1}^{-1}]G_p^H = [0] \qquad (4.56a)$$

so that after rearranging terms

$$- G_p^H[V_{p-1}^{-1}]^H[\hat{R}_{bb}]_{p-1}[V_{p-1}^{-1}]\Omega_{p-1}^{-1} - \Lambda_{p-1}^{-1}[U_{p-1}^{-1}]^H[\hat{R}_{ff}]_{p-1}[U_{p-1}^{-1}]G_p^H =$$

$$= [\hat{R}_{fb}]_{p-1}[V_{p-1}^{-1}][\Omega_{p-1}^{-1}] + [\Lambda_{p-1}^{-1}][U_{p-1}^{-1}]^H[\hat{R}_{fb}]_{p-1}. \qquad (4.56b)$$

However, from eq(4.49)

$$G_p^H \equiv - [\Delta]_p^H \qquad (4.57)$$

so that

$$[\hat{\Delta}]_p^H A^H + B^H[\hat{\Delta}]_p^H = C^H \qquad (4.58)$$

where $[\hat{\Delta}]_p^H$ is recognized as an estimate since limited data is being used in this equation and

$$A^H = [V_{p-1}^{-1}]^H[\hat{R}_{bb}]_{p-1}[V_{p-1}^{-1}]\Omega_{p-1}^{-1} \qquad (4.59a)$$

$$B^H = \Lambda_{p-1}^{-1}[U_{p-1}^{-1}]^H[\hat{R}_{ff}]_{p-1}[U_{p-1}^{-1}] \qquad (4.59b)$$

34

$$C^H = [\hat{R}_{fb}]_{p-1}[V_{p-1}^{-1}][\Omega_{p-1}^{-1}] + [\Lambda_{p-1}^{-1}][U_{p-1}^{-1}]^H[\hat{R}_{fb}]_{p-1} . \qquad (4.59c)$$

In reference [12], Nuttall examined several forms of the weighting matrices Λ_{p-1} and Ω_{p-1} and showed that stable conditions are achieved if

$$\Lambda_{p-1} = U_{p-1}^{-1} \equiv [\Sigma_f]_{p-1}^{-1} \qquad (4.60)$$

and

$$\Omega_{p-1} = V_{p-1}^{-1} \equiv [\Sigma_b]_{p-1}^{-1} . \qquad (4.61)$$

Thus, the constant matrices A^H, B^H and C^H simplify to

$$A^H = [V_{p-1}^{-1}]^H [\hat{R}_{bb}]_{p-1} = [V_{p-1}^{-1}]^H [\hat{R}_{bb}]_{p-1}^H \qquad (4.62a)$$

$$B^H = [\hat{R}_{ff}]_{p-1} [U_{p-1}^{-1}] = [\hat{R}_{ff}]_{p-1}^H [U_{p-1}^{-1}]^H \qquad (4.62b)$$

$$C^H = 2[\hat{R}_{fb}]_{p-1} \qquad (4.62c)$$

where $[\hat{R}_{bb}]_{p-1}$, $[\hat{R}_{ff}]_{p-1}$ and $[U_{p-1}^{-1}]$ are Hermitian. We note that A^H and B^H each contain the product of two matrices. The matrices $[U_{p-1}^{-1}]$ and $[V_{p-1}^{-1}]$ are the forward and backward error variances for a filter of order p-1, respectively. They are obtained from the Levinson-Wiggins-Robinson recursion. The matrices $[\hat{R}_{ff}]_{p-1}$ and $[\hat{R}_{bb}]_{p-1}$, however, are time-averaged estimates of these variances using limited data [see eqs(4.47)]. Using eqs(4.62), eq(4.58) is now written as

$$[\hat{\Delta}]_p^H[V_{p-1}^{-1}]^H [\hat{R}_{bb}]_{p-1}^H + [\hat{R}_{ff}]_{p-1}^H [U_{p-1}^{-1}]^H[\hat{\Delta}]_p^H = 2[\hat{R}_{fb}]_{p-1}. \qquad (4.63)$$

In the <u>single</u> channel case, each element is a scalar where

$$U_{p-1} = V_{p-1} \equiv \sigma_{p-1}^2 \qquad (4.64)$$

and $A_p^H(p) = [\Gamma_f]_p^H = - [\hat{\Delta}]_p^H[V_{p-1}^{-1}]^H$ becomes

$$a_p^*(p) = \hat{\Gamma}_p^* = - \frac{\hat{\Delta}_p^*}{\sigma_{p-1}^2} . \qquad (4.65)$$

From eqs(4.47), the terms $[\hat{R}_{bb}]_{p-1}$, $[\hat{R}_{ff}]_{p-1}$ and $[\hat{R}_{fb}]_{p-1}$ for the scalar case can be expressed as

$$[\hat{R}_{ff}]_{p-1} = [\hat{R}_{ff}]_{p-1}^* = \frac{1}{N-p} \sum_{k=p+1}^{N} |\varepsilon_{p-1}(k)|^2 \qquad (4.66a)$$

$$[\hat{R}_{fb}]_{p-1} = \frac{1}{N-p} \sum_{k=p+1}^{N} \varepsilon_{p-1}(k)\beta_{p-1}^*(k-1) \qquad (4.66b)$$

$$[\hat{R}_{bb}]_{p-1} = [\hat{R}_{bb}]_{p-1}^H = \frac{1}{N-p} \sum_{k=p+1}^{N} |\beta_{p-1}(k-1)|^2. \qquad (4.66c)$$

Using eqs(4.64) through (4.66), the scalar version of eq(4.63) can be written as

$$-a_p^*(p)\left[\sum_{k=p+1}^{N} |\beta_{p-1}(k-1)|^2\right] - \left[\sum_{k=p+1}^{N} |\varepsilon_{p-1}(k)|^2\right]a_p^*(p) = 2\left[\sum_{k=p+1}^{N} \varepsilon_{p-1}(k)\beta_{p-1}^*(k-1)\right].$$

$$(4.67)$$

Solving eq(4.67) for $a_p^*(p)$, we have

$$a_p^*(p) = \hat{\Gamma}_p^* = - \frac{2\displaystyle\sum_{k=p+1}^{N} [\varepsilon_{p-1}(k)\beta_{p-1}^*(k-1)]}{\displaystyle\sum_{k=p+1}^{N} \left[|\varepsilon_{p-1}(k)|^2 + |\beta_{p-1}(k-1)|^2\right]}. \qquad (4.68)$$

The result expressed in eq(4.68) is the estimate of the single channel Burg reflection coefficient. This result is equivalent to that obtained by minimizing eq(4.48b) with respect to Γ_p [13]. Thus the results presented here are a generalization of the single channel Burg algorithm.

4.4 SOME CONSIDERATIONS OF BIASED PARAMETER ESTIMATORS

In this section, we briefly develop a relationship that will be useful in evaluating the computed estimation results in chapter 5.0. Specifically, we develop a relationship between the error variance, the sample variance and the bias of the estimate.

Consider the estimate $\hat{a}$ of the parameter a. The error variance of $\hat{a}$ is expressed as

$$V_e = E\{[\hat{a} - a][\hat{a} - a]^*\} \tag{4.69a}$$

$$= E[|\hat{a}|^2] - aE(\hat{a}^*) - a^*E(\hat{a}) + |a|^2 \tag{4.69b}$$

For a biased estimator

$$E(\hat{a}) = a + B(a) \tag{4.70a}$$

$$E(\hat{a}^*) = a^* + B^*(a) \tag{4.70b}$$

so that

$$V_e = E[|\hat{a}|^2] - |a|^2 - aB^*(a) - a^*B(a). \tag{4.71}$$

Using eqs(4.70), the variance of $\hat{a}$ is expressed as

$$\sigma_{\hat{a}}^2 = E\{[\hat{a} - E(\hat{a})][\hat{a} - E(\hat{a})]^*\} \tag{4.72a}$$

$$= E[|\hat{a}|^2] - E(\hat{a})E(\hat{a}*) \tag{4.72b}$$

$$= E[|\hat{a}|^2] - |a|^2 - aB^*(a) - a^*B(a) + |B(a)|^2 \tag{4.72c}$$

Eqs(4.71) and (4.72c) yield

$$V_e = \sigma_{\hat{a}}^2 + |B(a)|^2 \tag{4.73}$$

The quantity $\sigma_{\hat{a}}^2$ can be estimated by the computation of the sample variance of $\hat{a}$. In chapter 5.0, we compute the quantities in eq(4.73) for verification of the results. In addition, we will note the dependence of each upon the correlation of the processes for various estimators.

4.5 SOME ERROR VARIANCE CONSIDERATIONS OF PARAMETER ESTIMATORS

As noted in the beginning of this chapter, expressions for the error variance of time-averaged parameter estimators are difficult to determine. This is due to the fact that the estimators generally involve ratios of correlated random

estimates. For example, from the Yule-Walker equation, the estimate $\hat{a}_1(1)$ for an AR(1) process is expressed as

$$\hat{a}_1(1) = -\frac{\hat{R}(-1)}{\hat{R}(0)} \tag{4.74}$$

while for an AR(2) process, we have the estimators

$$\hat{a}_2(1) = \frac{\hat{R}(2)\hat{R}(-1) - \hat{R}(1)\hat{R}(0)}{\hat{R}(0)\hat{R}(0) - \hat{R}(1)\hat{R}(-1)} \tag{4.75a}$$

and

$$\hat{a}_2(2) = \frac{\hat{R}(1)\hat{R}(1) - \hat{R}(2)\hat{R}(0)}{\hat{R}(0)\hat{R}(0) - \hat{R}(1)\hat{R}(-1)} \tag{4.75b}$$

The correlation among the estimates $\hat{R}(l)$ is due to the use of a single set of observation data in the estimation procedure. The above equations reveal a similar form to that noted in section 3.5 for the normalized correlation function estimators; ie., the deviation of the numerator terms about some mean level will be 'tracked' similarly by the denominator terms. If the numerator terms increase (or decrease), the denominator terms will also increase (or decrease). As a result, a type of 'normalization' results so that the estimator will be closer to its respective mean and its associated variance is reduced as compared to the corresponding performance of the individual estimates $\hat{R}(l)$.

5.0 RESULTS

5.1 COMPUTED VARIANCE OF THE AUTOCORRELATION FUNCTION ESTIMATOR

In this section, we validate eq(3.30) which is a special case of eq(3.27) using a real, exponentially shaped autocorrelation function. The real AR(1) process also has an exponential autocorrelation function and we use it here in the synthesis of the observation processes. Its autocorrelation function is expressed as

$$R_{AR}(k) = R_{AR}(0) \, [-a(1)]^{|k|} \tag{5.1a}$$

$$= \sigma_{AR}^2 \, [-a(1)]^{|k|}. \tag{5.1b}$$

where

$$R_{AR}(0) = \frac{\sigma_u^2}{1 - a^2(1)} = \sigma_{AR}^2 \tag{5.2}$$

and σ_u^2, $a(1)$ and σ_{AR}^2 are the white noise driving variance, the AR(1) parameter, and the variance of the AR(1) process, respectively. In the special case of the AR(1) process used in this example, the constants in eq(2.30) were chosen such that $\lambda_{ii} = -a(1)$, $\sigma_{ii}^2 = \sigma_{AR}^2$ and $\theta_{ii}(l) = 0$ for all l. Table 1 contains the parameters used in the process synthesis procedure described in section 2.4. The variance σ_{ii}^2 was held fixed at 4 while λ_{ii} was varied using 0.1, 0.7 and 0.99.

Fig.	σ_{ii}^2	λ_{ii}	N_T	N_R
2	4.0	0.1	100	10,000
3	4.0	0.7	100	10,000
4	4.0	0.99	100	10,000

Table 1 Parameters used in the synthesis of the processes analyzed in Figs.2 through 4.

Figs. 2 through 4 show the biased time-averaged autocorrelation functions computed with eq(3.1) and their associated variances for the processes described

39

in the Table 1. For each figure, plot (a) shows six realizations of the biased, time-averaged autocorrelation estimator $\hat{R}_{T_b}(l)$ plotted over 64 lag values using $N_T=100$ time samples. The corresponding ensemble averaged estimator $\hat{R}_E(l)$ is shown in plot b using $N_R=10,000$. The sample variance $Var[\hat{R}_{iiT_b}(l,N_T):N_R]$ of the biased time-averaged autocorrelation function computed using eq(3.28) with $N_R=10,000$ is displayed in c. The corresponding analytic calculation of $V_{B_{ii}}(l,N_T)$ using eq(3.30) is shown in plot d. The decrease in this quantity as a function of l is a result of the weighting associated with the biased estimator. A similar behavior is noted in [4] for continuous-time processes. The computed results (plots c) are in excellent agreement with the analytic expressions shown in plots d (note the scale change between plots c and d in Fig. 2).

In Fig. 5, the maximum value of $V_{B_{ii}}(l,N_T)$ which occurs at $l=0$ is plotted (solid curve) as a function of λ_{ii} for $N_T=100$ and $N_T=1000$ using the analytic expression of eq(3.30) for the AR(1) process. The corresponding sample variances of the time-averaged autocorrelation function estimates computed at lag zero using eq(3.28) with $i=j$ for the synthesized data processes are also plotted (•) on this curve. These values were computed using N_R realizations of the functions. For $N_T=100$, $N_R=10,000$ was used while for $N_T=1000$, the number of realizations was reduced to $N_R=1,000$. Reducing N_R decreases the confidence level associated with the computation of the sample variance $Var[\hat{R}_{ijT_b}(l,N_T):N_R]$.

However, the error bars representing one standard deviation from the mean are less than the size of the printed (•).

The results shown in Fig.5 indicate the significant increase in the variance $V_{B_{ii}}(l,N_T)$ as a function of λ_{ii}. In addition, it provides a measure of the required observation window size necessary to achieve a specific level of the variance. For example, the curve for $N_T=1000$ has a very distinct knee for $\lambda_{ii}\approx0.9$. For processes with a temporal correlation above this value, a larger observation data window would be required to reduce $V_{B_{ii}}(l,N_T)$ to values less than 0.15. We also note that for $N_T=100$, large variances can be obtained even for moderately low values of λ_{ii}. In [2], similar plots are shown for higher values of N_T.
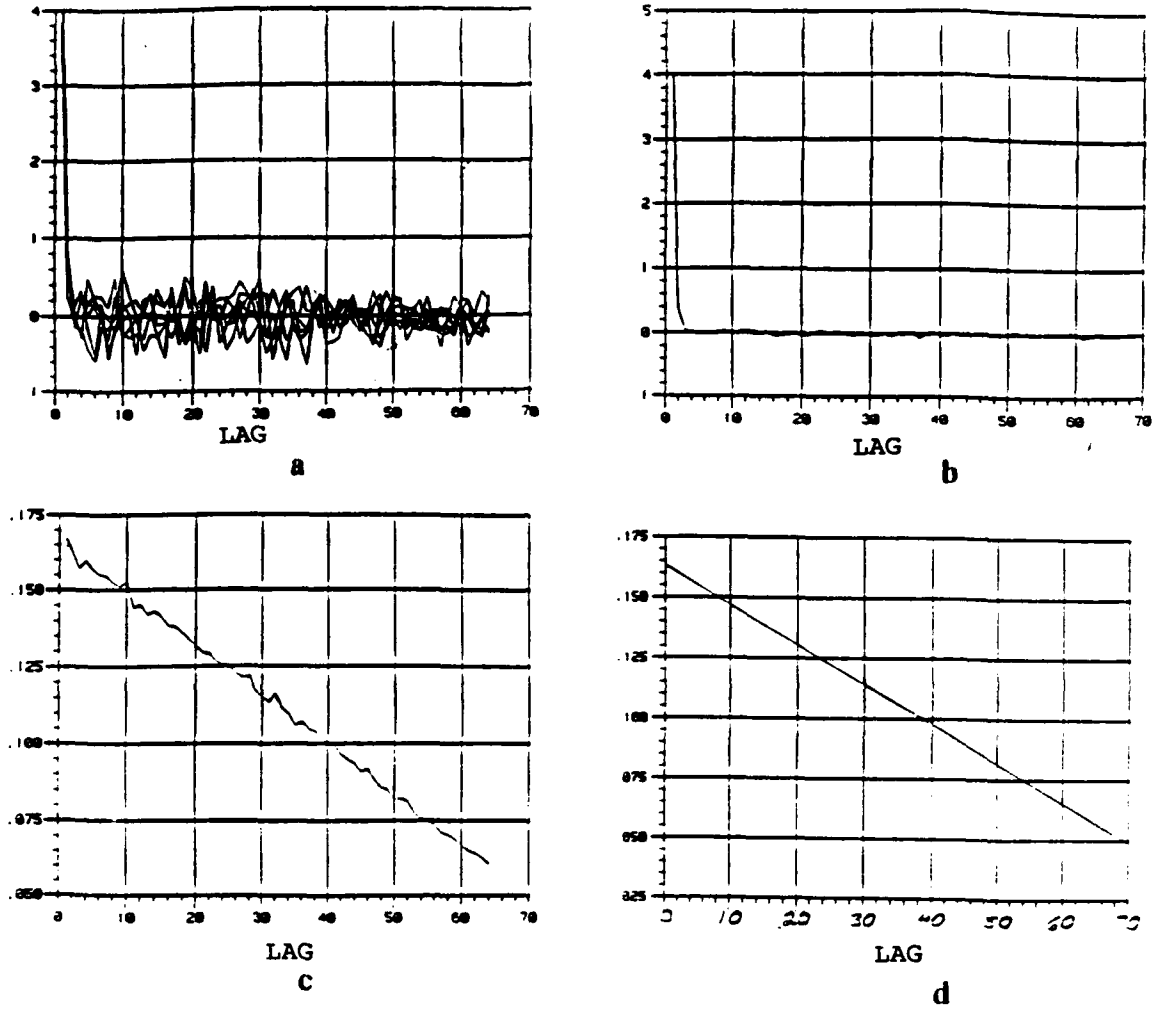
Figure 2 Time-averaged autocorrelation function and its variance for an AR(1) process; $\lambda=0.1$, $\sigma_s^2=4$ a.) biased $\hat{R}_{iiT_b}(l)$ (6 trials) using $N_T=100$ b.) ensemble averaged $\hat{R}_E(l)$ using 10,000 realizations c.) computed sample variance of the biased $\hat{R}_{iiT_b}(l)$ d.) analytical variance of the biased $\hat{R}_{iiT_b}(l)$.

41
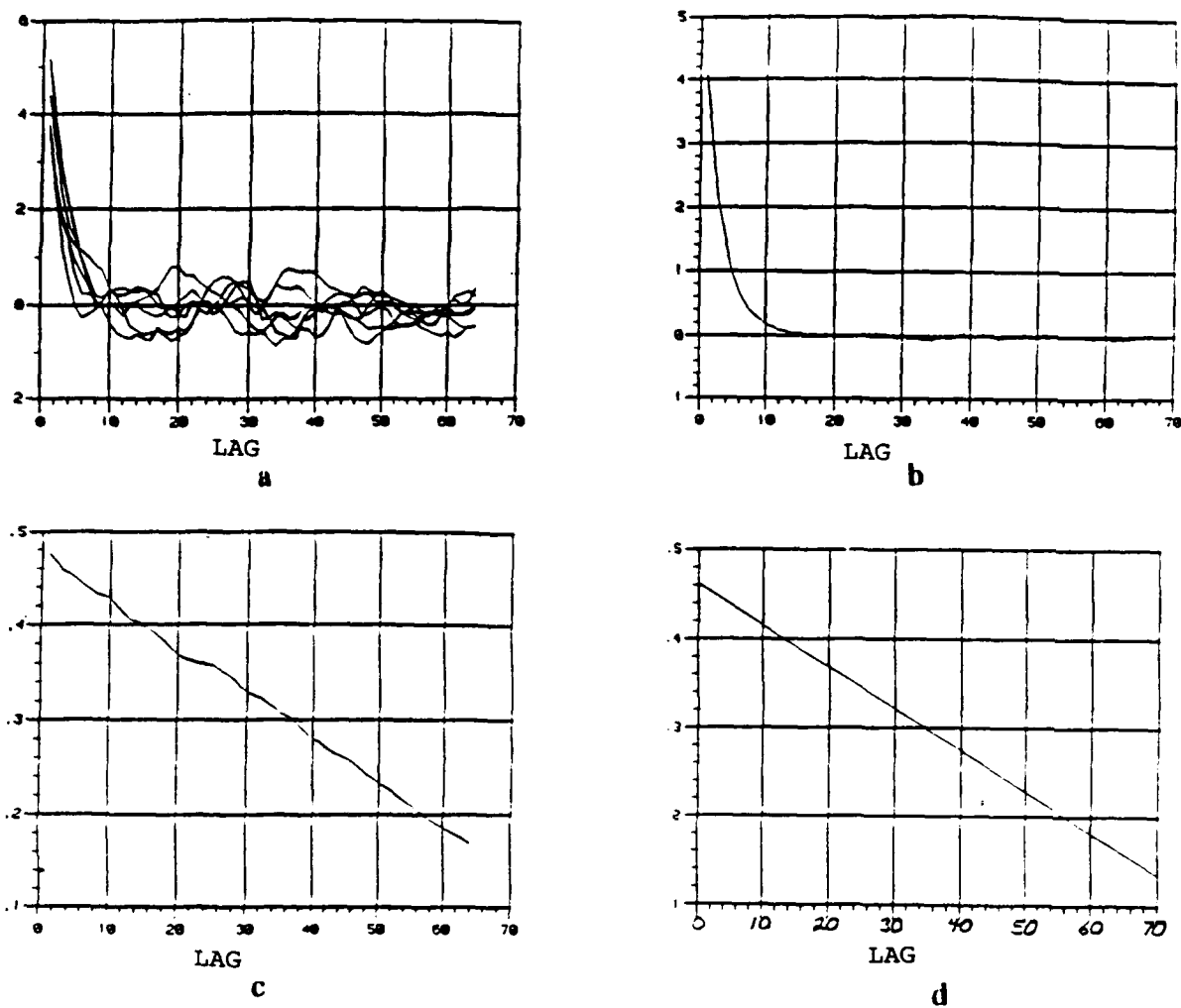
Figure 3 Time-averaged autocorrelation function and its variance for an AR(1) process; $\lambda=0.7$, $\sigma_s^2=4$ a.) biased $\hat{R}_{iiT_b}(l)$ (6 trials) using $N_T=100$ b.) ensemble averaged $\hat{R}_E(l)$ using 10,000 realizations c.) computed sample variance of the biased $\hat{R}_{iiT_b}(l)$ d.) analytical variance of the biased $\hat{R}_{iiT_b}(l)$.
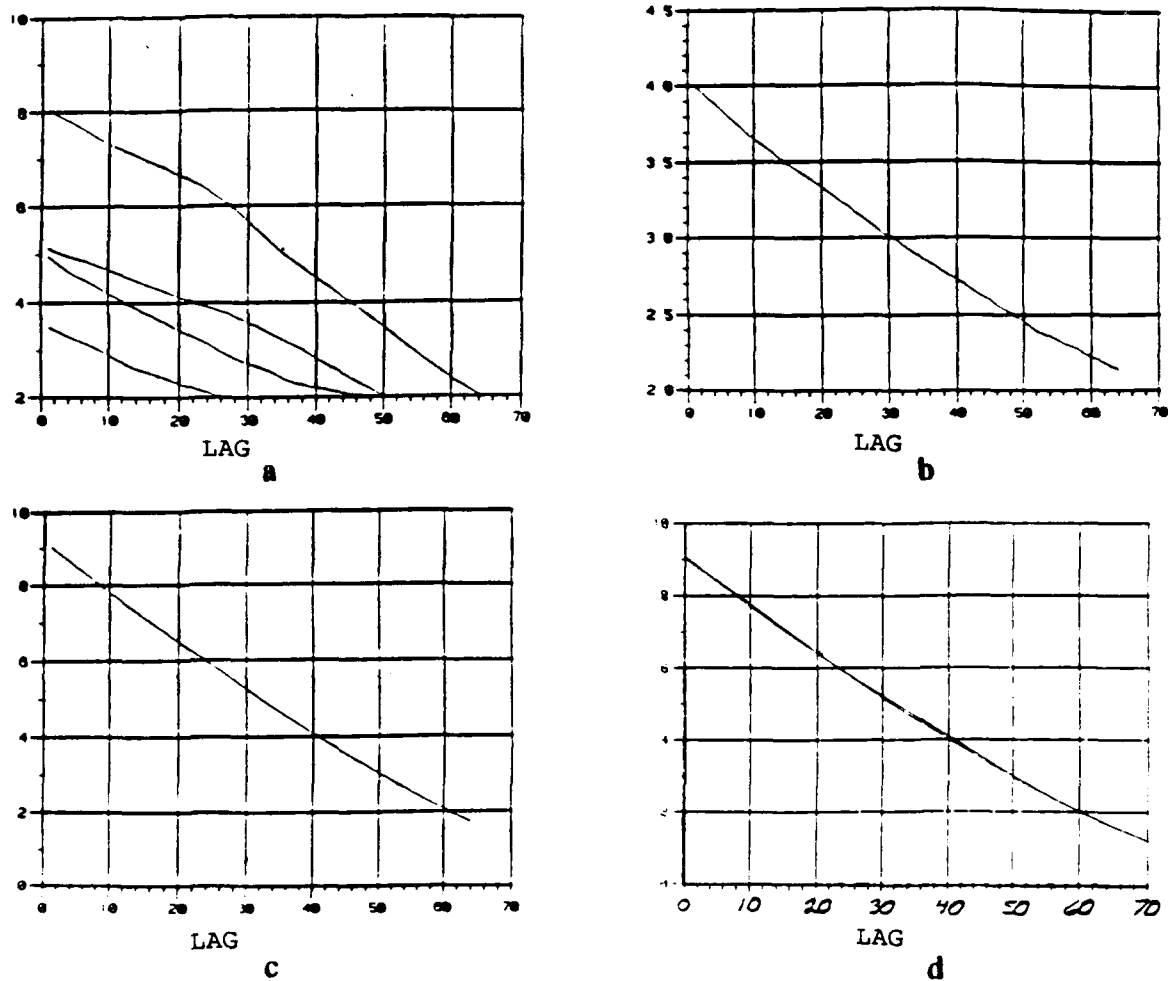
Figure 4 Time-averaged autocorrelation function and its variance for an AR(1) process; $\lambda=0.99$, $\sigma_s^2=4$ a.) biased $\hat{R}_{iiT_b}(l)$ (4 trials) using $N_T=100$ b.) ensemble averaged $\hat{R}_E(l)$ using 10,000 realizations c.) computed sample variance of the biased $\hat{R}_{iiT_b}(l)$ d.) analytical variance of the biased $\hat{R}_{iiT_b}(l)$.

43
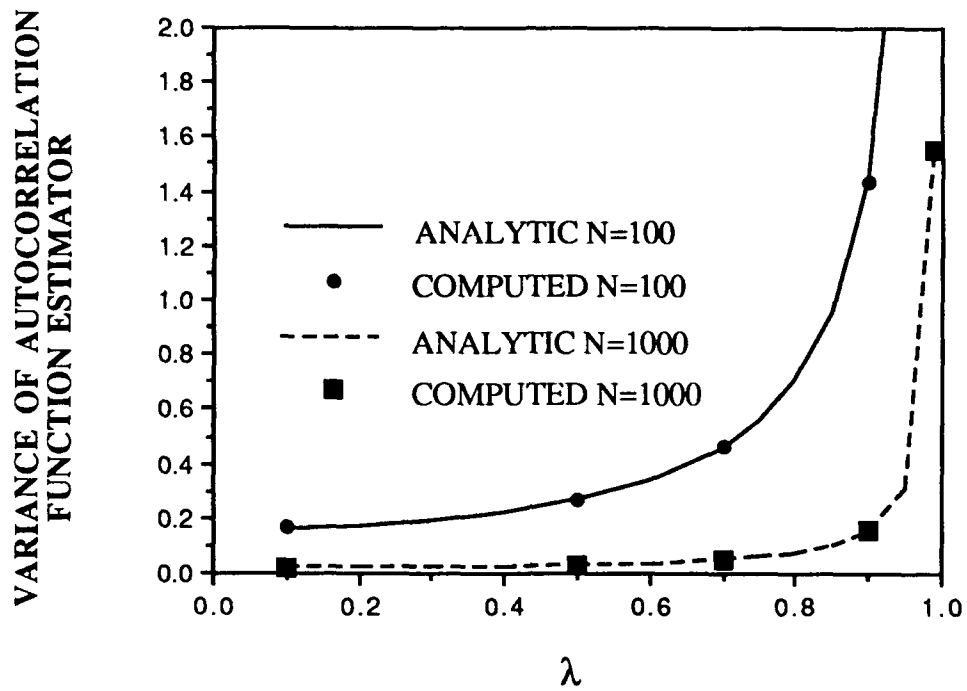
Figure 5 Maximum variance of the time-averaged autocorrelation function versus λ_{ii} for $\sigma_{ii}^2=4$; analytical (−) and computed (•).

5.2 Computed Variance of the Cross-Correlation Function

Table 2 contains the parameters used in the process synthesis procedure [1,2] for a two channel AR(1) process with real correlation functions. For the cases considered here, the variances of the two processes, denoted as σ_{11}^2 and σ_{22}^2, were both held fixed at 4 while λ_{11} and λ_{22} had values of 0.1, 0.5 and 0.99. The cross-correlation coefficient $|\rho_{12}|$ had values of 0.99, 0.5 and 0.0.

Fig.	σ_{11}^2	σ_{22}^2	λ_{11}	λ_{22}	λ_{12}	$|\rho_{12}|$	N_T	N_R	l_{12}
6	4	4	0.1	0.1	0.1	0.99	100	1000	0
7	4	4	0.1	0.1	0.1	0.50	100	1000	0
8	4	4	0.1	0.1	0.1	0.00	100	1000	0
9	4	4	0.5	0.5	0.5	0.50	100	1000	0
10	4	4	0.9	0.9	0.9	0.50	100	1000	0

Table 2 Parameters used in the synthesis of the processes analyzed in Figs.2 through 4.

Figs 6 through 10 show the variances of the time-averaged cross-correlation function estimates based on the computed values of eq(3.28) and the analytic expression of eq(3.31). The computed results are in excellent agreement with the analytic expressions. In Figs.6c, 7c and 8c, we observe that the computed sample variance is not affected by changes in $|\rho_{12}|$. This observation is consistent with the point made in section 3.2 that, in the special case where eqs.(3.26) hold, $F_{ij}(l,k)=0$ and the variance of the cross-correlation function estimator is independent of the cross-correlation parameter $|\rho_{12}|$.

In Fig.11, the maximum value of $V_{B_{ij}}(l,N_T)$, which occurs at $l=l_{12}=0$, is plotted (solid curves) as a function of $\lambda=\lambda_{11}=\lambda_{22}$ for $N_T=100$ and $N_T=1000$ using the analytic expression of eq(3.31) and $\sigma_{11}^2=\sigma_{22}^2=4$. The corresponding maximum

45
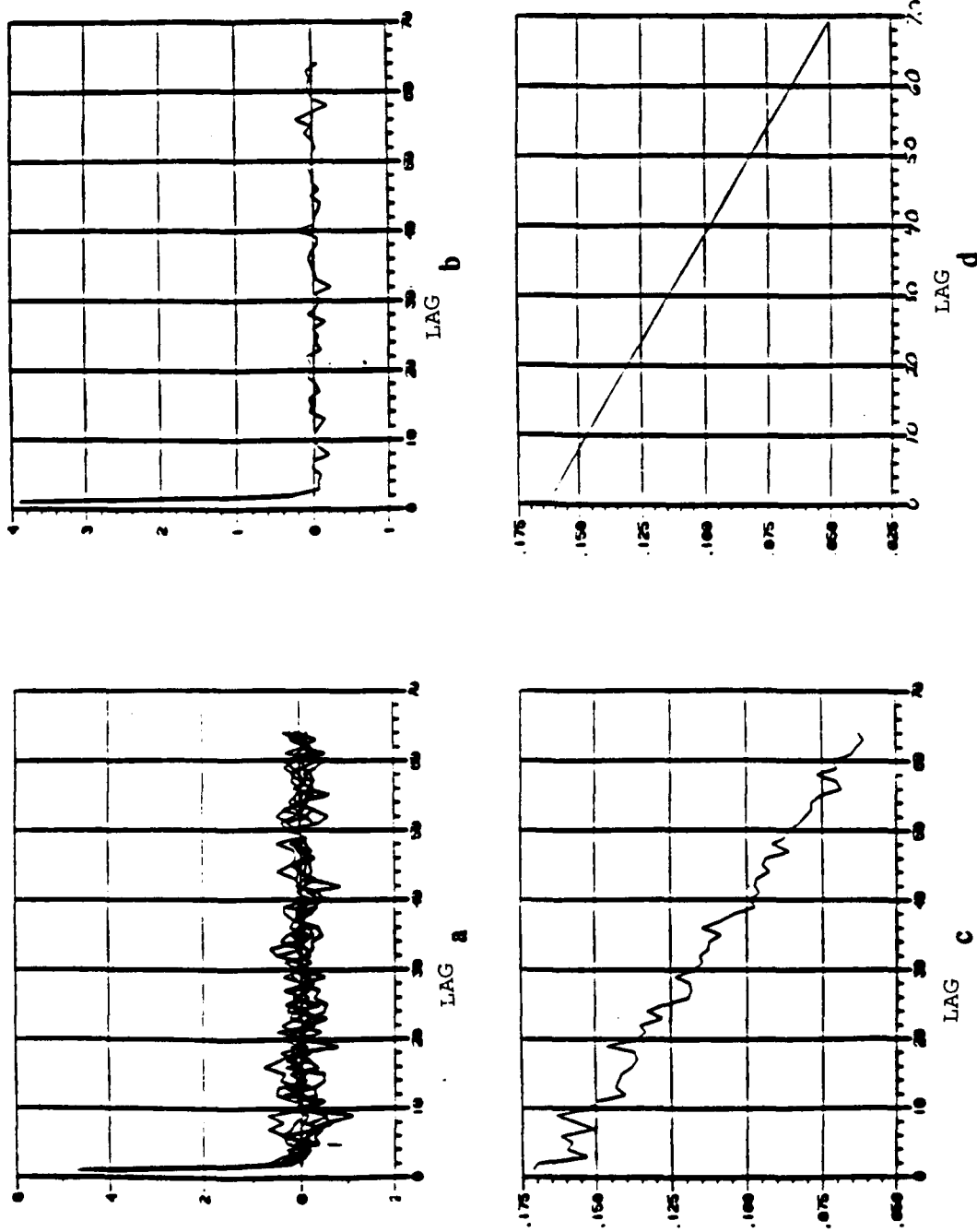
Figure 6 Time-averaged cross-correlation function and its variance for $|\rho_{12}|=0.99$, $\lambda_{11}=\lambda_{22}=\lambda_{12}=0.1$, $\sigma_{11}^2=\sigma_{22}^2=4$, $l_{12}=0$ a.) biased $\hat{R}_{ijT_b}(l)$ (6 trials) using $N_T=100$ b.) ensemble averaged $\hat{R}_E(l)$ using 1,000 realizations c.) sample variance of the biased $\hat{R}_{iiT_b}(l)$ d.) analytical variance of the biased $\hat{R}_{iiT_b}(l)$.

Figure 7 Time-averaged cross-correlation function and its variance for $|\rho_{12}|=0.50$, $\lambda_{11}=\lambda_{22}=\lambda_{12}=0.1$, $\sigma_{11}^2=\sigma_{22}^2=4$, $l_{12}=0$ a.) biased $\hat{R}_{ijT_b}(l)$ (6 trials) using $N_T=100$ b.) ensemble averaged $\hat{R}_E(l)$ using 1,000 realizations c.) sample variance of the biased $\hat{R}_{iiT_b}(l)$ d.) analytical variance of the biased $\hat{R}_{iiT_b}(l)$.

47

Figure 8 Time-averaged cross-correlation function and its variance for $|\rho_{12}|=0$, $\lambda_{11}=\lambda_{22}=\lambda_{12}=0.1$, $\sigma_{11}^2=\sigma_{22}^2=4$, $l_{12}=0$ a.) biased $\hat{R}_{ijT_b}(l)$ (6 trials) using $N_T=100$ b.) ensemble averaged $\hat{R}_E(l)$ using 1,000 realizations c.) sample variance of the biased $\hat{R}_{iiT_b}(l)$ d.) analytical variance of the biased $\hat{R}_{iiT_b}(l)$.

Figure 9 Time-averaged cross-correlation function and its variance for $|\rho_{12}|=0.50$, $\lambda_{11}=\lambda_{22}=\lambda_{12}=0.5$, $\sigma_{11}^2=\sigma_{22}^2=4$, $l_{12}=0$ a.) biased $\hat{R}_{ijT_b}(l)$ (6 trials) using $N_T=100$ b.) ensemble averaged $\hat{R}_E(l)$ using 1,000 realizations c.) sample variance of the biased $\hat{R}_{iiT_b}(l)$ d.) analytical variance of the biased $\hat{R}_{iiT_b}(l)$.

Figure 10 Time-averaged cross-correlation function and its variance for $|\rho_{12}|=0.50$, $\lambda_{11}=\lambda_{22}=\lambda_{12}=0.9$, $\sigma_{11}^2=\sigma_{22}^2=4$, $l_{12}=0$ a.) biased $\hat{R}_{ijT_b}(l)$ (6 trials) using $N_T=100$ b.) ensemble averaged $\hat{R}_E(l)$ using 1,000 realizations c.) sample variance of the biased $\hat{R}_{ijT_b}(l)$ d.) analytical variance of the biased $\hat{R}_{ijT_b}(l)$.
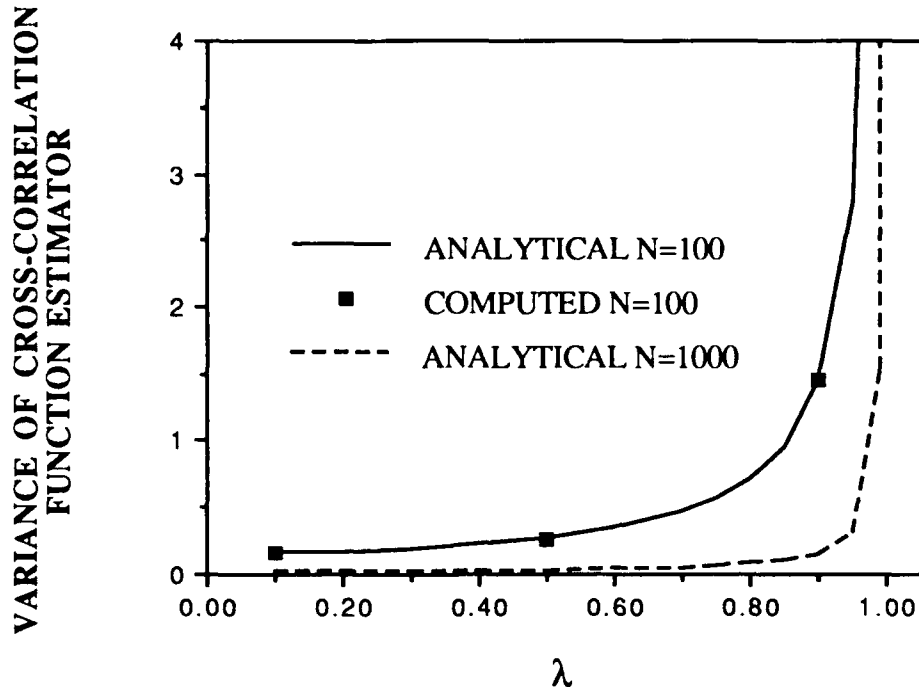
Figure 11 Variance of the time-averaged cross-correlation function at $l=l_{12}=0$ versus $\lambda=\lambda_{11}=\lambda_{22}$ for $\sigma_{11}^2=\sigma_{22}^2=4$; analytical($-$) and computed ($\bullet$).

values of the sample variances of the time-averaged cross-correlation function estimates computed using the synthesized data processes are also plotted ($\bullet$) on this curve. These values were computed using $N_R=1000$ realizations of the estimates. In several of the figures, we note the increase in the variance of $V_{B_{ij}}(l)$ over the results presented in the previous section. This is simply due to the decrease in N_R from 10,000 to 1,000 thus increasing the uncertainty of the statistical calculations.

51

5.3 COMPUTED ERROR VARIANCE OF SINGLE CHANNEL AUTO-REGRESSIVE MODEL PARAMETERS

In this section, we consider complex autoregressive (AR) time series models with known order and show computed simulation results for the error variance, the bias and the variance of the parameter estimates using the three estimators described in chapter 4.0. Both Gaussian and K-distributed processes are considered.

5.3.1 Performance with Gaussian Processes

Complex Gaussian autoregressive (AR) time series models are considered in this subsection. Tables 3a, b and c, show the estimated means, error variances and sample variances, respectively, of the $a(1)$ coefficient for N_T values ranging from 10 to 500. These values were obtained for each estimator using a complex single channel AR(1) process 'without noise'. The processes were synthesized with the real exponential correlation function of eq(5.1b). In Tables 4a through 4f, we focus on $N_T=10$ and 100 using more λ values. The value of the bias B (the difference between the estimates $\hat{a}(1)$ and the true value) for each estimator is also shown. The method described in section 2.4 was used to synthesize each process. In the special case of the AR(1) process, the one-lag temporal correlation parameter λ is the negative of the AR coefficient. Although the true parameters of the autoregressive process are real, the processes themselves are complex. Thus, an imaginary component of the estimate will, in general, be obtained. This component, however, becomes negligible in the limit as the estimate approaches the true value. Only the means of the real part of the estimated coefficients are shown here since the complex parts were small for these cases. Computed values of the error variance of $\hat{a}(1)$ and $\hat{\sigma}_u^2$ are obtained using $N_R=10,000$ realizations where $\hat{a}(1)$ and $\hat{\sigma}_u^2$ are the estimates of $a(1)$ and σ_u^2, respectively. Fig.12a shows the error variances of $\hat{a}(1)$ versus λ using $N_T=10$ for the three estimators. Corresponding log scale plots for $N_T=10$ and 100 are shown in Figs.12b and 12c, respectively. Each of these plots are compared to the exact unbiased Cramer-Rao bound [6]. We note that the error variances of the estimators lie below that of the Cramer-Rao bound for most values of λ. This observation is not unexpected since these estimators are not unbiased.

λ	true a(1)	N_T	mean Re â(1) YWUBC	mean Re â(1) YWBC	mean Re â(1) Burg Algorith.
0.1	- 0.1	10	- 8.9437×10^{-2}	- 8.0494×10^{-2}	- 8.9294×10^{-2}
	- 0.1	50	- 9.9174×10^{-2}	- 9.7190×10^{-2}	- 9.9191×10^{-2}
	- 0.1	100	- 9.9981×10^{-2}	- 9.8981×10^{-2}	- 1.0031×10^{-1}
	- 0.1	200	- 1.0006×10^{-1}	- 9.9560×10^{-2}	- 1.0006×10^{-1}
	- 0.1	500	- 1.0029×10^{-1}	- 1.0009×10^{-1}	- 1.0029×10^{-1}
0.5	- 0.5	10	- 4.5493×10^{-1}	- 4.0944×10^{-1}	- 4.5390×10^{-1}
	- 0.5	50	- 4.9035×10^{-1}	- 4.8055×10^{-1}	- 4.9029×10^{-1}
	- 0.5	100	- 4.9533×10^{-1}	- 4.9038×10^{-1}	- 4.9534×10^{-1}
	- 0.5	200	- 4.9724×10^{-1}	- 4.9475×10^{-1}	- 4.9722×10^{-1}
	- 0.5	500	- 4.9872×10^{-1}	- 4.9773×10^{-1}	- 4.9873×10^{-1}
0.9	- 0.9	10	- 8.3169×10^{-1}	- 7.4852×10^{-1}	- 8.3815×10^{-1}
	- 0.9	50	- 8.8284×10^{-1}	- 8.6518×10^{-1}	- 8.8369×10^{-1}
	- 0.9	100	- 8.9088×10^{-1}	- 8.8197×10^{-1}	- 8.9110×10^{-1}
	- 0.9	200	- 8.9557×10^{-1}	- 8.9109×10^{-1}	- 8.9562×10^{-1}
	- 0.9	500	- 8.9802×10^{-1}	- 8.9622×10^{-1}	- 8.9802×10^{-1}
0.99	- 0.99	10	- 9.6398×10^{-1}	- 8.6758×10^{-1}	- 9.6822×10^{-1}
	- 0.99	50	- 9.7772×10^{-1}	- 9.5817×10^{-1}	- 9.7979×10^{-1}
	- 0.99	100	- 9.8209×10^{-1}	- 9.7226×10^{-1}	- 9.8332×10^{-1}
	- 0.99	200	- 9.8573×10^{-1}	- 9.8080×10^{-1}	- 9.8623×10^{-1}
	- 0.99	500	- 9.8801×10^{-1}	- 9.8603×10^{-1}	- 9.8813×10^{-1}
0.9999	- 0.9999	10	- 9.9896×10^{-1}	- 8.9906×10^{-1}	- 9.9917×10^{-1}
	- 0.9999	50	- 9.9929×10^{-1}	- 9.7931×10^{-1}	- 9.9947×10^{-1}
	- 0.9999	100	- 9.9931×10^{-1}	- 9.8932×10^{-1}	- 9.9949×10^{-1}
	- 0.9999	200	- 9.9945×10^{-1}	- 9.9446×10^{-1}	- 9.9959×10^{-1}
	- 0.9999	500	- 9.9955×10^{-1}	- 9.9755×10^{-1}	- 9.9967×10^{-1}

Table 3a Tabulated values of the mean for the real part of â(1) with λ and N_T as parameters and computed using $N_R = 10,000$ realizations.

53

λ	N_T	error variance of $\hat{a}(1)$ YWUBC	error variance of $\hat{a}(1)$ YWBC	error variance of $\hat{a}(1)$ Burg Algorith.	unbiased exact Cramer-Rao bound
0.1	10	9.9742×10^{-2}	8.1081×10^{-2}	9.9524×10^{-2}	1.1088×10^{-1}
	50	1.94440×10^{-2}	1.8678×10^{-2}	1.9449×10^{-2}	
	100	9.9574×10^{-3}	9.7603×10^{-3}	9.8274×10^{-3}	1.0099×10^{-2}
	200	4.9522×10^{-3}	4.9030×10^{-3}	4.9518×10^{-3}	
	500	1.9872×10^{-3}	1.9791×10^{-3}	1.9871×10^{-3}	
0.5	10	8.4426×10^{-2}	7.4780×10^{-2}	8.2327×10^{-2}	1.04167×10^{-1}
	50	1.5339×10^{-2}	1.5021×10^{-2}	1.5196×10^{-2}	
	100	7.7212×10^{-3}	7.6388×10^{-3}	7.6932×10^{-3}	1.0034×10^{-2}
	200	3.7136×10^{-3}	3.6965×10^{-3}	3.7058×10^{-3}	
	500	1.5107×10^{-3}	1.5082×10^{-3}	1.5088×10^{-3}	
0.9	10	4.0044×10^{-2}	5.1605×10^{-2}	3.5420×10^{-2}	5.9975×10^{-2}
	50	5.1584×10^{-3}	5.8837×10^{-3}	4.7416×10^{-3}	
	100	2.2807×10^{-3}	2.4789×10^{-3}	2.1737×10^{-3}	9.3074×10^{-3}
	200	1.0532×10^{-3}	1.1026×10^{-3}	1.0269×10^{-3}	
	500	3.9503×10^{-4}	4.0380×10^{-4}	3.8968×10^{-4}	
0.99	10	8.2635×10^{-3}	2.1132×10^{-2}	6.6868×10^{-3}	1.024×10^{-2}
	50	1.1963×10^{-3}	2.0175×10^{-3}	9.1984×10^{-4}	
	100	4.8610×10^{-4}	7.2965×10^{-4}	3.8344×10^{-4}	5.0089×10^{-3}
	200	1.8450×10^{-4}	2.4927×10^{-4}	1.5359×10^{-4}	
	500	5.7238×10^{-5}	6.8802×10^{-5}	5.1501×10^{-5}	
0.9999	10	1.7938×10^{-4}	1.0314×10^{-2}	1.3863×10^{-4}	1.11×10^{-4}
	50	2.4836×10^{-5}	4.4756×10^{-4}	1.7980×10^{-5}	
	100	1.5377×10^{-5}	1.2665×10^{-4}	1.0509×10^{-5}	1.0×10^{-4}
	200	5.3456×10^{-6}	3.4784×10^{-5}	3.8399×10^{-6}	
	500	2.2383×10^{-6}	7.6558×10^{-6}	1.6141×10^{-6}	

Table 3b Tabulated values of the error variances of $\hat{a}(1)$ with λ and N_T as parameters and computed using $N_R=10,000$ realizations.

λ	N_T	sample variance of $\hat{a}(1)$ YWUBC	sample variance of $\hat{a}(1)$ YWBC	sample variance of $\hat{a}(1)$ Burg Algorith.
0.1	10	9.9627×10^{-2}	8.0698×10^{-2}	9.9406×10^{-2}
	50	1.9437×10^{-2}	1.8667×10^{-2}	1.9446×10^{-2}
	100	9.9569×10^{-3}	9.7588×10^{-3}	9.8249×10^{-3}
	200	4.9521×10^{-3}	4.9027×10^{-3}	4.9516×10^{-3}
	500	1.9871×10^{-3}	1.9791×10^{-3}	1.9870×10^{-3}
0.5	10	8.2194×10^{-2}	6.6577×10^{-2}	8.0201×10^{-2}
	50	1.5246×10^{-2}	1.4642×10^{-2}	1.5102×10^{-2}
	100	7.6993×10^{-3}	7.5461×10^{-3}	7.6714×10^{-3}
	200	3.7043×10^{-3}	3.6674×10^{-3}	3.6965×10^{-3}
	500	1.5090×10^{-3}	1.5029×10^{-3}	1.5070×10^{-3}
0.9	10	3.5373×10^{-2}	2.8652×10^{-2}	3.1590×10^{-2}
	50	4.8637×10^{-3}	4.6711×10^{-3}	4.4756×10^{-3}
	100	2.1974×10^{-3}	2.1537×10^{-3}	2.0945×10^{-3}
	200	1.0336×10^{-3}	1.0233×10^{-3}	1.0077×10^{-3}
	500	3.9107×10^{-4}	3.8951×10^{-4}	3.8572×10^{-4}
0.99	10	7.5861×10^{-3}	6.1448×10^{-3}	6.2120×10^{-3}
	50	1.0455×10^{-3}	1.0041×10^{-3}	8.1546×10^{-4}
	100	4.2336×10^{-4}	4.1493×10^{-4}	3.3881×10^{-4}
	200	1.6623×10^{-4}	1.6457×10^{-4}	1.3940×10^{-4}
	500	5.3270×10^{-5}	5.3057×10^{-5}	4.7999×10^{-5}
0.9999	10	1.7848×10^{-4}	1.4457×10^{-4}	1.3803×10^{-4}
	50	2.4469×10^{-5}	2.3500×10^{-5}	1.7759×10^{-5}
	100	1.5035×10^{-5}	1.4735×10^{-5}	1.0299×10^{-5}
	200	5.1416×10^{-6}	5.0902×10^{-6}	3.7203×10^{-6}
	500	2.1105×10^{-6}	2.1021×10^{-6}	1.5371×10^{-6}

Table 3c Tabulated values of the sample variances of $\hat{a}(1)$ with λ and N_T as parameters and computed using $N_R = 10,000$ realizations.

λ	N_T	true a(1)	mean Re $\hat{a}(1)$ YWBC	error variance of $\hat{a}(1)$ YWBC	sample variance of $\hat{a}(1)$ YWBC	bias B[$\hat{a}(1)$] YWBC
0.1	10	-0.1	-8.0494×10^{-2}	8.1081×10^{-2}	8.0698×10^{-2}	1.9506×10^{-2}
	100	-0.1	-9.8981×10^{-2}	9.7603×10^{-3}	9.7588×10^{-3}	1.0190×10^{-3}
0.2	10	-0.2	-1.6318×10^{-1}	8.0896×10^{-2}	7.9548×10^{-2}	3.6820×10^{-2}
	100	-0.2	-1.9633×10^{-1}	9.6344×10^{-3}	9.6219×10^{-3}	3.6700×10^{-2}
0.3	10	-0.3	-2.4547×10^{-1}	7.8376×10^{-2}	7.5409×10^{-2}	5.4530×10^{-2}
	100	-0.3	-2.9440×10^{-1}	9.0049×10^{-3}	8.9737×10^{-3}	5.6000×10^{-2}
0.4	10	-0.4	-3.2317×10^{-1}	7.7914×10^{-2}	7.2017×10^{-2}	7.6830×10^{-2}
	100	-0.4	-3.9142×10^{-1}	8.3293×10^{-3}	8.2560×10^{-3}	8.5800×10^{-3}
0.5	10	-0.5	-4.0944×10^{-1}	7.4780×10^{-2}	6.6577×10^{-2}	9.0560×10^{-2}
	100	-0.5	-4.9533×10^{-1}	7.6388×10^{-3}	7.5461×10^{-2}	4.6700×10^{-3}
0.6	10	-0.6	-4.8869×10^{-1}	7.3030×10^{-2}	6.0644×10^{-2}	1.1131×10^{-1}
	100	-0.6	-5.8840×10^{-1}	6.5236×10^{-3}	6.3896×10^{-3}	1.1600×10^{-2}
0.7	10	-0.7	-5.7702×10^{-1}	6.6399×10^{-2}	5.1278×10^{-2}	1.2298×10^{-1}
	100	-0.7	-6.8598×10^{-1}	5.3763×10^{-3}	5.1804×10^{-3}	1.4020×10^{-2}
0.8	10	-0.8	-6.6043×10^{-1}	6.1667×10^{-2}	4.2189×10^{-2}	1.3957×10^{-1}
	100	-0.8	-7.8483×10^{-1}	3.9796×10^{-3}	3.7496×10^{-3}	1.5170×10^{-2}
0.85	10	-0.85	-7.0213×10^{-1}	5.6941×10^{-2}	3.5080×10^{-2}	1.4787×10^{-1}
	100	-0.85	-8.3350×10^{-1}	3.2694×10^{-3}	2.9930×10^{-3}	1.6500×10^{-2}
0.9	10	-0.90	-7.4852×10^{-1}	5.1605×10^{-2}	2.8652×10^{-2}	1.5148×10^{-1}
	100	-0.90	-8.8197×10^{-1}	2.4789×10^{-3}	2.1537×10^{-3}	1.8030×10^{-2}
0.95	10	-0.95	-8.0363×10^{-1}	4.0403×10^{-2}	1.8980×10^{-2}	1.4637×10^{-1}
	100	-0.95	-9.3093×10^{-1}	1.6403×10^{-3}	1.2766×10^{-3}	1.9070×10^{-2}
0.99	10	-0.99	-8.6758×10^{-1}	2.1132×10^{-2}	6.1448×10^{-3}	1.2242×10^{-1}
	100	-0.99	-9.7226×10^{-1}	7.2965×10^{-4}	4.1493×10^{-4}	1.7740×10^{-2}
0.9999	10	-0.9999	-8.9906×10^{-1}	1.0314×10^{-2}	1.4457×10^{-4}	1.0084×10^{-1}
	100	-0.9999	-9.8932×10^{-1}	1.2665×10^{-4}	1.4735×10^{-5}	1.0580×10^{-2}

Table 4a Tabulated values of the statistics of $\hat{a}(1)$ for the YWBC with λ and N_T as parameters and computed using $N_R=10,000$ realizations.

56

λ	N_T	true σ_u^2	mean Re $\hat{\sigma}_u^2$ YWBC	error variance of $\hat{\sigma}_u^2$ YWBC	sample variance of $\hat{\sigma}_u^2$ YWBC	bias $B[\hat{\sigma}_u^2]$ YWBC
0.1	10	3.96	3.6359	1.5455	1.4405	3.2410×10^{-1}
	100	3.96	3.9215	1.6015×10^{-1}	1.5867×10^{-1}	3.8500×10^{-2}
0.2	10	3.84	3.5614	1.4756	1.3981	2.7860×10^{-1}
	100	3.84	3.8092	1.4627×10^{-1}	1.4534×10^{-1}	3.0800×10^{-2}
0.3	10	3.64	3.4152	1.3107	1.2603	2.2480×10^{-1}
	100	3.64	3.6099	1.3955×10^{-1}	1.3865×10^{-1}	3.0100×10^{-1}
0.4	10	3.36	3.1971	1.1324	1.1060	1.6290×10^{-1}
	100	3.36	3.3389	1.1306×10^{-1}	1.1262×10^{-1}	2.1100×10^{-2}
0.5	10	3.00	2.9463	9.7856×10^{-1}	9.7567×10^{-1}	5.3700×10^{-2}
	100	3.00	2.9920	8.8970×10^{-2}	8.8906×10^{-2}	8.0000×10^{-3}
0.6	10	2.56	2.6140	7.7840×10^{-1}	7.7556×10^{-1}	-5.4000×10^{-2}
	100	2.56	2.5659	6.7719×10^{-2}	6.7691×10^{-2}	-5.9000×10^{-3}
0.7	10	2.04	2.2396	6.5311×10^{-1}	6.1332×10^{-1}	-1.9960×10^{-1}
	100	2.04	2.0578	4.4638×10^{-2}	4.4324×10^{-2}	-1.7800×10^{-2}
0.8	10	1.44	1.797	5.9205×10^{-1}	4.6463×10^{-1}	-3.5700×10^{-1}
	100	1.44	1.4776	2.4925×10^{-2}	2.3512×10^{-2}	-3.7600×10^{-2}
0.85	10	1.11	1.5772	6.3943×10^{-1}	4.2122×10^{-1}	-4.6720×10^{-1}
	100	1.11	1.1602	1.8008×10^{-2}	1.5490×10^{-2}	-5.0200×10^{-2}
0.9	10	0.76	1.3101	7.0149×10^{-1}	3.9884×10^{-1}	-5.5010×10^{-1}
	100	0.76	8.1552×10^{-1}	8.7135×10^{-3}	1.1796×10^{-2}	-5.5520×10^{-2}
0.95	10	0.39	1.0394	8.3888×10^{-1}	4.1722×10^{-1}	-6.4940×10^{-1}
	100	0.39	4.5763×10^{-1}	9.2025×10^{-3}	4.6284×10^{-3}	-6.7630×10^{-2}
0.99	10	0.0796	8.2175×10^{-1}	1.0869	5.3602×10^{-1}	-7.4215×10^{-1}
	100	0.0796	1.5669×10^{-1}	9.6108×10^{-3}	3.6671×10^{-3}	-7.7090×10^{-2}
0.9999	10	$8.0013 \times^{-4}$	7.5213×10^{-1}	1.1240	5.5949×10^{-1}	-7.5133×10^{-1}
	100	$8.0013 \times^{-4}$	8.0369×10^{-2}	1.2688×10^{-2}	6.3565×10^{-3}	-7.9569×10^{-2}

Table 4b Tabulated values of the statistics of $\hat{\sigma}_u^2$ for the YWBC with λ and N_T as parameters and computed using $N_R=10{,}000$ realizations.

λ	N_T	true a(1)	mean Re $\hat{a}(1)$ YWUBC	error variance of $\hat{a}(1)$ YWUBC	sample variance of $\hat{a}(1)$ YWUBC	bias B[$\hat{a}(1)$] YWUBC
0.1	10	-0.1	-8.9437×10^{-2}	9.9742×10^{-2}	9.9627×10^{-2}	1.0563×10^{-2}
	100	-0.1	-9.9981×10^{-2}	9.9574×10^{-3}	9.9569×10^{-3}	1.9000×10^{-5}
0.2	10	-0.2	-1.8161×10^{-1}	9.9547×10^{-2}	9.9218×10^{-2}	1.8390×10^{-2}
	100	-0.2	-1.9781×10^{-1}	9.6865×10^{-3}	9.6827×10^{-3}	2.1900×10^{-3}
0.3	10	-0.3	-2.7341×10^{-1}	9.5300×10^{-2}	9.4582×10^{-2}	2.6590×10^{-2}
	100	-0.3	-2.9687×10^{-1}	9.0241×10^{-3}	9.0143×10^{-3}	3.1300×10^{-3}
0.4	10	-0.4	-3.6434×10^{-1}	9.0698×10^{-2}	8.9435×10^{-2}	3.5660×10^{-2}
	100	-0.4	-3.9608×10^{-1}	8.6024×10^{-3}	8.5877×10^{-3}	3.9200×10^{-3}
0.5	10	-0.5	-4.5493×10^{-1}	8.4426×10^{-2}	8.2194×10^{-2}	4.5070×10^{-2}
	100	-0.5	-4.9533×10^{-1}	7.7212×10^{-3}	7.6993×10^{-3}	4.6700×10^{-3}
0.6	10	-0.6	-5.4432×10^{-1}	7.7740×10^{-2}	7.4647×10^{-2}	5.5680×10^{-2}
	100	-0.6	-5.9340×10^{-1}	6.5662×10^{-3}	6.5231×10^{-3}	6.6000×10^{-3}
0.7	10	-0.7	-6.3791×10^{-1}	6.7425×10^{-2}	6.3568×10^{-2}	6.2090×10^{-2}
	100	-0.7	-6.9267×10^{-1}	5.2886×10^{-3}	5.2353×10^{-3}	7.3300×10^{-3}
0.8	10	-0.8	-7.3311×10^{-1}	5.5550×10^{-2}	5.1078×10^{-2}	6.6890×10^{-2}
	100	-0.8	-7.9232×10^{-1}	3.9145×10^{-3}	3.8551×10^{-3}	7.6800×10^{-3}
0.85	10	-0.85	-7.8411×10^{-1}	4.7431×10^{-2}	4.3093×10^{-2}	6.5890×10^{-2}
	100	-0.85	-8.4202×10^{-1}	3.1096×10^{-3}	3.0453×10^{-3}	7.9800×10^{-3}
0.90	10	-0.9	-8.3169×10^{-1}	4.0044×10^{-2}	3.5373×10^{-2}	6.8310×10^{-2}
	100	-0.9	-8.9088×10^{-1}	2.2807×10^{-3}	2.1974×10^{-3}	9.1200×10^{-3}
0.95	10	-0.95	-8.9609×10^{-1}	2.5219×10^{-2}	2.2315×10^{-2}	5.391×10^{-2}
	100	-0.95	-9.4101×10^{-1}	1.3332×10^{-3}	1.2522×10^{-3}	8.9900×10^{-3}
0.99	10	-0.99	-9.6398×10^{-1}	8.2635×10^{-3}	7.5861×10^{-3}	2.6020×10^{-2}
	100	-0.99	-9.8209×10^{-1}	4.8610×10^{-4}	4.2336×10^{-4}	7.9100×10^{-3}
0.9999	10	-0.9999	-9.9896×10^{-1}	1.7938×10^{-4}	1.7848×10^{-4}	9.4000×10^{-4}
	100	-0.9999	-9.9931×10^{-1}	1.5377×10^{-5}	1.5035×10^{-5}	5.9000×10^{-4}

Table 4c Tabulated values of the statistics of $\hat{a}(1)$ for the YWUBC with λ and N_T as parameters and computed using $N_R = 10,000$ realizations.

λ	N_T	true σ_u^2	mean Re $\hat{\sigma}_u^2$ YWUBC	error variance of $\hat{\sigma}_u^2$ YWUBC	sample variance of $\hat{\sigma}_u^2$ YWUBC	bias $B[\hat{\sigma}_u^2]$ YWUBC
0.1	10	3.96	3.5536	1.5976	1.4325	4.0640×10^{-1}
	100	3.96	3.9199	1.6020×10^{-1}	1.5860×10^{-1}	4.0100×10^{-2}
0.2	10	3.84	3.4482	1.4830	1.3297	3.9180×10^{-1}
	100	3.84	3.8051	1.4842×10^{-1}	1.4722×10^{-1}	3.4900×10^{-2}
0.3	10	3.64	3.2627	1.3887	1.2465	3.7730×10^{-1}
	100	3.64	3.6099	1.2943×10^{-1}	1.2853×10^{-1}	3.0100×10^{-2}
0.4	10	3.36	3.0185	1.1599	1.0433	3.4150×10^{-1}
	100	3.36	3.3219	1.1348×10^{-1}	1.1205×10^{-1}	3.8100×10^{-2}
0.5	10	3.00	2.6973	9.6695×10^{-1}	8.7529×10^{-1}	3.0270×10^{-1}
	100	3.00	2.9714	8.8579×10^{-2}	8.7761×10^{-2}	2.8600×10^{-2}
0.6	10	2.56	2.2974	7.2121×10^{-1}	6.5231×10^{-1}	2.6260×10^{-1}
	100	2.56	2.5329	6.5913×10^{-2}	6.5186×10^{-2}	2.7100×10^{-2}
0.7	10	2.04	1.8303	5.2519×10^{-1}	4.8125×10^{-1}	2.0970×10^{-1}
	100	2.04	2.0199	4.2119×10^{-2}	4.1721×10^{-2}	2.0100×10^{-2}
0.8	10	1.44	1.2782	3.4662×10^{-1}	3.2047×10^{-1}	1.6180×10^{-1}
	100	1.44	1.4227	2.1857×10^{-1}	2.1560×10^{-2}	1.7300×10^{-2}
0.85	10	1.11	0.98478	2.6197×10^{-1}	2.4632×10^{-1}	1.2522×10^{-1}
	100	1.11	1.0950	1.3562×10^{-2}	1.3349×10^{-2}	1.5000×10^{-2}
0.9	10	0.76	6.8370×10^{-1}	1.8335×10^{-1}	1.7752×10^{-1}	7.6300×10^{-2}
	100	0.76	7.5113×10^{-1}	7.8289×10^{-3}	7.7503×10^{-3}	8.8700×10^{-3}
0.95	10	0.39	3.5411×10^{-1}	9.9623×10^{-2}	9.8345×10^{-2}	3.5890×10^{-2}
	100	0.39	3.8545×10^{-1}	3.9760×10^{-3}	3.9557×10^{-3}	4.5500×10^{-3}
0.99	10	0.0796	7.3049×10^{-2}	1.8724×10^{-2}	1.8681×10^{-2}	6.5510×10^{-3}
	100	0.0796	7.8683×10^{-2}	1.7837×10^{-3}	1.7828×10^{-3}	9.1700×10^{-4}
0.9999	10	8.0013×10^{-4}	6.6967×10^{-4}	1.8188×10^{-4}	1.8186×10^{-4}	1.3046×10^{-4}
	100	8.0013×10^{-4}	7.8370×10^{-4}	2.1419×10^{-5}	2.1419×10^{-5}	1.6430×10^{-5}

Table 4d Tabulated values of the statistics of $\hat{\sigma}_u^2$ for the YWUBC with λ and N_T as parameters and computed using $N_R = 10,000$ realizations.

λ	N_T	true a(1)	mean Re $\hat{a}(1)$ BURG	error variance of $\hat{a}(1)$ BURG	sample variance of $\hat{a}(1)$ BURG	bias B[$\hat{a}(1)$] BURG
0.1	10	-0.1	-8.9294×10^{-2}	9.9524×10^{-2}	9.9406×10^{-2}	1.0706×10^{-2}
	100	-0.1	-1.0031×10^{-1}	9.8274×10^{-3}	9.8249×10^{-3}	-3.1000×10^{-4}
0.2	10	-0.2	-1.8327×10^{-1}	9.9120×10^{-2}	9.8850×10^{-2}	1.6730×10^{-2}
	100	-0.2	-1.9729×10^{-1}	9.6306×10^{-3}	9.6242×10^{-3}	2.7100×10^{-3}
0.3	10	-0.3	-2.7314×10^{-1}	9.3171×10^{-2}	9.2458×10^{-2}	2.6860×10^{-2}
	100	-0.3	-2.9661×10^{-1}	9.2899×10^{-3}	9.2793×10^{-3}	3.3900×10^{-3}
0.4	10	-0.4	-3.6327×10^{-1}	8.8534×10^{-2}	8.7192×10^{-2}	3.6730×10^{-2}
	100	-0.4	-3.9625×10^{-1}	8.4301×10^{-3}	8.4168×10^{-3}	3.7500×10^{-3}
0.5	10	-0.5	-4.5390×10^{-1}	8.2327×10^{-2}	8.0201×10^{-2}	4.6100×10^{-2}
	100	-0.5	-4.9534×10^{-1}	7.6932×10^{-3}	7.6714×10^{-3}	4.6600×10^{-3}
0.6	10	-0.6	-5.4378×10^{-1}	7.5013×10^{-2}	7.1847×10^{-2}	5.6220×10^{-2}
	100	-0.6	-5.9440×10^{-1}	6.4842×10^{-3}	6.4531×10^{-3}	5.6000×10^{-3}
0.7	10	-0.7	-6.3707×10^{-1}	6.4977×10^{-2}	6.1022×10^{-2}	6.2930×10^{-2}
	100	-0.7	-6.9288×10^{-1}	5.2134×10^{-3}	5.1632×10^{-3}	7.1200×10^{-3}
0.8	10	-0.8	-7.3561×10^{-1}	5.1247×10^{-2}	4.7091×10^{-2}	6.4390×10^{-2}
	100	-0.8	-7.9190×10^{-1}	3.8491×10^{-3}	3.7838×10^{-3}	8.1000×10^{-3}
0.85	10	-0.85	-7.8489×10^{-1}	4.3703×10^{-2}	3.9469×10^{-2}	6.5110×10^{-2}
	100	-0.85	-8.4187×10^{-1}	3.0015×10^{-3}	2.9356×10^{-3}	8.1300×10^{-3}
0.9	10	-0.9	-8.3815×10^{-1}	3.5420×10^{-2}	3.1590×10^{-2}	6.1850×10^{-2}
	100	-0.9	-8.9110×10^{-1}	2.1737×10^{-3}	2.0945×10^{-3}	8.9000×10^{-3}
0.95	10	-0.95	-8.9749×10^{-1}	2.3537×10^{-2}	2.0781×10^{-2}	5.2510×10^{-2}
	100	-0.95	-9.4120×10^{-1}	1.2599×10^{-3}	1.1822×10^{-3}	8.8000×10^{-3}
0.99	10	-0.99	-9.6822×10^{-1}	6.6868×10^{-3}	6.2120×10^{-3}	2.1780×10^{-2}
	100	-0.99	-9.8332×10^{-1}	3.8344×10^{-4}	3.3881×10^{-4}	6.6800×10^{-3}
0.9999	10	-0.9999	-9.9917×10^{-1}	1.3863×10^{-4}	1.3803×10^{-4}	7.3000×10^{-4}
	100	-0.9999	-9.9949×10^{-1}	1.0509×10^{-5}	1.0299×10^{-5}	4.1000×10^{-4}

Table 4e Tabulated values of the statistics of $\hat{a}(1)$ for the Burg estimator with λ and N_T as parameters and computed using $N_R=10,000$ realizations.

λ	N_T	true σ_u^2	mean Re $\hat{\sigma}_u^2$ BURG	error variance of $\hat{\sigma}_u^2$ BURG	sample variance of $\hat{\sigma}_u^2$ BURG	bias $B[\hat{\sigma}_u^2]$ BURG
0.1	10	3.96	3.5694	1.6092	1.4566	3.9060×10^{-1}
	100	3.96	3.9199	1.6018×10^{-1}	1.5858×10^{-1}	4.0100×10^{-2}
0.2	10	3.84	3.4634	1.4662	1.3245	3.7660×10^{-1}
	100	3.84	3.7938	1.4626×10^{-1}	1.4414×10^{-1}	4.6200×10^{-2}
0.3	10	3.64	3.2607	1.3007	1.1569	3.7930×10^{-1}
	100	3.64	3.6014	1.3610×10^{-1}	1.3463×10^{-1}	3.8600×10^{-2}
0.4	10	3.36	3.0320	1.1482	1.0407	3.2800×10^{-1}
	100	3.36	3.3264	1.1364×10^{-1}	1.1252×10^{-1}	3.3600×10^{-2}
0.5	10	3.00	2.7151	9.1918×10^{-1}	8.3800×10^{-1}	2.8490×10^{-1}
	100	3.00	2.9715	8.8333×10^{-2}	8.7523×10^{-2}	2.8500×10^{-2}
0.6	10	2.56	2.3152	6.5754×10^{-1}	5.9765×10^{-1}	2.4480×10^{-1}
	100	2.56	2.5322	6.4634×10^{-2}	6.3870×10^{-2}	2.7800×10^{-2}
0.7	10	2.04	1.8583	4.1647×10^{-1}	3.8349×10^{-1}	1.8170×10^{-1}
	100	2.04	2.0216	5.2134×10^{-3}	4.0778×10^{-2}	1.8400×10^{-2}
0.8	10	1.44	1.3143	2.1044×10^{-1}	1.9466×10^{-1}	1.2570×10^{-1}
	100	1.44	1.4238	2.0554×10^{-2}	2.0294×10^{-2}	1.6200×10^{-2}
0.85	10	1.11	1.0187	1.2332×10^{-1}	1.1500×10^{-1}	9.1300×10^{-2}
	100	1.11	1.0992	1.2353×10^{-2}	1.2238×10^{-2}	8.0000×10^{-2}
0.9	10	0.76	6.9803×10^{-1}	5.9288×10^{-2}	5.5448×10^{-2}	6.1970×10^{-2}
	100	0.76	7.5200×10^{-1}	5.7107×10^{-3}	5.6467×10^{-3}	8.0000×10^{-3}
0.95	10	0.39	3.6265×10^{-1}	1.5734×10^{-2}	1.4988×10^{-2}	2.735×10^{-2}
	100	0.39	3.8643×10^{-1}	1.5107×10^{-3}	1.4981×10^{-3}	3.5700×10^{-3}
0.99	10	0.0796	7.4523×10^{-2}	6.5985×10^{-4}	6.3407×10^{-4}	5.0770×10^{-3}
	100	0.0796	7.9082×10^{-2}	6.4060×10^{-5}	6.3791×10^{-5}	5.1800×10^{-4}
0.9999	10	$8.0013 \times^{-4}$	7.5184×10^{-4}	6.9146×10^{-8}	6.6810×10^{-8}	4.8290×10^{-5}
	100	$8.0013 \times^{-4}$	7.9691×10^{-4}	6.3769×10^{-9}	6.3663×10^{-9}	3.2200×10^{-7}

Table 4f Tabulated values of the statistics of $\hat{\sigma}_u^2$ for the Burg estimator with λ and N_T as parameters and computed using $N_R = 10,000$ realizations.

61

Figure 12a Error variance of â(1) for the time averaged parameter estimators of an AR(1) process versus the one-lag temporal correlation parameter λ using N_T=10.

Figure 12b Error variance of $\hat{a}(1)$ for the time averaged parameter estimators of an AR(1) process versus the one-lag temporal correlation parameter λ using $N_T=10$ plotted on a log scale.

Figure 12c Error variance of $\hat{a}(1)$ for the time averaged parameter estimators of an AR(1) process versus the one-lag temporal correlation parameter λ using $N_T=100$.

Unlike the correlation function estimators, the error variance of the AR parameter estimators decreases with increasing temporal correlation. Between $\lambda=0.9$ and 0.9999, the decrease in error variance for these estimators is nearly three orders of magnitude as shown by the log scale plots of Figs.12b and 12c. In Fig.12a, it is also interesting to note that for the small N_T size used here (ie., $N_T=10$), the error variance for (YWBC) is the lowest of the three for processes with low temporal correlation (ie., $\lambda \approx 0.1$). However, in Fig.13, we also observe that the bias $B[\hat{a}(1)]$ of the (YWBC) estimate $\hat{a}(1)$ computed over the 10,000 realizations is larger compared to the other two estimators for all values of λ and N_T. The explanation for this apparently contradictory behavior is found in Fig.14 where we observe that the variance of $\hat{a}(1)$ using (YWBC) is much smaller than the other estimators. From eq(4.73) in section 4.4, we note that a very small variance $\sigma_{\hat{a}}^2$ can compensate for a large bias thus resulting in a low error variance. At a value of $\lambda \approx 0.65$, however, a cross-over occurs in the curves shown in Fig.12a so that the error variances of the Burg and (YWUBC) algorithms are lower than the (YWBC) at higher temporal correlation values. This results from the lower biases of the former algorithms as well as the fact that the $\sigma_{\hat{a}}^2$ values for the three estimators converge at high λ (see Fig.14).

In Figs.15a, b and c, we show the convergence of the mean estimate $\hat{a}(1)$ to the true parameter value as N_T increases for values of $\lambda=0.1$, 0.9, and 0.9999, respectively. For small time window sizes (ie., small N_T), the bias of the YWUBC is barely, but slightly, smaller than that of the Burg estimator (see Fig.15a). As the temporal correlation increases, however, the performance of the Burg estimator is superior as shown in Figs.15b and c. Finally, although the bias of the YWBC estimator appears to be increasing dramatically for increasing temporal correlation (see Fig.15c) as compared to the other estimators, the percentage error is actually decreasing thus showing performance improvement with increasing temporal correlation. In Figs.16, 17 and 18, we show plots for the error variance, the bias and the estimator variance for $\hat{\sigma}_u^2$.

Tables 5a, b and c list the means, error variances and estimator variances $\sigma_{\hat{a}}^2$, respectively, of $\hat{a}(1)$, $\hat{a}(2)$ and $\hat{\sigma}_u^2$ for single channel AR(2) processes with various one-lag temporal correlation parameters λ using the order 2 Burg
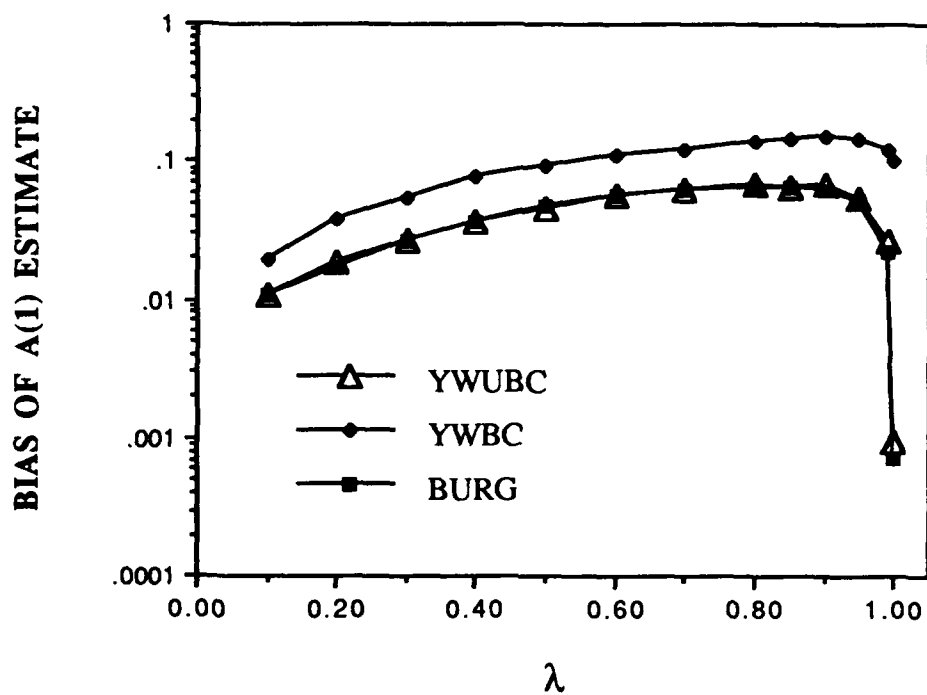
Figure 13 Bias B[$\hat{a}(1)$] for the time-averaged parameter estimators of an AR(1) process versus the one-lag temporal correlation parameter using $N_T=10$.
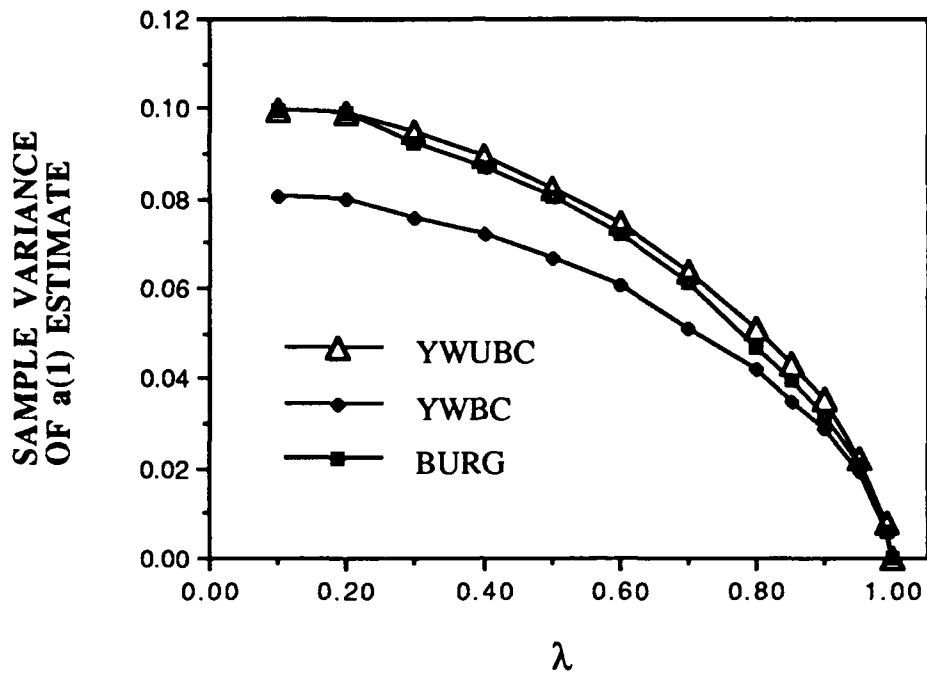
Figure 14a Sample variance of $\hat{a}(1)$ for the time averaged parameter estimators of an AR(1) process versus the one-lag temporal correlation parameter λ using $N_T=10$.
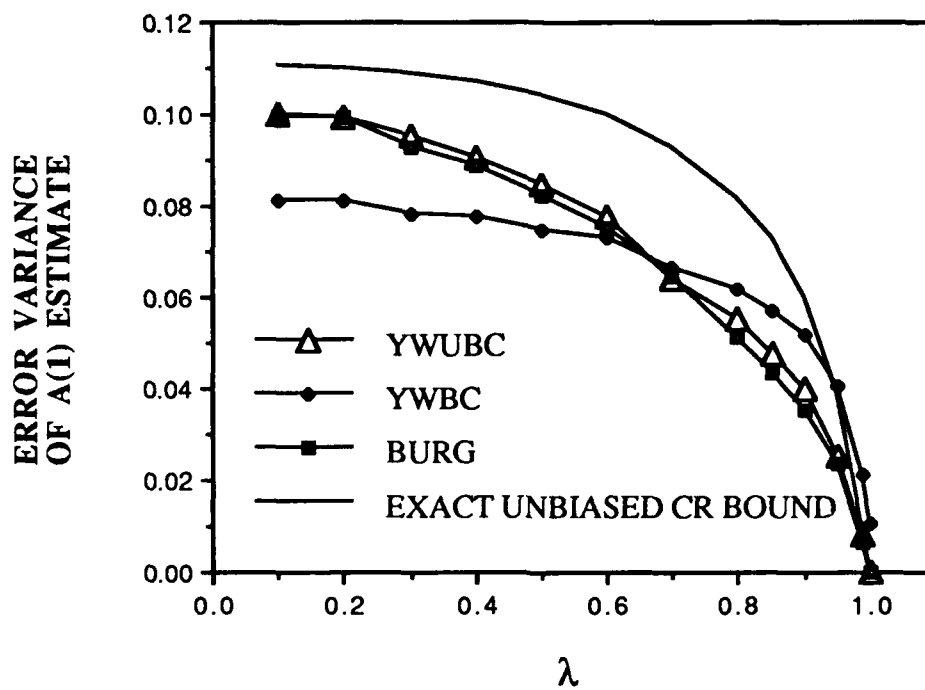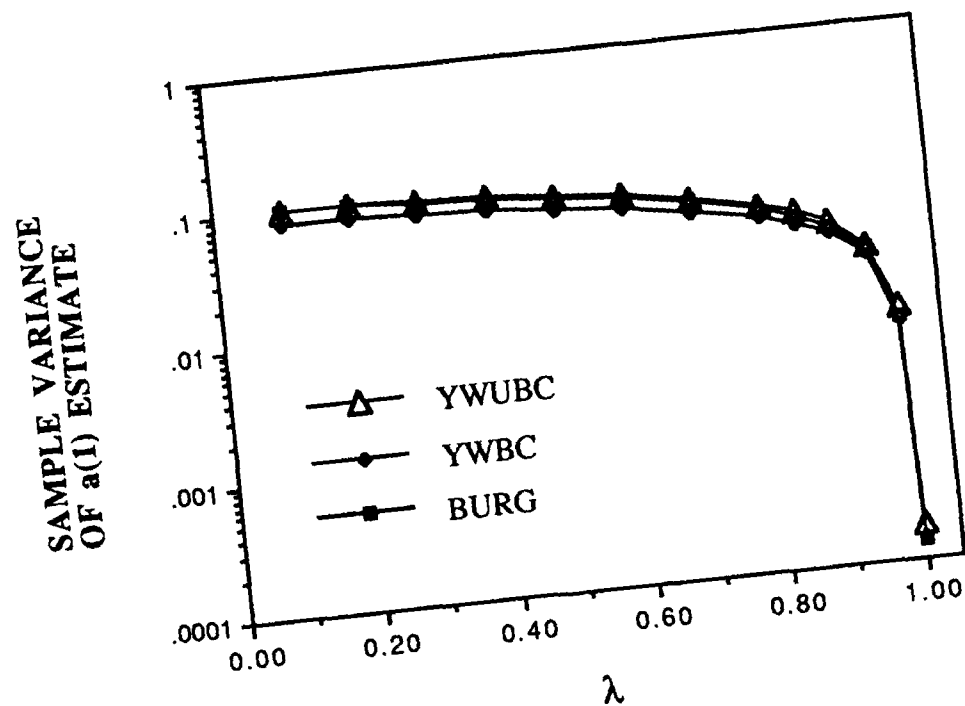
Figure 14b Sample variance of $\hat{a}(1)$ for the time averaged parameter estimators of an AR(1) process versus the one-lag temporal correlation parameter λ using $N_T=10$ plotted on a log scale.
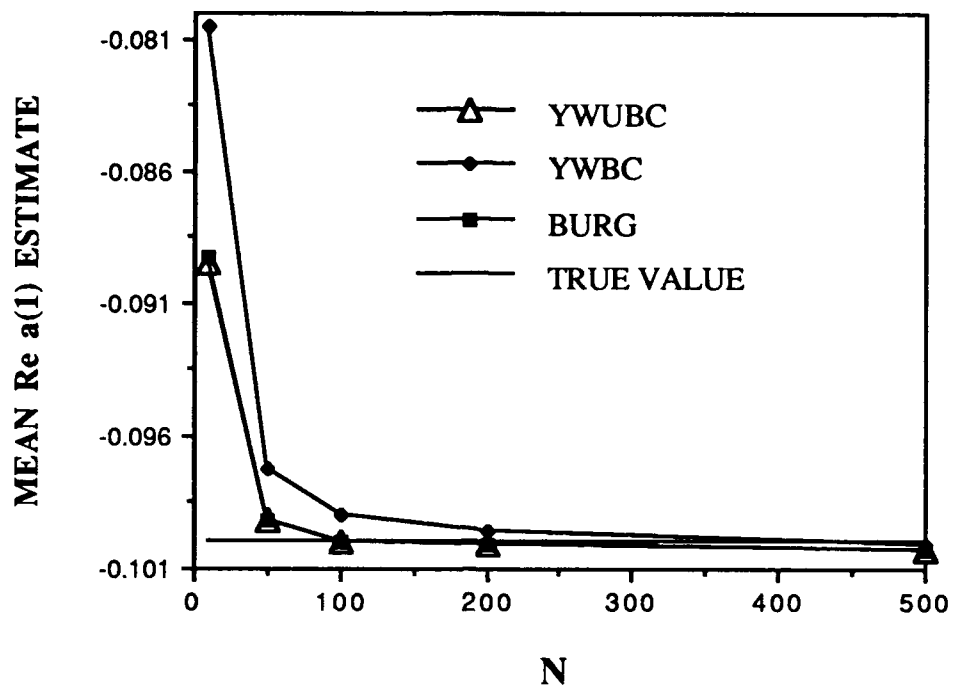
Figure 15a   Mean of $\hat{a}(1)$ versus N_T for an AR(1) process with a one-lag temporal correlation parameter $\lambda=0.1$.
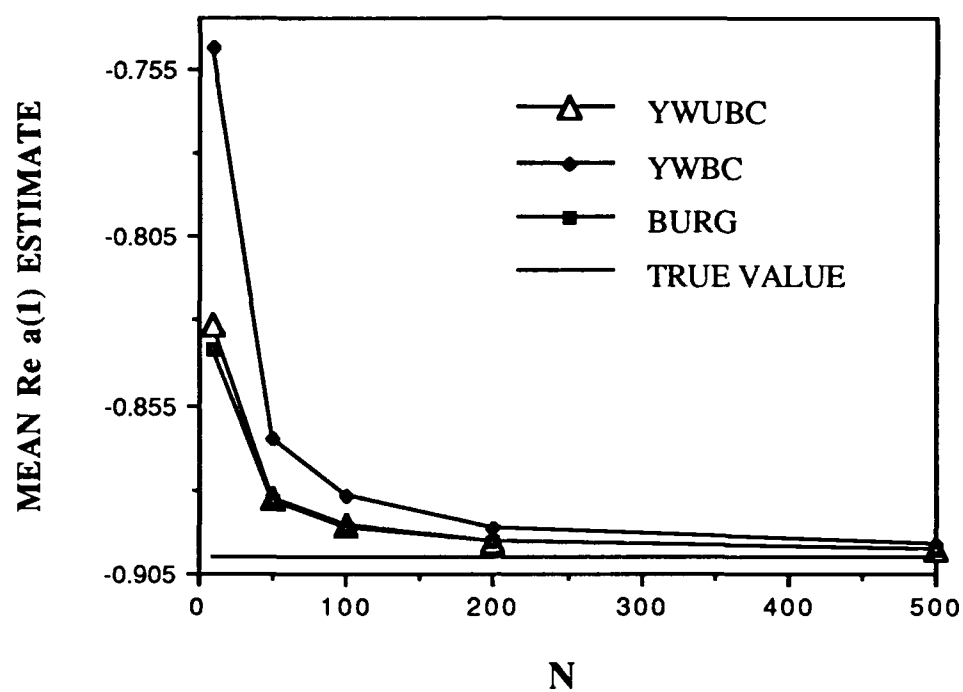
Figure 15b   Mean of $\hat{a}(1)$ versus N_T for an AR(1) process with a one-lag temporal correlation parameter $\lambda=0.9$.
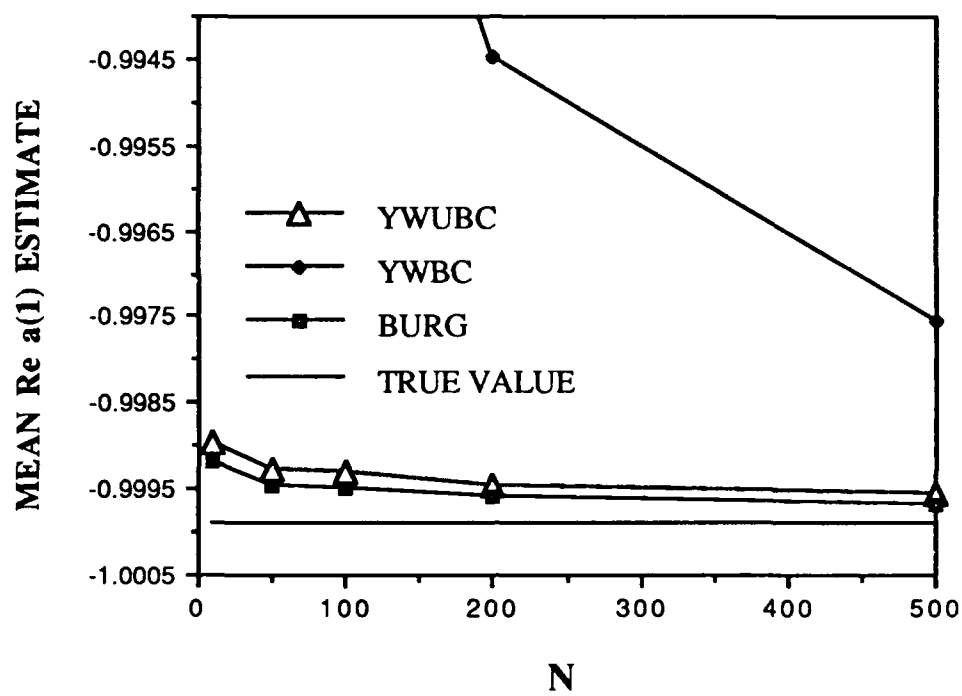
Figure 15c Mean of $\hat{a}(1)$ versus N_T for an AR(1) process with a one-lag temporal correlation parameter $\lambda=0.9999$.
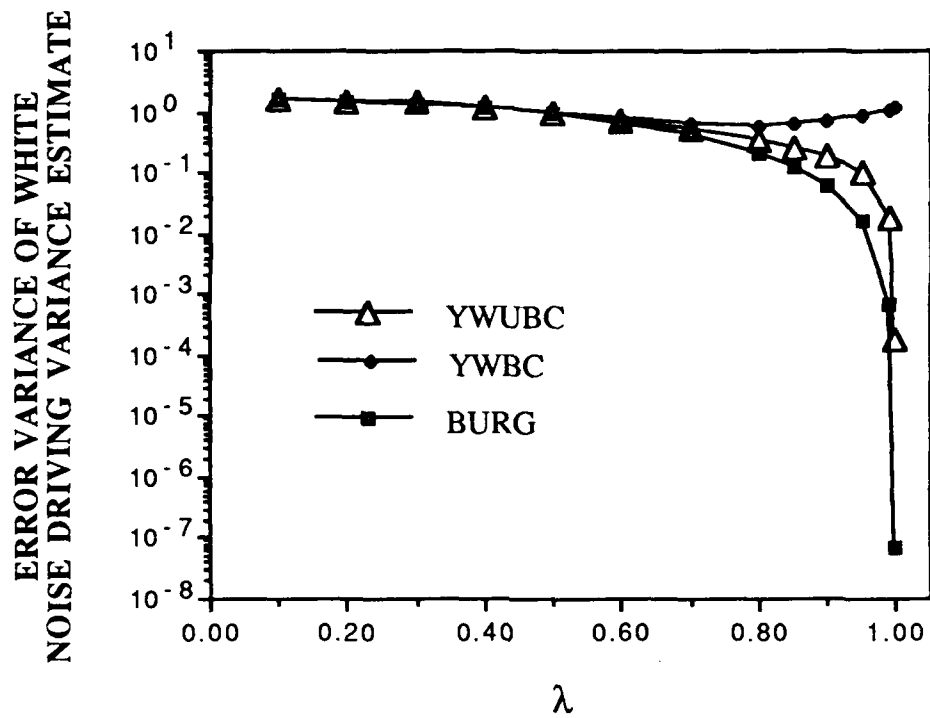
Figure 16 Error variance of $\hat{\sigma}_u^2$ for the time-averaged parameter estimators of an AR(1) process versus the one-lag temporal correlation parameter λ using $N_T=10$.
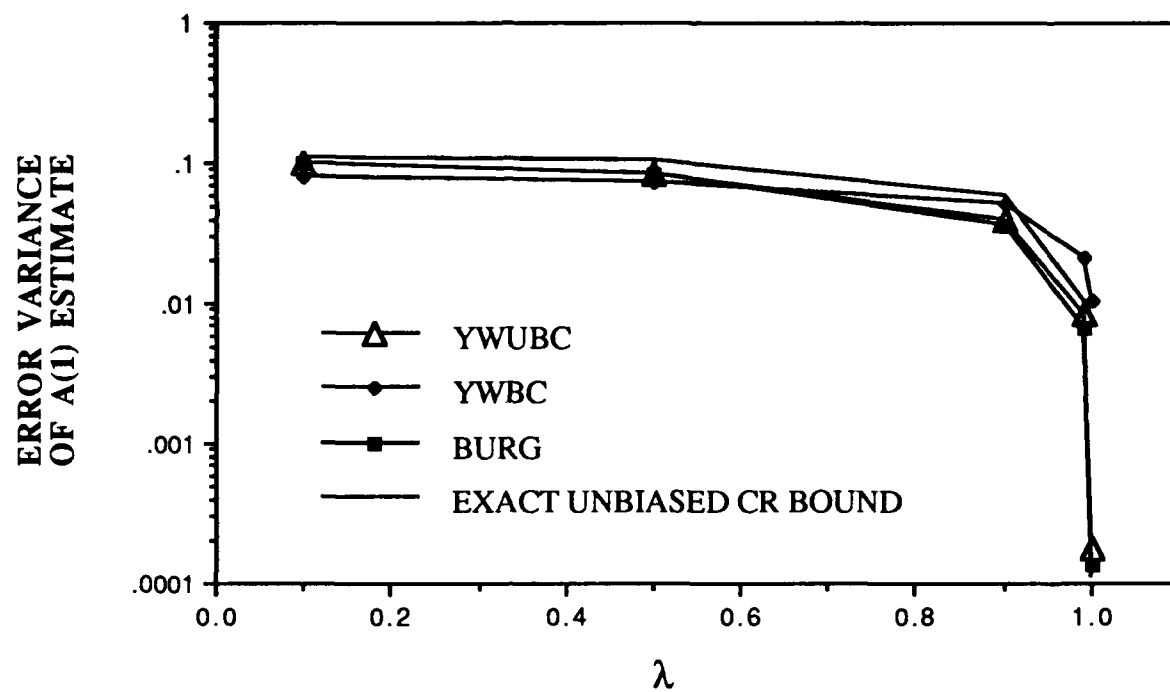
Figure 17 Bias of $\hat{\sigma}_u^2$ for the time-averaged parameter estimators of an AR(1) process versus the one-lag temporal correlation parameter λ using $N_T=10$.

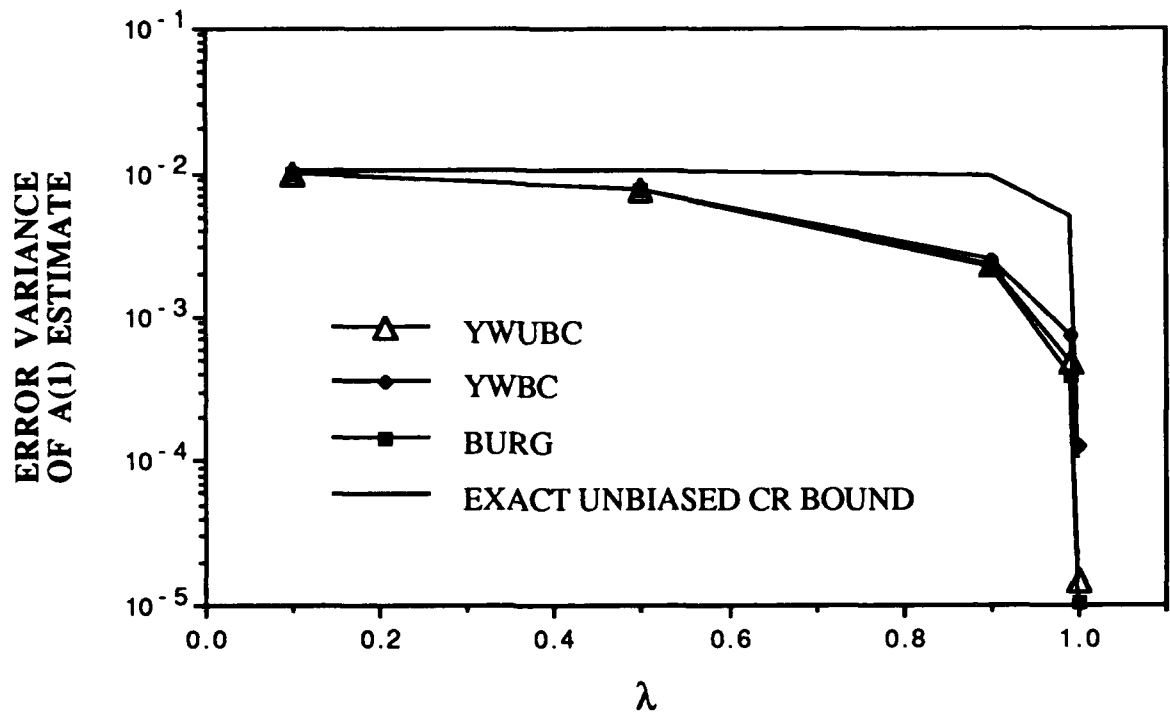Figure 18 Sample variance of $\hat{\sigma}_u^2$ for the time-averaged parameter estimators of an AR(1) process versus the one-lag temporal correlation parameter λ using $N_T=10$.

λ	N_T	true a(1)	mean Re $\hat{a}(1)$ Burg Algorith.	true a(2)	mean Re $\hat{a}(2)$ Burg Algorith.	true σ_u^2	mean Re $\hat{\sigma}_u^2$ Burg Algorith
0.1	10	-0.101	-0.089682	0.01	0.012920	3.9596	3.1581
	100	-0.101	-0.099617	0.01	0.0098845	3.9596	3.8812
0.5	10	-0.625	-0.56279	0.25	0.20679	2.8125	2.249
	100	-0.625	-0.61665	0.25	0.24397	2.8125	2.7597
0.6	10	-0.816	-0.73757	0.36	0.29377	2.2282	1.7904
	100	-0.816	-0.80760	0.36	0.35263	2.2282	2.1835
0.7	10	-1.043	-0.94039	0.49	0.40322	1.5502	1.2639
	100	-1.043	-1.0317	0.49	0.47984	1.5502	1.519
0.8	10	-1.312	-1.1861	0.64	0.52919	0.8502	0.70077
	100	-1.312	-1.2994	0.64	0.62764	0.8502	0.83313
0.85	10	-1.464	-1.3292	0.7225	0.6045	0.53057	0.44617
	100	-1.464	-1.4494	0.7225	0.70769	0.53057	0.52050
0.9	10	-1.629	-1.4964	0.81	0.6955	0.26136	0.22303
	100	-1.629	-1.6133	0.81	0.7948	0.26136	0.25648
0.99	10	-1.9603	-1.8633	0.98	0.89688	3.1361e-3	4.4644×10^{-3}
	100	-1.9603	-1.9470	0.98	0.96703	3.1361e-3	3.0977×10^{-3}
0.9999	10	-1.9995	-1.9809	0.9997	0.98197	4.7677e-7	1.9573×10^{-6}
	100	-1.9995	-1.9974	0.9997	0.99774	4.7677e-7	6.3050×10^{-7}

Table 5a   Mean of estimated parameters for a Gaussian AR(2) process using the Burg algorithm with λ and N_T as parameters and N_R=10,000.

λ	N_T	error var $\hat{a}(1)$ Burg Algorith.	error var $\hat{a}(2)$ Burg Algorith.	error var $\hat{\sigma}_u^2$ Burg Algorith
0.1	10	1.1012×10^{-1}	1.1393×10^{-1}	1.9373
	100	1.0019×10^{-2}	1.0303×10^{-2}	1.6370×10^{-1}
0.5	10	1.1239×10^{-2}	1.1166×10^{-1}	9.398×10^{-1}
	100	9.6568×10^{-3}	9.5378×10^{-3}	8.0525×10^{-2}
0.6	10	1.1145×10^{-1}	1.0946×10^{-1}	5.9132×10^{-1}
	100	9.1010×10^{-3}	9.0057×10^{-3}	5.0494×10^{-2}
0.7	10	1.0683×10^{-1}	1.0539×10^{-1}	2.8203×10^{-1}
	100	7.9729×10^{-3}	8.040×10^{-3}	2.4269×10^{-2}
0.8	10	9.9714×10^{-2}	9.6516×10^{-2}	8.5696×10^{-2}
	100	6.4081×10^{-3}	6.2261×10^{-3}	7.3920×10^{-3}
0.85	10	9.39520×10^{-2}	8.9116×10^{-2}	3.3739×10^{-2}
	100	5.2861×10^{-3}	5.2873×10^{-3}	2.8461×10^{-3}
0.9	10	7.992×10^{-2}	7.3954×10^{-2}	8.181×10^{-3}
	100	4.0572×10^{-3}	4.006×10^{-3}	7.026×10^{-4}
0.99	10	3.2103×10^{-2}	3.0368×10^{-2}	1.2169×10^{-5}
	100	8.405×10^{-4}	8.3077×10^{-4}	9.938×10^{-8}
0.9999	10	5.6797×10^{-3}	4.6069×10^{-3}	1.7209×10^{-10}
	100	$5.0524 xx 10^{-5}$	5.0442×10^{-5}	1.1187×10^{-13}

Table 5b   Error variances of the estimated parameters for a Gaussian AR(2) process using the Burg algorithm with λ and N_T as parameters and $N_R = 10,000$.

λ	N_T	sample var $\hat{a}(1)$ Burg Algorith.	sample var $\hat{a}(2)$ Burg Algorith.	sample var $\hat{\sigma}_u^2$ Burg Algorith
0.1	10	1.1000×10^{-1}	1.1394×10^{-1}	1.2950
	100	1.0018×10^{-2}	1.0304×10^{-2}	1.5756×10^{-1}
0.5	10	1.0851×10^{-1}	1.0978×10^{-1}	6.2231×10^{-1}
	100	9.5875×10^{-3}	9.5023×10^{-3}	7.7746×10^{-2}
0.6	10	1.0530×10^{-1}	1.0508×10^{-1}	3.9965×10^{-1}
	100	9.0303×10^{-3}	8.9521×10^{-3}	4.8494×10^{-2}
0.7	10	9.6310×10^{-2}	9.7858×10^{-2}	2.0006×10^{-1}
	100	7.8448×10^{-3}	7.9375×10^{-3}	2.3301×10^{-2}
0.8	10	8.3871×10^{-2}	8.4242×10^{-2}	6.3381×10^{-2}
	100	6.2500×10^{-3}	6.0740×10^{-3}	7.1021×10^{-3}
0.85	10	7.5749×10^{-2}	7.5200×10^{-2}	2.6618×10^{-2}
	100	5.0711×10^{-3}	5.0684×10^{-3}	2.7448×10^{-3}
0.9	10	6.2334×10^{-2}	6.0849×10^{-2}	6.7118×10^{-3}
	100	3.8104×10^{-3}	3.7745×10^{-3}	6.7881×10^{-4}
0.99	10	2.2685×10^{-2}	2.3444×10^{-2}	1.0406×10^{-5}
	100	6.6275×10^{-4}	6.5986×10^{-4}	9.7917×10^{-8}
0.9999	10	4.3379×10^{-3}	4.2963×10^{-3}	1.7008×10^{-10}
	100	4.6262×10^{-5}	4.6589×10^{-5}	8.8243×10^{-14}

Table 5c Sample variances of the estimated parameters for a Gaussian AR(2) process using the Burg algorithm with λ and N_T as parameters and $N_R = 10,000$.

estimator. The estimates were obtained using batch sizes of $N_T=10$ and 100. Again, the number of repeated realizations was $N_R=10,000$. Figs.19, 20 and 21 show the error variances of $\hat{a}(1)$, $\hat{a}(2)$ and $\hat{\sigma}_u^2$, respectively. Again, a significant decrease in the error variance is noted at high values of temporal correlation. For $\hat{\sigma}_u^2$, the reduction in error variance using $N_T=100$ is approximately 12 orders of magnitude between $\lambda=0.1$ and 0.9999.

The important point to be made regarding the above observations is that the error variance, the estimator variance and the bias of the estimators are not only dependent upon N_T, but also on process correlation. Furthermore, the superiority of a given estimator may change significantly depending upon process correlation especially for low valuses of N_T.
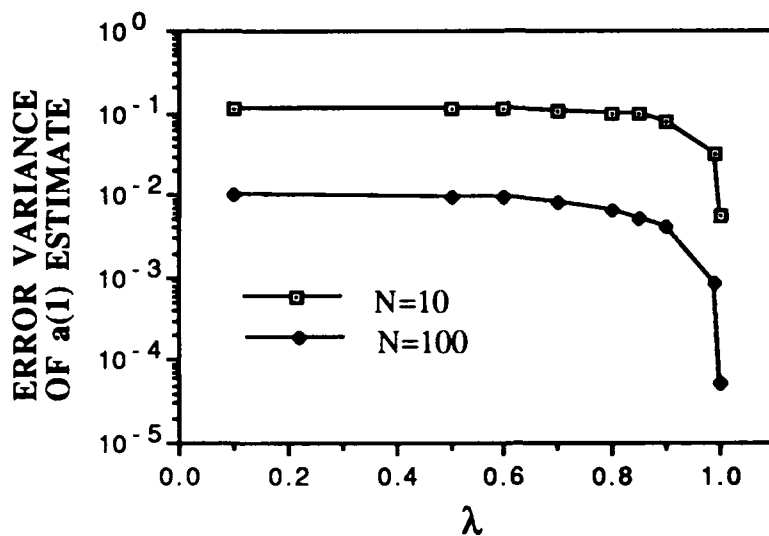
Figure 19 Error variance of $\hat{a}(1)$ for an AR(2) process using the Burg algorithm with $N_T=10$ and 100.
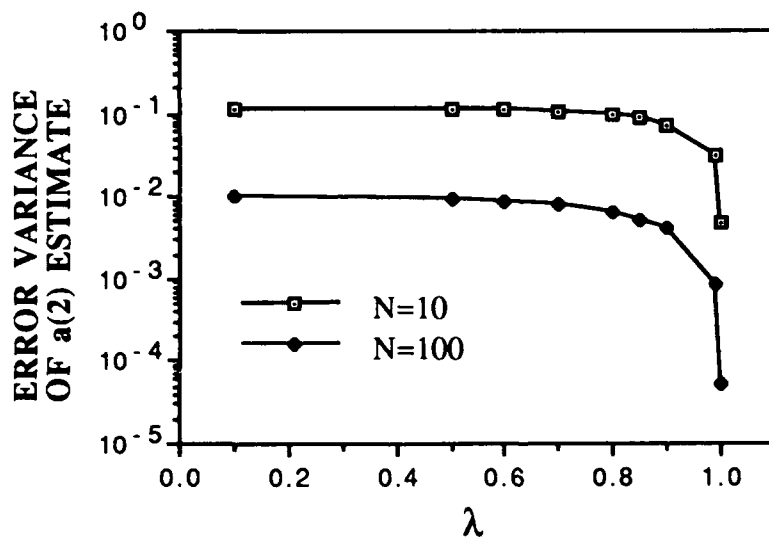
Figure 20 Error variance of $\hat{a}(2)$ for an AR(2) process using the Burg algorithm with $N_T=10$ and 100.
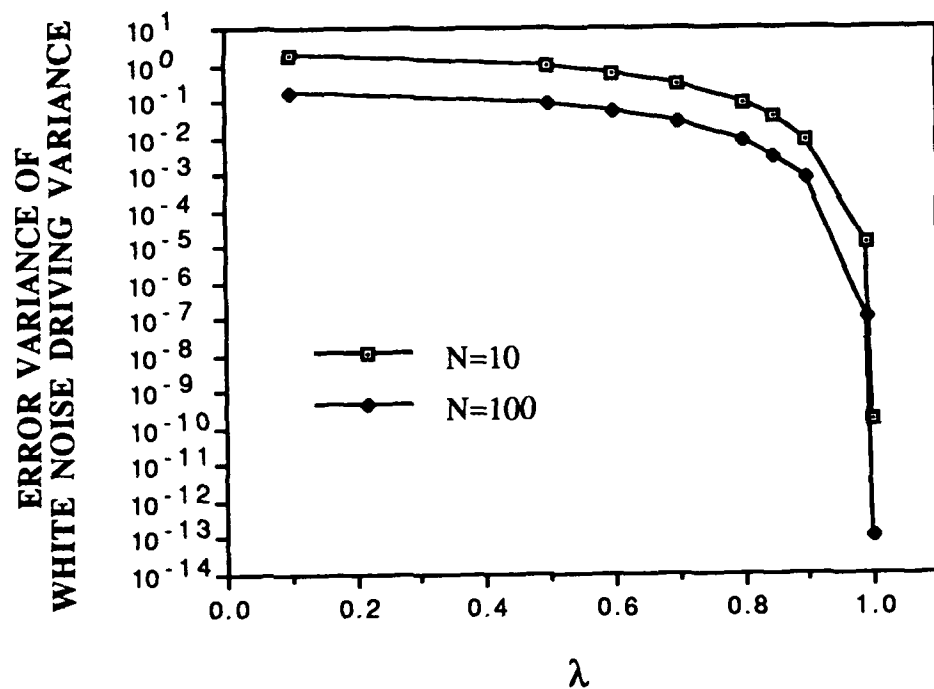
Figure 21 Error variance of $\hat{\sigma}_u^2$ for an AR(2) process using the Burg algorithm with N_T=10 and 100.

5.3.2 Performance with Non-Gaussian SIRP Processes

In this subsection, computed simulation results of the error variances are presented using the Burg estimator for autoregressive (AR) time series models where the white noise driving process is non-Gaussian. Again, the order of the process is assumed known. The non-Gaussian processes are modeled from the general class known as spherically invariant random processes (SIRP). In [7], the synthesis of such processes is developed. The special case of a K-distributed SIRP process is considered here. Detection analyses involving K-distributed clutter processes are presented in [8]. For processes consisting of in-phase (real) and quadrature (imaginary) components, the K-distributed envelope PDF is expressed as

$$f_R(r) = \frac{2\sqrt{\alpha}}{\Gamma(\alpha)}\left[\frac{\sqrt{\alpha}\,r}{2}\right]^\alpha K_{\alpha-1}(\sqrt{\alpha}\,r) \qquad (0 \le r \le \infty)$$

where $\Gamma(\alpha)$ is the Eulerian Gamma function, $K_\alpha(\bullet)$ is the modified Bessel function of the second kind with order α. Here, α is refered to as the shape parameter.

AR(4) processes with various degrees of temporal correlation are synthesized using various shape parameters, α. The sample mean, sample variance and error variances of the estimated AR parameters and white noise driving variances are listed in Tables 6a through 6d for several values of α and λ. In all cases, N_T=1000 time samples were used to obtain each estimate and N_R=1000 realizations were used to obtain the statistics.

Examination of the tables reveals that using N_T=1000 time samples, good estimates with low error variances are obtained for the a(k) coefficients, k=1 to 4, for nearly all values of α and λ. Furthermore, the error variances for the estimates of a(k) are insensitive to α. The same point cannot be made for the estimate of the white noise driving variance, $\hat{\sigma}_u^2$, however. Although, the estimates of the mean values of $\hat{\sigma}_u^2$ are quite good (using N_T=1000), the associated error variances are quite revealing. In Figs. 18 and 19, we plot the error variances of $\hat{\sigma}_u^2$ as a function of α with λ as a parameter. Each curve reveals a significant decrease in the error variance with increasing α (approximately two orders of magnitude between α=0.1 and 10). This result is explained by first noting that in the limit as $\alpha \rightarrow \infty$, K-distributed processes approach that of the

81

α		true value	sample mean	sample variance	error variance	bias
	a(1)	-0.32965	-0.32885	9.6365×10^{-4}	9.6442×10^{-4}	$+8.000 \times 10^{-4}$
	a(2)	0.09963	0.099624	1.0361×10^{-3}	1.0361×10^{-3}	-6.000×10^{-6}
0.1	a(3)	-0.02967	-0.030629	1.0648×10^{-3}	1.0665×10^{-3}	-9.590×10^{-4}
	a(4)	0.0081	0.009436	1.0500×10^{-3}	1.0518×10^{-3}	$+1.336 \times 10^{-3}$
	σ_u^2	3.6076	3.7466	169.19	169.21	0.139
	a(1)	-0.32965	-0.32946	1.0004×10^{-3}	1.0004×10^{-3}	$+1.900 \times 10^{-4}$
	a(2)	0.09963	0.099045	1.0895×10^{-3}	1.0899×10^{-3}	-5.850×10^{-4}
0.5	a(3)	-0.02967	-0.02976	1.0977×10^{-3}	1.0978×10^{-3}	-9.000×10^{-5}
	a(4)	0.0081	0.008522	9.9183×10^{-4}	9.9223×10^{-4}	$+4.220 \times 10^{-4}$
	σ_u^2	3.6076	3.6551	26.818	26.820	$+4.750 \times 10^{-2}$
	a(1)	-0.32965	-0.3302	9.4419×10^{-4}	9.4479×10^{-4}	-5.500×10^{-4}
	a(2)	0.09963	0.09920	1.0639×10^{-3}	1.0644×10^{-3}	-4.300×10^{-4}
1.0	a(3)	-0.02967	-0.028524	1.1300×10^{-3}	1.1320×10^{-3}	$+1.146 \times 10^{-3}$
	a(4)	0.0081	0.007151	9.7787×10^{-4}	9.7973×10^{-4}	-9.490×10^{-4}
	σ_u^2	3.6076	3.6619	13.606	13.609	$+5.430 \times 10^{-2}$
	a(1)	-0.32965	-0.33011	9.5535×10^{-4}	9.5572×10^{-4}	-4.600×10^{-4}
	a(2)	0.09963	0.10060	1.0742×10^{-3}	1.0752×10^{-3}	$+9.700 \times 10^{-4}$
10	a(3)	-0.02967	-0.029265	1.0702×10^{-3}	1.0752×10^{-3}	$+4.050 \times 10^{-4}$
	a(4)	0.0081	0.0078392	1.0327×10^{-3}	1.0328×10^{-3}	-2.610×10^{-4}
	σ_u^2	3.6076	3.6188	1.237	1.2378	$+1.120 \times 10^{-2}$
	a(1)	-0.32965	-0.32947	1.0314×10^{-3}	1.0310×10^{-3}	$+1.800 \times 10^{-4}$
	a(2)	0.09963	0.098557	1.0885×10^{-3}	1.0886×10^{-3}	-1.073×10^{-3}
∞	a(3)	-0.02967	-0.028013	1.1002×10^{-3}	1.1034×10^{-3}	$+1.657 \times 10^{-3}$
	a(4)	0.0081	0.0066742	1.0106×10^{-3}	1.0124×10^{-3}	-1.426×10^{-3}
	σ_u^2	3.6076	3.5965	1.3756×10^{-2}	1.3866×10^{-2}	-1.110×10^{-2}

Table 6a. Performance of the Burg estimator for an AR(4) process with α as a parameter and $\lambda = 0.3$, $N_T = 1000$ and $N_R = 1000$.

α		true value	sample mean	sample variance	error variance	bias
0.1	$a(1)$	-1.2934	-1.2914	9.4170×10^{-4}	9.456×10^{-4}	$+2.000 \times 10^{-3}$
	$a(2)$	1.0513	1.0486	2.0586×10^{-3}	2.066×10^{-3}	-2.700×10^{-3}
	$a(3)$	-0.63378	-0.6312	2.0904×10^{-3}	2.099×10^{-3}	$+2.580 \times 10^{-3}$
	$a(4)$	0.2401	0.2388	9.0343×10^{-4}		-1.300×10^{-3}
	σ_u^2	1.2891	1.2810	3.137×10^{-2}	3.144×10^{-2}	-8.100×10^{-3}
0.5	$a(1)$	-1.2934	-1.2911	9.3737×10^{-4}	9.4255×10^{-4}	$+2.300 \times 10^{-3}$
	$a(2)$	1.0513	1.0492	2.1866×10^{-3}	2.1910×10^{-3}	-2.100×10^{-3}
	$a(3)$	-0.63378	-0.63199	2.2355×10^{-3}	2.2390×10^{-3}	$+1.790 \times 10^{-3}$
	$a(4)$	0.2401	0.23968	9.0611×10^{-4}	9.0646×10^{-4}	-4.200×10^{-4}
	σ_u^2	1.2890	1.2807	8.1152×10^{-3}	8.1839×10^{-3}	-8.300×10^{-3}
1.0	$a(1)$	-1.2934	-1.2925	9.0805×10^{-4}	9.0888×10^{-4}	$+9.000 \times 10^{-4}$
	$a(2)$	1.0513	1.0485	2.0950×10^{-3}	2.1027×10^{-3}	-2.800×10^{-3}
	$a(3)$	-0.63378	-0.6299	2.1903×10^{-3}	2.2059×10^{-3}	$+3.880 \times 10^{-3}$
	$a(4)$	0.2401	0.2377	9.3840×10^{-4}	9.4483×10^{-4}	-2.400×10^{-3}
	σ_u^2	1.2890	1.2841	4.9590×10^{-3}	4.9826×10^{-3}	-4.900×10^{-3}
10	$a(1)$	-1.2934	-1.2917	9.3806×10^{-4}	9.4155×10^{-4}	$+1.700 \times 10^{-3}$
	$a(2)$	1.0513	1.0484	2.2654×10^{-3}	2.2762×10^{-3}	-2.900×10^{-3}
	$a(3)$	-0.63378	-0.63092	2.3454×10^{-3}	2.3551×10^{-3}	$+2.860 \times 10^{-3}$
	$a(4)$	0.2401	0.2383	9.8906×10^{-4}	9.9259×10^{-4}	-1.800×10^{-3}
	σ_u^2	1.2890	1.2830	2.0194×10^{-3}	2.0554×10^{-3}	-6.000×10^{-3}
∞	$a(1)$	-1.2934	-1.2923	9.0910×10^{-4}	9.0947×10^{-4}	$+1.100 \times 10^{-3}$
	$a(2)$	1.0513	1.0497	2.0942×10^{-3}	2.0951×10^{-3}	-1.600×10^{-3}
	$a(3)$	-0.63378	-0.63156	2.1302×10^{-3}	2.1340×10^{-3}	$+2.220 \times 10^{-3}$
	$a(4)$	0.2401	0.23923	9.2802×10^{-4}	9.2785×10^{-4}	-8.700×10^{-4}
	σ_u^2	1.2890	1.2834	1.6744×10^{-3}	1.7038×10^{-3}	-5.600×10^{-3}

Table 6b. Performance of the Burg estimator for an AR(4) process with α as a parameter and $\lambda=0.7$, $N_T=1000$ and $N_R=1000$.

α		true value	sample mean	sample variance	error variance	bias
	$a(1)$	-2.6978	-2.6949	5.9992×10^{-4}	6.0853×10^{-4}	$+2.900 \times 10^{-3}$
	$a(2)$	3.3081	3.3013	3.2060×10^{-3}	3.2524×10^{-3}	-6.800×10^{-3}
0.1	$a(3)$	-2.1852	-2.1788	3.1615×10^{-3}	3.2027×10^{-3}	$+6.400 \times 10^{-3}$
	$a(4)$	0.6561	0.65389	5.8826×10^{-4}	5.9325×10^{-4}	-2.210×10^{-3}
	σ_u^2	0.069747	0.067509	5.8782×10^{-2}	5.8787×10^{-2}	-2.238×10^{-3}
	$a(1)$	-2.6978	-2.6939	5.6190×10^{-4}	5.7698×10^{-4}	$+3.900 \times 10^{-3}$
	$a(2)$	3.3081	3.2985	3.1312×10^{-3}	3.2225×10^{-3}	-9.600×10^{-3}
0.5	$a(3)$	-2.1852	-2.1753	3.1650×10^{-3}	3.2641×10^{-3}	$+9.90 \times 10^{-3}$
	$a(4)$	0.6561	0.6519	5.9119×10^{-4}	6.0818×10^{-4}	-4.200×10^{-3}
	σ_u^2	0.069747	0.070988	9.9154×10^{-3}	9.9169×10^{-3}	$+1.241 \times 10^{-3}$
	$a(1)$	-2.6978	-2.6945	5.5612×10^{-4}	5.6765×10^{-4}	$+3.300 \times 10^{-3}$
	$a(2)$	3.3081	3.3006	3.0109×10^{-3}	3.0704×10^{-3}	-7.500×10^{-3}
1.0	$a(3)$	-2.1852	-2.1778	3.0589×10^{-3}	3.1154×10^{-3}	$+7.400 \times 10^{-3}$
	$a(4)$	0.6561	0.65298	5.6884×10^{-4}	5.7859×10^{-4}	-3.120×10^{-3}
	σ_u^2	0.069747	0.07194	5.1243×10^{-3}	5.1291×10^{-3}	$+2.193 \times 10^{-3}$
	$a(1)$	-2.6978	-2.6953	5.7912×10^{-4}	5.8551×10^{-4}	$+2.500 \times 10^{-3}$
	$a(2)$	3.3081	3.3014	3.0688×10^{-3}	3.1151×10^{-3}	-6.700×10^{-3}
10	$a(3)$	-2.1852	-2.1781	2.9719×10^{3}	3.0236×10^{-3}	$+7.100 \times 10^{-3}$
	$a(4)$	0.6561	0.65319	5.3793×10^{-4}	5.4664×10^{-4}	-2.910×10^{-3}
	σ_u^2	0.069747	0.069316	4.9057×10^{-4}	4.9076×10^{-4}	-4.310×10^{-4}
	$a(1)$	-2.6978	-2.695	5.5435×10^{-4}	5.6151×10^{-4}	$+2.800 \times 10^{-3}$
	$a(2)$	3.3081	3.3008	2.9622×10^{-3}	3.0152×10^{-3}	-7.300×10^{-3}
∞	$a(3)$	-2.1852	-2.1773	2.9584×10^{-3}	3.0199×10^{-3}	$+7.900 \times 10^{-3}$
	$a(4)$	0.6561	0.6526	5.6196×10^{-4}	5.7378×10^{-4}	-3.500×10^{-3}
	σ_u^2	0.069747	0.069499	4.9018×10^{-6}	4.9591×10^{-6}	-2.480×10^{-4}

Table 6c. Performance of the Burg estimator for an AR(4) process with α as a parameter and $\lambda=0.9$, $N_T=1000$ and $N_R=1000$.

α		true value	sample mean	sample variance	error variance	bias
0.1	$a(1)$	-3.8729	-3.8696	2.7532×10^{-5}	3.8603×10^{-5}	$+3.30 \times 10^{-3}$
	$a(2)$	5.7379	5.7280	2.3402×10^{-4}	3.3179×10^{-4}	-9.900×10^{-3}
	$a(3)$	-3.8542	-3.8442	2.3299×10^{-4}	3.3238×10^{-4}	$+1.100 \times 10^{-2}$
	$a(4)$	0.99033	0.98695	2.7189×10^{-5}	3.8638×10^{-5}	-3.380×10^{-3}
	σ_u^2	3.4907×10^{-6}	2.8519×10^{-6}	7.5142×10^{-11}	7.555×10^{-11}	-6.388×10^{-7}
0.5	$a(1)$	-3.8729	-3.8698	2.6899×10^{-5}	3.6670×10^{-5}	$+3.100 \times 10^{-3}$
	$a(2)$	5.7379	5.7286	2.2970×10^{-4}	3.1683×10^{-4}	-9.300×10^{-3}
	$a(3)$	-3.8542	-3.8448	2.2980×10^{-4}	3.1921×10^{-4}	$+9.400 \times 10^{-3}$
	$a(4)$	0.99033	0.98711	2.6922×10^{-5}	3.7300×10^{-5}	-3.220×10^{-3}
	σ_u^2	3.4907×10^{-6}	3.5639×10^{-6}	2.6984×10^{-11}	2.6990×10^{-11}	$+7.320 \times 10^{-8}$
1.0	$a(1)$	-3.8729	-3.8698	2.6217×10^{-5}	3.5597×10^{-5}	$+3.100 \times 10^{-3}$
	$a(2)$	5.7379	5.7287	2.2341×10^{-4}	3.0717×10^{-4}	-9.200×10^{-3}
	$a(3)$	-3.8542	-3.8449	2.2297×10^{-4}	3.0913×10^{-4}	$+9.300 \times 10^{-3}$
	$a(4)$	0.99033	0.98717	2.6076×10^{-5}	3.6103×10^{-5}	-3.160×10^{-3}
	σ_u^2	3.4907×10^{-6}	3.1827×10^{-6}	9.7524×10^{-12}	9.8023×10^{-12}	-3.080×10^{-7}
10	$a(1)$	-3.8729	-3.8697	2.6989×10^{-5}	3.7185×10^{-5}	$+3.200 \times 10^{-3}$
	$a(2)$	5.7379	5.7284	2.2932×10^{-4}	3.2023×10^{-4}	-9.500×10^{-3}
	$a(3)$	-3.8542	-3.8445	2.2859×10^{-4}	3.2206×10^{-4}	$+9.700 \times 10^{-3}$
	$a(4)$	0.99033	0.98703	2.6732×10^{-5}	3.7627×10^{-5}	-3.300×10^{-3}
	σ_u^2	3.4907×10^{-6}	3.5003×10^{-6}	1.2889×10^{-12}	1.2890×10^{-12}	$+9.600 \times 10^{-9}$
∞	$a(1)$	-3.8729	-3.8698	2.5457×10^{-5}	3.4981×10^{-5}	$+3.100 \times 10^{-3}$
	$a(2)$	5.7379	5.7288	2.1643×10^{-4}	2.9991×10^{-4}	-9.100×10^{-3}
	$a(3)$	-3.8542	-3.8449	2.1575×10^{-4}	3.0044×10^{-4}	$+9.300 \times 10^{-3}$
	$a(4)$	0.99033	0.98717	2.5218×10^{-5}	3.5166×10^{-5}	-3.160×10^{-3}
	σ_u^2	3.4907×10^{-6}	3.4796×10^{-6}	1.1347×10^{-14}	1.1458×10^{-14}	-1.110×10^{-8}

Table 6d. Performance of the Burg estimator for an AR(4) process with α as a parameter and $\lambda=0.99$, $N_T=1000$ and $N_R=1000$.

Gaussian. Thus, for small values of α, we have processes which depart most significantly from Gaussianity. For these processes, the tails of the PDF distribution are highest. Thus, for a fixed sample size N_T, the uncertainty in the estimate of the variance is expected to increase as α decreases. In Fig.19, we show an expanded view of the upper three curves from Fig.18. In this figure, we note a two order of magnitude decrease in the error variance over the range of α values from $\alpha=0.1$ to 10. From the tables, we observe that these curves continue to decrease by nearly two additional orders of magnitude as $\alpha \to \infty$. We also note the drastic reduction in the error variance with increasing temporal correlation expressed by the one-lag temporal correlation parameter λ.

Fig.22 The error variance of the estimate $\hat{\sigma}_u^2$ versus the shape parameter α with the one-lag temporal correlation parameter λ fixed.
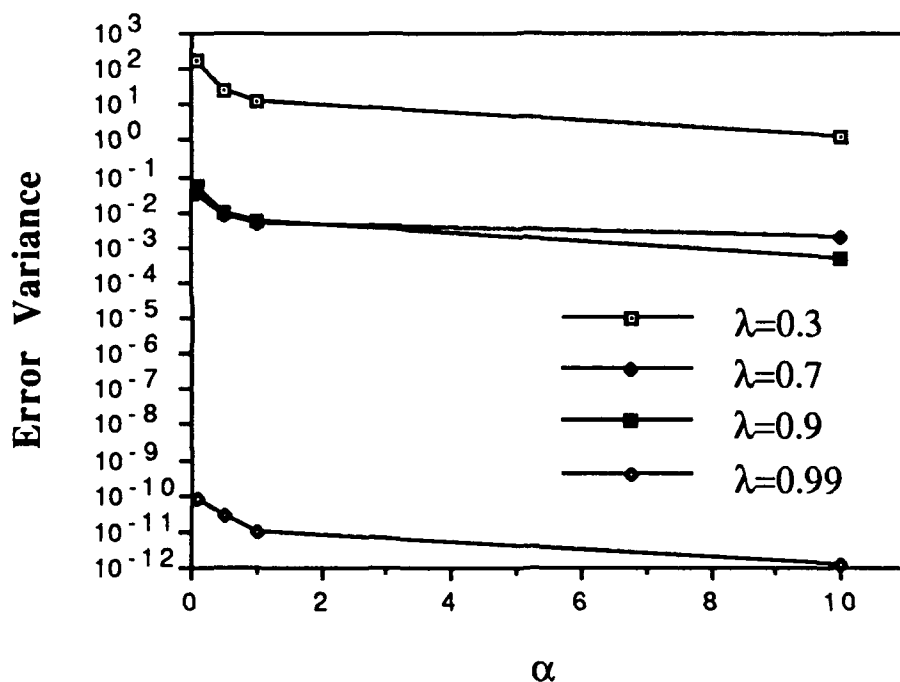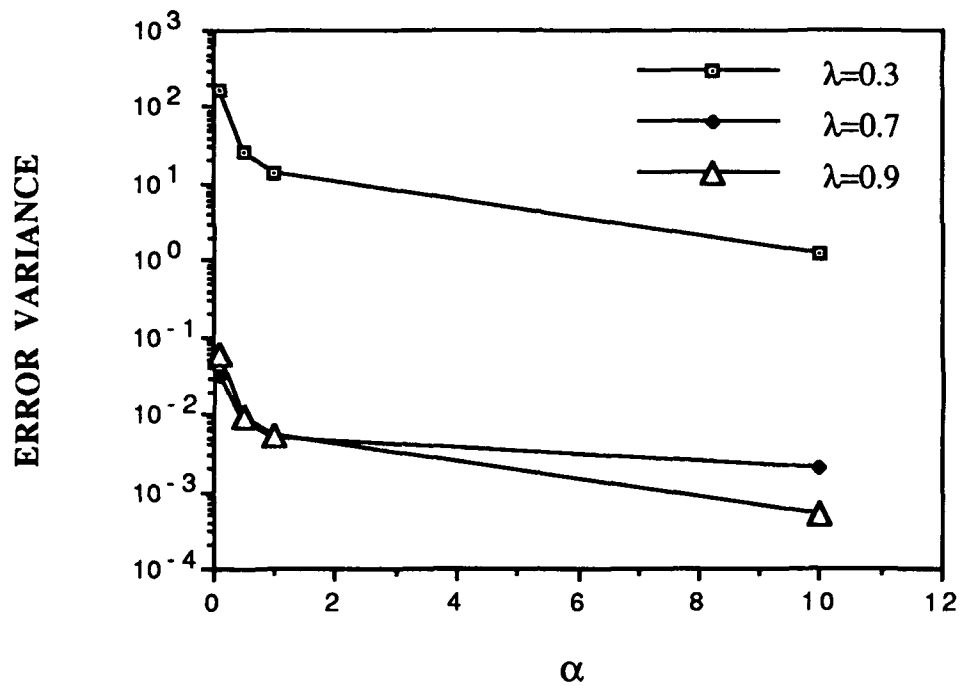
Fig.23 The error variance of the estimate $\hat{\sigma}_u^2$ versus the shape parameter α with the one-lag temporal correlation parameter λ fixed using an expanded scale from Fig. 22.

5.4 Computed Error Variance of Multichannel AR Model Parameters

In this section, we present the computed results for the means and error variances associated with the multichannel estimates of the JxJ matrix coefficients $A(k)$ and $[\Sigma_f]_u$ defined by eqs.(2.1) and (2.6), respectively. The Strand-Nuttall algorithm is used in all the cases presented here. Specific consideration is given to the performance of the estimator not only as a function of the temporal correlation on each channel, but also the cross-channel correlation. We consider multichannel AR(2) processes with J=2 channels and various values of the one-lag temporal correlation parameter λ_{jj} on channel j and the cross-channel correlation parameter, $|\rho_{ij}|$. In this case, we have parameters

$$A(k) = \begin{bmatrix} a_{11}(k) & a_{12}(k) \\ a_{21}(k) & a_{22}(k) \end{bmatrix} \qquad k=1,2 \tag{5.4}$$

and

$$[\Sigma_f]_u = \begin{bmatrix} \Sigma_{11} & \Sigma_{12} \\ \Sigma_{21} & \Sigma_{22} \end{bmatrix} \tag{5.5}$$

Table 7 contains the computed results for the estimates $\hat{a}_{11}(1)$, $\hat{a}_{12}(1)$, $\hat{\Sigma}_{11}$ and $\hat{\Sigma}_{12}$. The number of time samples used to obtain each estimate was $N_T=100$ while the statistics were computed with $N_R=1000$ realizations. In Figs. 22 and 23, we plot the error variances of the matrix element estimates $\hat{a}_{11}(1)$ and $\hat{\Sigma}_{11}$. Similar results were obtained for the estimates of the other elements.

Consistent with the results noted for single channel processes, the error variances associated with the estimates of these coefficients decrease with increasing temporal correlation. However, we now observe in Figs 22 and 23 that the error variance associated with the estimates $\hat{a}_{11}(1)$ and $\hat{a}_{12}(1)$ increases with increasing cross-channel correlation. In Figs.24 and 25, however, we observe that the error variance associated with the estimates of the white driving noise covariance matrix elements $\hat{\Sigma}_{11}$ and $\hat{\Sigma}_{12}$ are independent of the cross-channel correlation. This result is consistent with the presentation made in section 3.2 that error variances of cross-correlation function estimates are independent of the cross-channel correlation for the special case of wide-sense jointly stationary narrowband bandpass processes as considered here.

λ_{11}	λ_{22}	λ_{12}	$|\rho_{12}|$		TRUE VALUE	MEAN OF ESTIMATE	SAMPLE VARIANCE	ERROR VARIANCE
0.1	0.1	0.01	0	a_{11}	-0.101	-0.099721	1.0272×10^{-2}	1.0263×10^{-2}
				a_{12}	0	-2.1981×10^{-3}	1.0529×10^{-2}	1.0525×10^{-2}
				Σ_{11}	3.9596	3.8077	1.4491×10^{-1}	1.6783×10^{-1}
				Σ_{12}	0	1.9938×10^{-2}	1.4529×10^{-1}	1.4556×10^{-1}
0.5	0.5	0.01	0	a_{11}	-0.625	-0.61265	9.7337×10^{-3}	9.8814×10^{-3}
				a_{12}	0	4.3440×10^{-4}	9.3721×10^{-3}	9.3647×10^{-3}
				Σ_{11}	2.8125	2.7058	7.4709×10^{-2}	8.6021×10^{-2}
				Σ_{12}	0	1.4185×10^{-3}	7.7050×10^{-2}	7.7009×10^{-2}
0.7	0.7	0.01	0	a_{11}	-1.043	-1.0209	8.6619×10^{-3}	9.1400×10^{-3}
				a_{12}	0	-2.3376×10^{-3}	8.3557×10^{-3}	8.3803×10^{-3}
				Σ_{11}	1.5502	1.4824	2.3082×10^{-2}	2.7649×10^{-2}
				Σ_{12}	0	2.5259×10^{-3}	2.4681×10^{-2}	2.4676×10^{-2}
0.9	0.9	0.01	0	a_{11}	-1.6290	-1.5929	4.7884×10^{-3}	6.0843×10^{-3}
				a_{12}	0	-6.4223×10^{-4}	4.8277×10^{-3}	4.8239×10^{-3}
				Σ_{11}	0.26136	0.25166	6.5474×10^{-4}	7.4833×10^{-4}
				Σ_{12}	0	1.9544×10^{-4}	6.5406×10^{-4}	6.5357×10^{-4}
0.99	0.99	0.01	0	a_{11}	-1.9603	-1.9180	1.8241×10^{-3}	3.6105×10^{-3}
				a_{12}	0	1.8338×10^{-5}	2.2002×10^{-3}	2.1980×10^{-3}
				Σ_{11}	3.1361×10^{-3}	3.0368×10^{-3}	9.3876×10^{-8}	1.0365×10^{-7}
				Σ_{12}	0	-6.4657×10^{-6}	9.8708×10^{-8}	9.8692×10^{-8}

Table 7a   Tabulated values of the mean and variances for the multichannel coefficient estimates $\hat{a}_{11}(1)$, $\hat{a}_{12}(1)$, $\hat{\Sigma}_{11}(1)$ and $\hat{\Sigma}_{12}(1)$ for AR(2) processes with specified temporal and cross-channel correlation using the Strand-Nuttall estimator.

λ_{11}	λ_{22}	λ_{12}	$|\rho_{12}|$		TRUE VALUE	MEAN OF ESTIMATE	SAMPLE VARIANCE	ERROR VARIANCE
0.1	0.1	0.1	0.7	a_{11}	-0.101	-0.10209	1.9722×10^{-2}	1.9706×10^{-2}
				a_{12}	0	5.6071×10^{-3}	2.0244×10^{-2}	2.0256×10^{-2}
				Σ_{11}	3.9596	3.8016	1.4683×10^{-1}	1.7166×10^{-1}
				Σ_{12}	2.7717	2.6534	1.4752×10^{-1}	1.6142×10^{-1}
0.5	0.5	0.5	0.7	a_{11}	-0.625	-0.61097	1.9408×10^{-2}	1.9587×10^{-2}
				a_{12}	0	2.0894×10^{-3}	1.9262×10^{-2}	1.9249×10^{-2}
				Σ_{11}	2.8125	2.7092	7.8848×10^{-2}	8.9437×10^{-2}
				Σ_{12}	1.9687	1.9026	7.3984×10^{-2}	7.8289×10^{-2}
0.7	0.7	0.7	0.7	a_{11}	-1.043	-1.0235	1.6809×10^{-2}	1.7196×10^{-2}
				a_{12}	2.557×10^{-7}	1.5809×10^{-3}	1.7263×10^{-2}	2.6020×10^{-2}
				Σ_{11}	1.5502	1.4890	2.3195×10^{-2}	2.6915×10^{-2}
				Σ_{12}	1.0851	1.0405	2.4046×10^{-2}	2.6020×10^{-2}
0.9	0.9	0.9	0.7	a_{11}	-1.6290	-1.5993	8.7113×10^{-3}	9.9725×10^{-3}
				a_{12}	-2.1458×10^{-7}	-7.7136×10^{-4}	8.9255×10^{-3}	8.9177×10^{-3}
				Σ_{11}	0.26136	0.25214	6.1706×10^{-4}	7.0158×10^{-4}
				Σ_{12}	0.18295	0.17707	6.4987×10^{-4}	6.8409×10^{-4}
0.99	0.99	0.99	0.7	a_{11}	-1.9603	-1.9168	4.1238×10^{-3}	6.0096×10^{-3}
				a_{12}	5.9009×10^{-7}	-7.0187×10^{-4}	4.3465×10^{-3}	4.3438×10^{-3}
				Σ_{11}	3.1361×10^{-3}	3.0342×10^{-3}	1.0060×10^{-7}	1.1090×10^{-7}
				Σ_{12}	2.195×10^{-3}	2.1211×10^{-3}	9.8467×10^{-8}	1.0388×10^{-7}

Table 7b Tabulated values of the mean and variances for the multichannel coefficient estimates $\hat{a}_{11}(1)$, $\hat{a}_{12}(1)$, $\hat{\Sigma}_{11}(1)$ and $\hat{\Sigma}_{12}(1)$ for AR(2) processes with specified temporal and cross-channel correlation using the Strand-Nuttall estimator.

90

λ_{11}	λ_{22}	λ_{12}	$|\rho_{12}|$		TRUE VALUE	MEAN OF ESTIMATE	SAMPLE VARIANCE	ERROR VARIANCE
0.1	0.1	0.1	0.99	a_{11}	-0.101	-0.1027	4.9512×10^{-1}	4.9503×10^{-1}
				a_{12}	4.8161×10^{-7}	3.1909×10^{-3}	4.9880×10^{-1}	4.9871×10^{-1}
				Σ_{11}	3.9596	3.8008	1.5615×10^{-1}	1.8122×10^{-1}
				Σ_{12}	3.92	3.7651	1.5696×10^{-1}	1.8080×10^{-1}
0.5	0.5	0.5	0.99	a_{11}	-0.625	0.6230	5.1454×10^{-1}	5.1421×10^{-1}
				a_{12}	0	1.0188×10^{-2}	5.1596×10^{-1}	5.1579×10^{-1}
				Σ_{11}	2.8125	2.6910	7.7955×10^{-2}	9.2635×10^{-2}
				Σ_{12}	2.7844	2.6650	7.7097×10^{-2}	9.1265×10^{-2}
0.7	0.7	0.7	0.99	a_{11}	-1.043	-1.0390	4.2740×10^{-1}	4.2803×10^{-1}
				a_{12}	-1.503×10^{-5}	1.6488×10^{-2}	4.2911×10^{-1}	4.3012×10^{-1}
				Σ_{11}	1.5502	1.4899	2.3652×10^{-2}	2.7263×10^{-2}
				Σ_{12}	1.5347	1.4759	2.3821×10^{-2}	2.7255×10^{-2}
0.9	0.9	0.9	0.99	a_{11}	-1.6290	-1.5976	2.3052×10^{-1}	2.3128×10^{-1}
				a_{12}	1.0300×10^{-5}	2.5663×10^{-3}	2.3220×10^{-1}	2.3197×10^{-1}
				Σ_{11}	0.26136	0.25186	6.6874×10^{-4}	7.5798×10^{-4}
				Σ_{12}	0.25873	0.24928	6.6927×10^{-4}	7.5788×10^{-4}
0.99	0.99	0.99	0.99	a_{11}	-1.9603	-1.9143	1.1510×10^{-1}	1.1712×10^{-1}
				a_{12}	-7.1755×10^{-5}	-3.7304×10^{-3}	1.1472×10^{-1}	1.1462×10^{-1}
				Σ_{11}	3.1361×10^{-3}	2.9814×10^{-3}	1.0885×10^{-7}	1.2240×10^{-7}
				Σ_{12}	3.067×10^{-3}	2.9483×10^{-3}	1.1691×10^{-7}	1.3090×10^{-7}

Table 7c   Tabulated values of the mean and variances for the multichannel coefficient estimates $\hat{a}_{11}(1)$, $\hat{a}_{12}(1)$, $\hat{\Sigma}_{11}(1)$ and $\hat{\Sigma}_{12}(1)$ for AR(2) processes with specified temporal and cross-channel correlation using the Strand-Nuttall estimator.

ERROR VARIANCE
FOR a11(1) ESTIMATE

10^0

10^{-1}

10^{-2}

10^{-3}

|ρ12|=0

|ρ12|=0.7

|ρ12|=0.99

0.0   0.2   0.4   0.6   0.8   1.0

λ

Figure 24 Error variance for the estimate $\hat{a}_{11}(1)$ coefficient versus the one-lag temporal correlation parameter $\lambda=\lambda_{11}=\lambda_{12}$ using the Strand-Nuttall algorithm with order 2, $N_T=100$ time samples, and $|\rho_{12}|$ as a parameter.
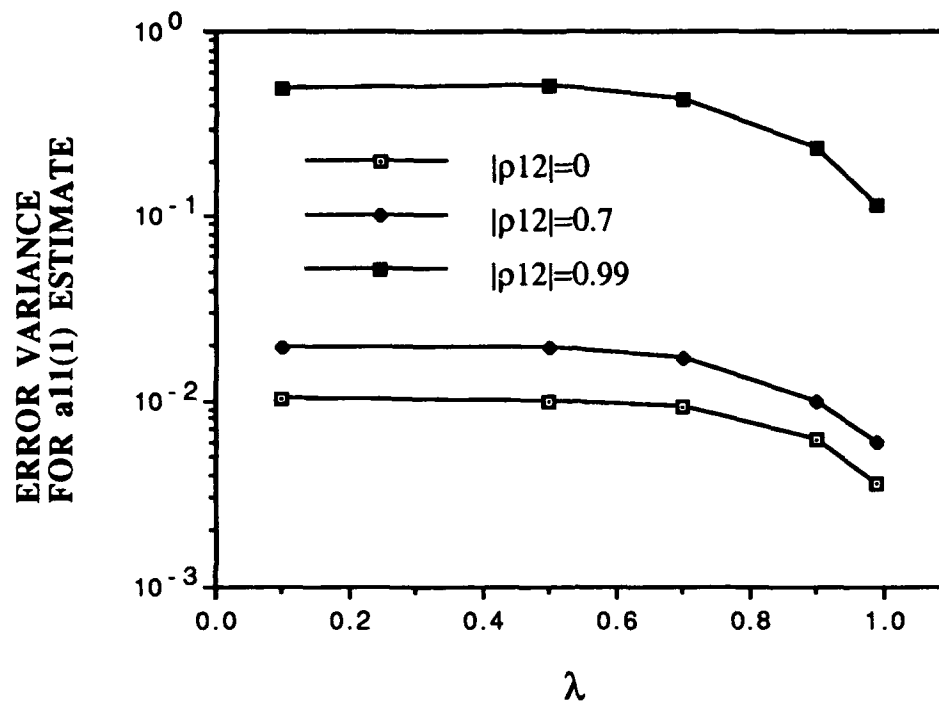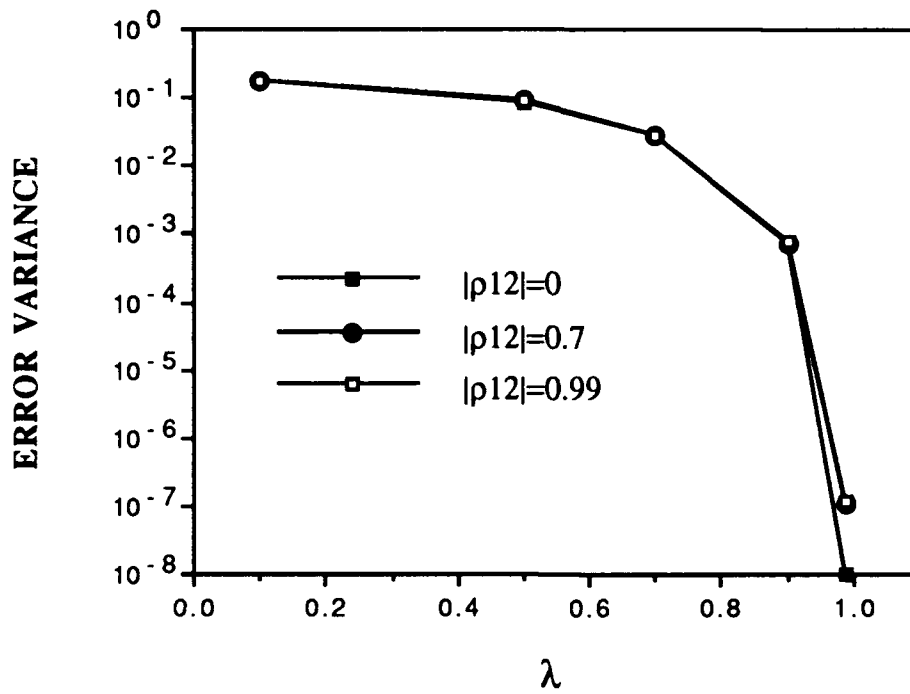
Figure 25 Error variance for the estimate $\hat{\Sigma}_{11}(1)$ coefficient versus the one-lag temporal correlation parameter $\lambda=\lambda_{11}=\lambda_{12}$ using the Strand-Nuttall algorithm with order 2, $N_T=100$ time samples, and $|\rho_{12}|$ as a parameter.

6.0 SUMMARY

In this study, the performance of time-averaged estimators is considered not only as a function of the observation window size of the data, but also in terms of the pertinent correlation parameters of the underlying observation processes. Specifically, the error variances and sample variances of both correlation function and parameter estimators are considered for Gaussian as well as non-Gaussian processes. In addition, multichannel processes are analyzed. Analytic expressions are derived for the variance of the time-averaged complex auto- and cross-correlation functions. The unique aspect of this development is the determination of the functional dependence of these expressions in terms of process correlation parameters. Specifically, the variance of the time-averaged cross-correlation function is shown to depend upon the temporal correlation and variance of each process, as well as (in the more general case of processes with unconstrained Gaussian quadrature components [5]) the cross-correlation coefficient. These expressions provide a performance measure which can be used to specify the window size of the observation interval required to achieve a specific value of this variance.

REFERENCES

[1]   Michels, J. H., Varshney, P., Weiner, D., "A Synthesis Method for Multichannel AR Processes", presented at the 24th Annual Asilomar Conference on Signals, Systems and Computers, Pacific Grove, California, 5-7 November, 1990.

[2]   Michels, J. H., "Synthesis of Multichannel Autoregressive Random Processes and Ergodicity Considerations", RADC-TR-90-211, July, 1990.

[3]   Papoulis, A., Signal Analysis, McGraw-Hill Book Co., 1977.

[4]   Jenkins, G., Watts, D., Spectral Analysis and its applications, Holden Day,1968.

[5]   Michels, J. H., Multichannel Detection Using the Discrete-Time Model-Based Innovations Approach, PhD dissertation, Syracuse University, Syracuse, N.Y., May 1991.

[6]   Porat, B., Friedlander, B., "The Exact Cramer-Rao Bound for Gaussian Autoregressive Processes," IEEE Trans. on Aerospace and Electronic Systems, vol. AES-23, no. 4, July 1987.

[7]   Rangaswami, M., 'Spherically Invariant Random Processes for Radar Clutter Modeling, Simulation and Distributed Identification', PhD dissertation, Syracuse University, 1992.

[8]   Rangaswami, M., Weiner, D., Michels, J.H., "Innovations Based Detection Algorithm for Correlated Non-Gaussian Random Processes," accepted for presentation at the Sixth SSAP Workshop on Statistical Signal and Array Processing, Victoria, British Columbia, Canada, 7-9 Oct., 1992.

[9]   Yule, G.V., "On the method of investigating periodicities in diturbed series, with special reference to Wolfer's sunspot numbers," Phil. Trans. Royal Soc. (London), vol. A226, pp. 267-298, 1927.

[10]   Walker, G. "On periodicity in time series of related terms," Proc. Royal Soc. (London), vol. A131, pp. 518-532, 1931.

[11]   Strand, O. N., "Multichannel complex maximum entropy (auto-regressive) spectral analysis," IEEE Trans. Antom. Control, vol, AC-22, pg 634-640, Aug 1977.

[12]   Nuttall, A.H., "Multivariate linear predictive spectral analysis employing weighted forward and backward averaging: A generalization of Burg's algorithm," Naval Underwater Systems Center TR-5501, New London, Conn. Oct. 1976.

[13] Burg, J.P., "Maximum Entropy Spectral Analysis," Ph.D. dissertation, Stanford University, Stanford, California, 1975.

[14] Levinson, N., "Wiener RMS (Root Mean Square) Error Criterion in Filter Design and Prediction," J. Math. Physics, Vol. 25, pp. 261-278, 1947.

[15] Lu, C.S., "Solution of the Matrix Equation AX+XB=C," Electronics Letters, vol. 7, no.8, April 22, 1971, pp. 185-186.

[16] Wiggins, R., Robinson, E., "Recursive solution to the multichannel filtering problem," JGR, Vol. 70, 1965.

[17] Jacovitti, G., Cusani, R., "Performance of Normalized Correlation Estimators for Complex Processes", IEEE Transactions on Signal Processing, vol. 40, no. 1, January 1992.

APPENDIX A

In this Appendix, we derive the result expressed in eq.(29b) of the text. From eqs(11)

$$E[\phi(n,l)] = R_{ii}(l) \tag{A.1a}$$

and

$$E[\phi^*(n-k,l)] = R_{ii}^*(l) \tag{A.1b}$$

so that from eq(2d)

$$C_{\phi\phi}(k,l) = R_{\phi\phi}(k,l) - |R_{ii}(l)|^2. \tag{A.2}$$

And so, eq(3c) becomes

$$V_{B_{ii}}(l,N_T) = \frac{1}{N_T} \sum_{k=-(N_T-|l|-1)}^{N_T-|l|-1} \left[1 - \frac{|l|+|k|}{N_T} \right] [R_{\phi\phi}(k,l) - |R_{ii}(l)|^2]. \tag{A.3}$$

We now consider,

$$R_{\phi\phi}(k,l) = E[\phi(n,l)\phi^*(n-k,l)] \tag{A.4a}$$

$$= E[x_i(n)x_i^*(n-l)x_i^*(n-k)x_i(n-l-k)]. \tag{A.4b}$$

For processes with zero-mean, jointly stationary Gaussian quadrature components $x_{iI}(n)$ and $x_{iQ}(n)$, eq(A.4b) can be expressed as [see Appendix B]

$$R_{\phi\phi}(k,l) = |R_{ii}(l)|^2 + |R_{ii}(k)|^2 + F_{ii}(l,k) \tag{A.5}$$

where

$$F_{ii}(l,k) = E[x_i(n)x_i(n-l-k)]E[x_i^*(n-l)x_i^*(n-k)] \tag{A.6a}$$

$$= \{ R_{ii}^{II}(l+k) - R_{ii}^{QQ}(l+k) \} \{ R_{ii}^{II}(l-k) - R_{ii}^{QQ}(l-k) \}$$

$$+ \{ R_{ii}^{QI}(l+k) + R_{ii}^{IQ}(l+k) \} \{ R_{ii}^{QI}(l-k) + R_{ii}^{IQ}(l-k) \}$$

$$- j \{ R_{ii}^{II}(l+k) - R_{ii}^{QQ}(l+k) \} \{ R_{ii}^{QI}(l-k) + R_{ii}^{IQ}(l-k) \}$$

$$+ j \{ R_{ii}^{II}(l-k) - R_{ii}^{QQ}(l-k) \} \{ R_{ii}^{QI}(l+k) + R_{ii}^{IQ}(l+k) \}. \tag{A.6b}$$

Using eq(A.5) in (A.3), we have

$$V_{B_{ii}}(l,N_T) = \frac{1}{N_T} \sum_{k=-(N_T-|l|-1)}^{N_T-|l|-1} \left[1 - \frac{|l|+|k|}{N_T}\right] \left[|R_{ii}(k)|^2 + F_{ii}(l,k)\right]. \qquad (A.7)$$

By examination of eq(A.6b), we note that the imaginary terms in eq(A.7) sum to zero. This can be seen by first noting that $F_{ii}(l,k)$ is real for $k=0$. We also note that imaginary terms evaluated with negative values of k serve to cancel the corresponding imaginary terms for positive values of k. And so, only the real part of the function $F_{ii}(l,k)$ contributes to the $V_{B_{ii}}(l,N_T)$ function. Therefore,

$$V_{B_{ii}}(l,N_T) = \frac{1}{N_T} \sum_{k=-(N_T-|l|-1)}^{N_T-|l|-1} \left[1 - \frac{|l|+|k|}{N_T}\right] \left[|R_{ii}(k)|^2 + \mathrm{Re}\{F_{ii}(l,k)\}\right] \qquad (A.8)$$

which is eq(4) in the text.

APPENDIX B

In this appendix, we derive eq(A.5) of Appendix A. Consider eq(A.4b) expressed as

$$R_{\phi\phi}(k,l) = E[x_i(n)x_i^*(n-l)x_i^*(n-k)x_i(n-l-k)]. \tag{B.1}$$

In the special case where the process $x_i(n)$ is Gaussian, then [6]

$$R_{\phi\phi}(k,l) = E[x_i(n)x_i^*(n-l)]E[x_i^*(n-k)x_i(n-l-k)]$$

$$+ E[x_i(n)x_i^*(n-k)]E[x_i^*(n-l)x_i(n-l-k)]. \tag{B.2}$$

However, we do not wish to constrain this discussion to this restrictive case. Rather, we wish to consider the more general case of a process $x_i(n)$ with jointly Gaussian quadrature components. We therefore consider

$$x_i(n) = x_{iI}(n) + j\, x_{iQ}(n) \tag{B.3}$$

where the processes $x_{iI}(n)$ and $x_{iQ}(n)$ are jointly Gaussian. Using eq(B.3) in (B.1), we obtain

$$R_{\phi\phi}(k) = E\{ [x_{iI}(n) + j\, x_{iQ}(n)][x_{iI}(n-l) - j\, x_{iQ}(n-l)]$$

$$\bullet\ [x_{iI}(n-k) - j\, x_{iQ}(n-k)][x_{iI}(n-l-k) + j\, x_{iQ}(n-l-k)]\} \tag{B.4a}$$

$$= E\{ [x_{iI}(n)x_{iI}(n-l)+x_{iQ}(n)x_{iQ}(n-l)+jx_{iQ}(n)x_{iI}(n-l)-jx_{iI}(n)x_{iQ}(n-l)]$$

$$\bullet\ [x_{iI}(n-k)x_{iI}(n-l-k)+x_{iQ}(n-k)x_{iQ}(n-l-k)+jx_{iI}(n-k)x_{iQ}(n-l-k)$$

$$-jx_{iQ}(n-k)x_{iI}(n-l-k)]\} \tag{B.4b}$$

$$= E[x_{iI}(n)x_{iI}(n-l)x_{iI}(n-k)x_{iI}(n-l-k)] + E[x_{iQ}(n)x_{iQ}(n-l)x_{iI}(n-k)x_{iI}(n-l-k)]$$

$$+ E[x_{iI}(n)x_{iI}(n-l)x_{iQ}(n-k)x_{iQ}(n-l-k)] + E[x_{iQ}(n)x_{iQ}(n-l)x_{iQ}(n-k)x_{iQ}(n-l-k)]$$

$$- E[x_{iQ}(n)x_{iI}(n-l)x_{iI}(n-k)x_{iQ}(n-l-k)] + E[x_{iI}(n)x_{iQ}(n-l)x_{iI}(n-k)x_{iQ}(n-l-k)]$$

$$+ E[x_{iQ}(n)x_{iI}(n-l)x_{iQ}(n-k)x_{iI}(n-l-k)] - E[x_{iI}(n)x_{iQ}(n-l)x_{iQ}(n-k)x_{iI}(n-l-k)]$$

$$+jE[x_{iI}(n)x_{iI}(n-l)x_{iI}(n-k)x_{iQ}(n-l-k)] - jE[x_{iI}(n)x_{iI}(n-l)x_{iQ}(n-k)x_{iI}(n-l-k)]$$

$$+jE[x_{iQ}(n)x_{iQ}(n-l)x_{iI}(n-k)x_{iQ}(n-l-k)] - jE[x_{iQ}(n)x_{iQ}(n-l)x_{iQ}(n-k)x_{iI}(n-l-k)]$$

$$+jE[x_{iQ}(n)x_{iI}(n-l)x_{iI}(n-k)x_{iI}(n-l-k)] + jE[x_{iQ}(n)x_{iI}(n-l)x_{iQ}(n-k)x_{iQ}(n-l-k)]$$

$$-jE[x_{iI}(n)x_{iQ}(n-l)x_{iI}(n-k)x_{iI}(n-l-k)] - j\, E[x_{iI}(n)x_{iQ}(n-l)x_{iQ}(n-k)x_{iQ}(n-l-k)]$$

$$\tag{B.4c}$$

For Gaussian, zero-mean quadrature components, eq(B.4c) can be expressed as

$$R_{\phi\phi}(k) = [R_{ii}^{II}(l)]^2 + [R_{ii}^{II}(k)]^2 + R_{ii}^{II}(l+k)R_{ii}^{II}(k-l)$$

$$+ R_{ii}^{QQ}(l)R_{ii}^{II}(l) + [R_{ii}^{QI}(k)]^2 + R_{ii}^{QI}(l+k)R_{ii}^{QI}(k-l)$$

$$+ R_{ii}^{II}(l)R_{ii}^{QQ}(l) + [R_{ii}^{IQ}(k)]^2 + R_{ii}^{IQ}(l+k)R_{ii}^{IQ}(k-l)$$

$$+ [R_{ii}^{QQ}(l)]^2 + [R_{ii}^{QQ}(k)]^2 + R_{ii}^{QQ}(l+k)R_{ii}^{QQ}(k-l)$$

$$- R_{ii}^{QI}(l)R_{ii}^{IQ}(l) - R_{ii}^{QI}(k)R_{ii}^{IQ}(k) - R_{ii}^{QQ}(l+k)R_{ii}^{II}(k-l)$$

$$+ [R_{ii}^{IQ}(l)]^2 + R_{ii}^{II}(k)R_{ii}^{QQ}(k) + R_{ii}^{IQ}(l+k)R_{ii}^{QI}(k-l)$$

$$+ [R_{ii}^{QI}(l)]^2 + R_{ii}^{QQ}(k)R_{ii}^{II}(k) + R_{ii}^{QI}(l+k)R_{ii}^{IQ}(k-l)$$

$$- R_{ii}^{IQ}(l)R_{ii}^{QI}(l) - R_{ii}^{IQ}(k)R_{ii}^{QI}(k) - R_{ii}^{II}(l+k)R_{ii}^{QQ}(k-l)$$

$$+j\left\{ R_{ii}^{II}(l)R_{ii}^{IQ}(l) + R_{ii}^{II}(k)R_{ii}^{IQ}(k) + R_{ii}^{IQ}(l+k)R_{ii}^{II}(k-l) \right\}$$

$$-j\left\{ R_{ii}^{II}(l)R_{ii}^{QI}(l) + R_{ii}^{IQ}(k)R_{ii}^{II}(k) + R_{ii}^{II}(l+k)R_{ii}^{IQ}(k-l) \right\}$$

$$+j\left\{ R_{ii}^{QQ}(l)R_{ii}^{IQ}(l) + R_{ii}^{QI}(k)R_{ii}^{QQ}(k) + R_{ii}^{QQ}(l+k)R_{ii}^{QI}(k-l) \right\}$$

$$-j\left\{ R_{ii}^{QQ}(l)R_{ii}^{QI}(l) + R_{ii}^{QQ}(k)R_{ii}^{QI}(k) + R_{ii}^{QI}(l+k)R_{ii}^{QQ}(k-l) \right\}$$

$$+j\left\{ R_{ii}^{QI}(l)R_{ii}^{II}(l) + R_{ii}^{QI}(k)R_{ii}^{II}(k) + R_{ii}^{QI}(l+k)R_{ii}^{II}(k-l) \right\}$$

$$+j\left\{ R_{ii}^{QI}(l)R_{ii}^{QQ}(l) + R_{ii}^{QQ}(k)R_{ii}^{IQ}(k) + R_{ii}^{QQ}(l+k)R_{ii}^{IQ}(k-l) \right\}$$

$$-j\left\{ R_{ii}^{IQ}(l)R_{ii}^{II}(l) + R_{ii}^{II}(k)R_{ii}^{QI}(k) + R_{ii}^{II}(l+k)R_{ii}^{QI}(k-l) \right\}$$

$$-j\left\{ R_{ii}^{IQ}(l)R_{ii}^{QQ}(l) + R_{ii}^{IQ}(k)R_{ii}^{QQ}(k) + R_{ii}^{IQ}(l+k)R_{ii}^{QQ}(k-l) \right\}$$

$$(B.5)$$

where we note that the first two terms in each parenthesis for the imaginary terms cancel. Since

$$R(l) = [R_{ii}^{II}(l) + R_{ii}^{QQ}(l)] + j[R_{ii}^{QI}(l) - R_{ii}^{IQ}(l)] \tag{B.6}$$

then

$$|R(l)|^2 = [R_{ii}^{II}(l)]^2 + 2R_{ii}^{II}(l)R_{ii}^{QQ}(l) + [R_{ii}^{QQ}(l)]^2$$
$$+ [R_{ii}^{QI}(k)]^2 - 2R_{ii}^{QI}(l)R_{ii}^{IQ}(l) + [R_{ii}^{IQ}(l)]^2 \tag{B.7}$$

and similarly for $|R(k)|^2$ so that

$$R_{\phi\phi}(k) = |R_{ii}(l)|^2 + |R_{ii}(k)|^2 + F_{ii}(l,k) \tag{B.8}$$

100

where

$$F_{ii}(l,k) = \left\{ R_{ii}^{II}(l+k) - R_{ii}^{QQ}(l+k) \right\} \left\{ R_{ii}^{II}(l-k) - R_{ii}^{QQ}(l-k) \right\}$$

$$+ \left\{ R_{ii}^{QI}(l+k) + R_{ii}^{IQ}(l+k) \right\} \left\{ R_{ii}^{QI}(l-k) + R_{ii}^{IQ}(l-k) \right\}$$

$$- j \left\{ R_{ii}^{II}(l+k) - R_{ii}^{QQ}(l+k) \right\} \left\{ R_{ii}^{QI}(l-k) + R_{ii}^{IQ}(l-k) \right\}$$

$$+ j \left\{ R_{ii}^{II}(l-k) - R_{ii}^{QQ}(l-k) \right\} \left\{ R_{ii}^{QI}(l+k) + R_{ii}^{IQ}(l+k) \right\} \qquad (B.9)$$

as noted in eq(A.6b) of Appendix A.

MISSION

OF

ROME LABORATORY

Rome Laboratory plans and executes an interdisciplinary program in re-
search, development, test, and technology transition in support of Air
Force Command, Control, Communications and Intelligence (C^3I) activities
for all Air Force platforms. It also executes selected acquisition programs
in several areas of expertise. Technical and engineering support within
areas of competence is provided to ESD Program Offices (POs) and other
ESD elements to perform effective acquisition of C^3I systems. In addition,
Rome Laboratory's technology supports other AFSC Product Divisions, the
Air Force user community, and other DOD and non-DOD agencies. Rome
Laboratory maintains technical competence and research programs in areas
including, but not limited to, communications, command and control, battle
management, intelligence information processing, computational sciences
and software producibility, wide area surveillance/sensors, signal proces-
sing, solid state sciences, photonics, electromagnetic technology, super-
conductivity, and electronic reliability/maintainability and testability.